Application of Raman spectroscopy and mass spectrometry to study growth and interaction processes of the white-rot fungus *Schizophyllum commune*

DISSERTATION

Zur Erlangung des akademischen Grades

Doctor rerum naturalium (Dr. rer. nat.)

vorgelegt dem Rat der Biologisch-Pharmazeutischen Fakultät

der Friedrich-Schiller-Universität Jena

von

Riya Christina Menezes (MSc. Biotechnology)

geboren am 16.08.1986 in Mangalore, Indien

Jena, im März 2014

GUTACHTER (REVIEWER)

1. Prof. Dr. Erika Kothe, Institut für Mikrobiologie, Friedrich-Schiller-Universität, Neugasse 25, 07743 Jena Germany
2. Prof. Dr. Jürgen Popp, Leibniz-Institut für Photonische Technologien e.V, Albert-Einstein-Straße 9, 07745 Jena Germany
3. Prof. Dr. Max Diem, Department of Chemistry and Chemical Biology, Northeastern University, 316 Hurtig Hall, Boston, MA 02115 USA

TAG DER ÖFFENTLICHEN VERTEIDIGUNG (DAY OF PUBLIC DEFENCE)

January 27th, 2015

Table of contents

Abbreviations

2, 4-D	2,4-Dichlorophenoxyacetic acid
2, 4, 5-T	2,4,5-Trichlorophenoxyacetic acid
BF	bright field
CARS	coherent anti-Stokes Raman scattering
DAPI	4', 6-Diamidin-2'phenylindol-dihydrochloride
DIC	differential interference contrast
GC	gas chromatography
HPLC	high performance liquid chromatography
IAA	indole-3-acetic acid
LESA	liquid extraction surface analysis
LTQ	linear ion trap quadrupole
MIC	minimum inhibitory concentration
NLO	nonlinear optics
PC	phase contrast
PTR-MS	proton transfer reaction – mass spectrometry
RMS	Raman microspectroscopy
RT	room temperature
SHG	second harmonic generation
SPE	solid phase extraction
THG	third harmonic generation
TPEF	two-photon excitation fluorescence
UHPLC-ESI-MS/MS	ultra high performance liquid chromatography – electro-spray ionization – tandem mass spectrometry
WT	wild type

1. Introduction

1.1 *Schizophyllum commune*: Life cycle and characteristics

The common split-gill mushroom *S. commune* belongs to the group of gilled mushrooms. Its distribution is circum-global, occurring in temperate to tropical climates, and growing predominantly on hardwoods like *Fagus* and *Quercus*, fruit woods, conifers, bamboos, straw, tea-leaves, or coconut fibers. Its fruiting bodies (Fig. 1) are perennial, leathery, shell-shaped, 1–5 cm and typically monomitic with a tetrapolar mating type system (Raper & Miles, 1958) and usually in groups. Its lower surface shows split gills (Schmidt, 2006). It is a widely occurring saprophyte which grows on dead, rotting wood causing white rot. It also occurs as a wound parasite on

Figure 1: *S. commune* 12-43 x 4-39 on solid media and fruiting bodies *in vitro*

living trees after bark fire damage, on stumps or stored stems; and is frequently found on beech as a first colonizer. In the tropics, *S. commune* is a serious wood destroyer, and forms fruit bodies often on imported timber. However, *in vitro,* only modest wood decay has been observed (Schmidt & Liese, 1980).

S. commune has been used as a model system for the investigation of mating and sexual development for decades since it can be grown from spore to spore through its entire life cycle within 14 days on artificial media (Fig 2), and it shows easily distinguished phenotypes for a tetrapolar mating behavior facilitating genetic analyses (Kothe, 1996). Its genome is 38.5 megabases in size, and has 14 chromosomes, ranging in size from 1.6 to 4.7 Mbp (Ásgeirsdóttir*, et al.*, 1994).

The molecular study of gene function has been enabled by DNA-mediated transformation (Munoz-Rivas, *et al.*, 1986) and by the ability to perform targeted gene disruption by homologous integration (Horton, *et al.*, 1999, Berends, *et al.*, 2013). The status of *S. commune* as a model system was elevated as a result of the Joint Genome Institute sequencing the entire genome of this organism (Ohm, *et al.*, 2010).

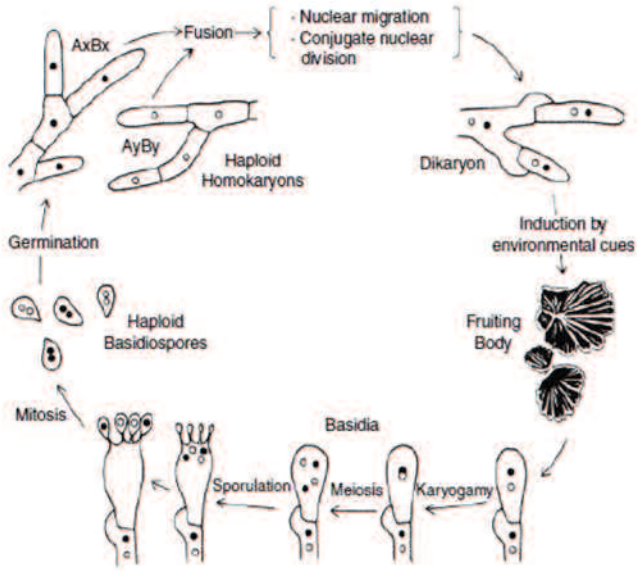

Figure 2: The life cycle of *Schizophyllum commune* (Stankis, *et al.*, 1992)

The life cycle of most basidiomycetes encompasses two distinct phases: those of the monokaryon and the dikaryon (Fig 2). Initially, a meiotic haploid spore germinates, giving rise to a mycelium with uninucleate cells, the monokaryon. This mycelium can grow vegetatively and, when it meets another monokaryon of the same species, hyphal fusions occur between the two mycelia. At that moment, fertilization of the mycelium can occur. In most mushroom-forming basidiomycetes, fusion is followed by exchange of nuclei, but not cytoplasm (Hintz, *et al.*, 1988, May & Taylor, 1988) resulting in a mycelium with binucleate cells, the dikaryon. The life cycle of *S. commune* allows comparison of evolutionary change between two contrasting conformations of nuclei: a) in mycelia consisting of uninucleate cells with genetically uniform haploid nuclei and b) in mycelia consisting of dikaryotic cells, each of which contains the two haploid gametic nuclear types in paired association. In tetrapolar species, incompatibility is controlled by two series of multiple alleles at two loci on different chromosomes. The two pairs segregate independently at meiosis. The first mating type genes in basidiomycetes were identified in *S. commune* (Giasson, *et al.*,

1989). The term tetrapolar describes the phenomenon which was attributed to two separate mating type factors, called *A* and *B* in homobasidiomycetes (Kniep, 1920, 1928). In this fungus, both *A* and *B* factors are found to be composed of two separate genetic loci, *Aα* and *Aβ*, and *Bα* and *Bβ* for *A* and *B*, respectively. In tetrapolar basidiomycetes four different reactions can be distinguished upon mating. They include (1) compatible matings between two isolates with different *A* and *B* mating type genes, which is necessary for fruit body formation and spore production; (2) incompatible matings between isolates with identical A and B mating type genes, resulting in growth indistinguishable from the monokaryotic strains; and (3 & 4) two semi compatible mating reactions where the mating type genes of the confronted mycelia differ either in *A* alone (also called a common-*B* reaction) or in *B* alone (also known as common-*A* reaction). Upon plasmogamy, which is observed regardless of mating type, nuclear migration is induced to transport the mate's nuclei throughout the entire mycelium as a prerequisite to nuclear pairing. In a compatible mating, the nuclei pair and perform conjugate divisions forming clamps which ensure the proper distribution of both genetically distinct nuclei in the daughter cells. Karyogamy takes place within the fruit body hymenium immediately before meiosis. If only the *A* factors are different, part of this developmental pathway is switched on. Nuclear pairing and clamp cell formation can be seen only at the mating zone between the two isolates, but clamp cell fusion and nuclear migration are missing. The latter event apparently is under control of the *B* factor as seen in matings of strains different only in *B* (Raper, 1966, Raper, 1983).

1.2 Nuclear migration

After cell fusion, septal breakdown and fast nuclear migration allow reciprocal nuclear exchange between the two mates. After the pairing of the migrant and resident nuclei, dikaryotic hyphal tips are established. Subsequent conjugate nuclear division is accompanied by formation of clamp connections (Fig. 3). Clamp connections are short, backwardly directed branches that fuse with the sub apical cell and provide a bypass for one of the nuclei produced during synchronous division of the dikaryon, ensuring the equal distribution of the two different nuclei between mother and daughter cells. Initiation of conjugate nuclear division is accompanied by formation of a lateral branch, the hook (Schubert*, et al.*, 2006). After nuclear division and septum formation, one nucleus is temporarily entrapped in the hook until the hook cell fuses

with the subapical cell, forming a clamp connection. The hook cell does not fuse with the sub apical cell directly but with a peg formed by the sub apical cell growing toward the hook (Badalyan*, et al.*, 2004). Finally, the entrapped nucleus migrates from the clamp back into the sub apical cell to restore the nuclear pairing. Clamp formation is repeated at each subsequent cellular division (Kniep, 1915).

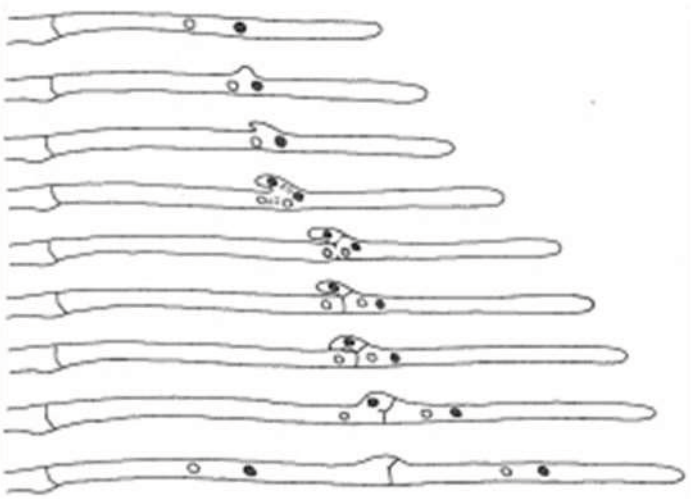

Figure 3: Schematic representation of the formation of clamp connections (Clémençon, 2004). The process begins at a dikaryotic hyphal end cell. Lateral ramifications near the nuclei indicate the commencement of division. The ramification grows backward, opposite in direction to the general growth of the hypha. This is a specialized projection that connects the two adjacent hyphal cells. Then, synchronous nuclear divisions occur with one of the daughter nuclei migration into the clamp cell. The formation of septa occurs facilitating the segregation of two daughter nuclei, one of each mating type, into distinct cellular compartments to prevent the nuclei from falling back and thus, a three-cell state occurs. At this point, the terminal cell is dikaryotic, the subterminal cell and the clamp cell are monokaryotic and form a sexually compatible system. By sexual reaction the clamp cell bends towards the subterminal cell until it touches the hypha. The walls between the tip of the clamp cell and the subterminal cell are lysed and the nucleus in the clamp cell migrates into the subterminal cell. Finally, both nuclear pairs migrate towards the middle of the cells.

There's a paucity of information on the regulation of nuclear dynamics in many basidiomycete mushrooms. The dikaryon stage dominates the life cycles of many basidiomycetes. The receipt of an unknown environmental signal ends the dikaryon stage and triggers rapid karyogamy, meiosis and fruiting body development. The process of dikaryon formation involves nuclear migration and sorting of the nuclei by genotype to ensure that each dikaryon contains a balance of each parental genome. When hyphae of compatible mating types fuse, the nuclei rapidly migrate (for

example, up to 2–3 mm per hour in *S. commune* (Niederpruem, 1980) and a remarkable 4 cm per hour in *Coprinellus congregates* (Ross, 1976) to the distal reaches of the partner mycelium (Raudaskoski, 1998). Distinct from *S. commune,* in *C. cinereus,* the two nuclei alternate in taking the leading and second positions in the apical cell at almost every conjugate division in the dikaryon (Iwasa*, et al.*, 1998). Unlike yeast, filamentous fungi that form dikaryons do not use pheromones to recognize mates extracellularly, as the hyphae will anastomosize regardless of mating type (Gladfelter & Berman, 2009). Nuclei do not initiate migration when cell fusion is with the same mating type, so the rapid increase in motility is triggered by the coexistence of compatible nuclei, as defined by their mating-type loci (Brown & Casselton, 2001).

1.3 Production of secondary metabolites by *S. commune* in co-culture with white-rot fungi

Fungi share important functional roles within ecosystems as nutrient recyclers and decomposers (Johnson*, et al.*, 2005) with wood decay fungi being a major component of woodland ecosystems. The white rot basidiomycetes, are the dominant organisms able to decompose all wood lignocellulose components, both in coniferous softwood and angiosperm hardwoods, including the lignin heteropolymers (Kirk & Farrell, 1987, Eriksson*, et al.*, 1990, Hatakka, 1994). In forest ecosystems, enormous amounts of lignocellulose from dead trees (trunks, litter) is biodegraded mainly by specific basidiomycetous filamentous fungi causing white or brown rot type of decay, a task which is indispensable for the Earth's carbon cycle (Lundell*, et al.*, 2010). In their niche, these fungi interact with competitors which may be other fungi or bacteria also widely distributed in soil and on decaying wood. Thereby, mycelial interactions within fungal communities are believed to have a significant impact on distribution, abundance, indeterminacy and ubiquity (Rayner*, et al.*, 1994).

In order to survive, a fungus must reduce the effect of potential competitors or utilise effective competitive mechanisms. A sizable body of experimental work has investigated the mycelial distributions of confrontations between wood-decay species, usually paired on agar plates (e.g. Rayner & Webber, 1984, White & Boddy, 1992, Rayner*, et al.*, 1994). Interspecific fungal interactions may be mediated at a distance or via contact. The result of these interactions is dependent on species

compatibility and are characterised by physiological responses including cessation of mycelial extension, pigmentation, barrage formation, and increased secretion of phenol oxidases, leading to the premise that fungi possess a ‘recognition’ mechanism that allows them to detect and respond to nonself mycelia (Rayner, 1991, Griffith*, et al.*, 1994, Boddy, 2000). Such mechanisms allow fungi to defend their territories, thereby restricting access to captured nutrients by opposing species (Rayner, 1991, Boddy, 2000).

Wood colonized by white and brown rot fungi can be shown to be occupied by different fungi, each colonizing a discrete zone. These zones often show clear boundaries demarcated by visible black 'zone lines' (Fig 4) where different individuals meet, and antagonistic interactions are common in such encounters (Ueyama, 1966, Rayner & Todd, 1980, Rayner & Todd, 1982, Cooke & Rayner, 1984, Coates & Rayner, 1985, Chapela & Boddy, 1988, Chapela*, et al.*, 1988, Boddy*, et al.*, 1989).

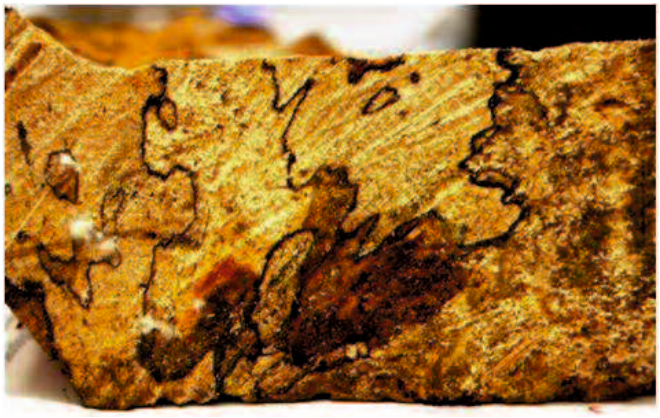

Figure 4: Zone lines on a log of wood colonized by multiple fungi

Trametes versicolor and some other fungi show black demarcation lines by which different species, or incompatible mycelia of the same species separate themselves from each other, or mycelia dissociate themselves from not yet colonized wood. The lines result from fungal phenol oxidases, whereby fungal compounds or also host-own substances are transformed to melanin (Li, 1981, Butin & Lonsdale, 1995). The different interaction types observed in cultures where confrontation assays are performed can be described with 'deadlock' or 'replacement' (Cooke & Rayner, 1984, Rayner & Webber, 1984, Rayner & Boddy, 1988). In 'deadlock', neither species is capable of dominance and a thin zone of uncolonized agar is seen between the

fungal colonies (Cooke & Rayner, 1984, Rayner & Boddy, 1988). The edge of the colony frequently is bordered by a region of dense mycelial growth, proliferating aerial hyphae, or pigment production; in wood, such a 'deadlock' region often shows pigmented zonation (Boddy*, et al.*, 1989). Deadlock often occurs due to each species detecting non-native chemical compound(s) that inhibit growth, although the chemical basis of the myriad of compounds produced and how they are sensed is unclear (White & Boddy, 1992). Replacement may result from one individual completely engulfing the other as a prelude to complete replacement. Replacement may induce autophagy, which promotes degradation and recycling of long-lived proteins and organelles in eukaryotic cells (Yorimitsu & Klionsky, 2005). The key genes of autophagy are also active in filamentous fungi (Pinan-Lucarre*, et al.*, 2005). For the replacement to be successful, the membrane of one of the genetically incompatible colonies will lyse (cellular necrosis), releasing the hyphal content that can subsequently be used by an antagonist (Falconer*, et al.*, 2008).

In an extensive strain collection, pigmented isolates of *Schizophyllum commune* showing blue coloration identified as indigo have been observed. The pigment was first observed in *S. commune* by Papazian (1950) and identified by Miles *et al*. (1956) as indigo. Other blue pigments reported from fungi include lactarazulene described in *Lactarius deliciosus* (Willstaedt, 1935, 1936); thelephoric acid in *Hydnum ferrugineum* and species of *Thelephora* (Kögl*, et al.*, 1930); boletol described in *Boletus luridus* and *B. satanas* (Kögl & Deijs, 1935); and the blue stain of *Ceratostomella* (Cartwright & Findlay, 1946). In order, to understand the interactions of *S. commune* with fungi and bacteria, Hardiman (2012) used the dual culture method on artificial media and wood blocks. This study also investigated extracellular enzymes activity, including laccase, amylase, cellulase, and lipase, during interactions, *S. commune* was found to produce a blue colouration in the interaction zones with different wood-decay fungi and bacteria. Indigo production in *S. commune* can occur by the utilization of nitrogen in the form of ammonium ion (Miles*, et al.*, 1956). The pathway of indigo biosynthesis however, remains elusive. The biosynthetic pathways of indigo synthesis have been well characterized in bacteria. In most cases, indole is first regioselectively hydroxylated by an oxygenase to indoxyl which spontaneously dimerizes to form indigo (McClay*, et al.*, 2005, Royo*, et al.*, 2005, Kwon*, et al.*, 2008). Confrontation assays between *S. commune* and *Trichoderma viride* on synthetic media could show

changes in metabolite profiles, lipid peroxidation, protein carbonylation, and calcium influx as a result of combat in *S. commune* (Ujor*, et al.*, 2012). However, there was no observation of indigoids.

1.4 *S. commune* and Indole-3-acetic acid

The auxin indole-3-acetic acid (IAA), a phytohormone is best known for its role in plant cell elongation, division, and differentiation (Halliday*, et al.*, 2009, Moller & Weijers, 2009, Sundberg & Ostergaard, 2009, Abel & Athanosios, 2010, McSteen, 2010, Scarpella*, et al.*, 2010, Zazímalová*, et al.*, 2010). IAA was first detected by Dolk and Thimman (Dolk & Thimann, 1932) in culture filtrates of the fungus *Rhizopus suinus*, even before IAA was identified in plants. The other fungi include *Rhizoctonia* (Furukawa*, et al.*, 1996), *Colletotrichum* (Robinson*, et al.*, 1998), *Ustilago maydis* (Reineke*, et al.*, 2008) and yeast (Nielsen, 1931, Gruen, 1959). Auxin production was demonstrated for 30 of 34 genera and for 67 (89 per cent) of 75 species of fungi including some varieties of *Fusarium* (Anker, 1949). Microbial IAA plays a significant role in plant–microbe interactions (Glick*, et al.*, 1999), both pathogenic and symbiotic (Hirsch*, et al.*, 1989 , Reineke*, et al.*, 2008). Predominantly a plant hormone, it is not clear how microbes developed the trait of IAA production during their evolution, but it most probably, could have been developed as a signal to manipulate the host metabolic and defense systems, since most microbes producing IAA are plant-associated. Whereas there is convincing evidence to support this hypothesis in bacteria (Spaepen*, et al.*, 2007), where bacterial IAA was shown to modulate plant IAA signaling or host defense responses, the physiological role of fungal IAA in host interaction is still largely speculative (Asiimwe, 2010).

In fungi, IAA has been generally proposed as a metabolite of tryptophan (Hazelwood*, et al.*, 2008) but this has been conclusively demonstrated only in *Ustilago maydis* (Reineke*, et al.*, 2008) and *Saccharomyces uvarum* (Shin*, et al.*, 1991). In most studies, IAA was found in the culture medium but there are also reports on the accumulation of IAA inside the mycelium. External conditions such as light, nitrogen level, pH, temperature and aeration had variable, or no effects on IAA production (Tudzynski & Sharon, 2001). Most fungal species have the capacity to produce IAA and some utilize more than a single biosynthetic pathway. These findings strongly argue for an essential role of IAA in fungi. Two major aspects of auxin action include:

a direct effect on the fungus and a role during fungal infection of plants. Numerous investigations have established the synthesis of IAA by fungi belonging to different taxonomic groups including the basidiomycetes (Gruen, 1959). Most of the reports involve pathogenic fungi, which produce IAA after the addition of tryptophan to the medium. Asiimwe (2010) showed that IAA increased ectomycorrhiza development as observed by significantly higher Hartig' net formation in cultures supplemented with 100 µM IAA. It was suggested that the growth and ramification effects of IAA on *T. vaccinum* observed *in vitro* represented a new mechanism involved in mycorrhiza morphogenesis. Interestingly, the results also suggested that IAA acts as a signal in the fungal-plant interaction in ectomycorrhizal symbiosis.

S. commune has a large number of biochemical and morphological mutants, many of which produce the blue pigment indigo (Raper & Miles, 1958). Epstein and Miles (1967) found that only the indigo-producing mutants produced detectable amounts of IAA which indicated the possibility of a relationship between the formation of IAA and indigo. They could not detect IAA in the non-indigo producing strains that they studied.

1.5 Why Vibrational Spectroscopy?

Breakthroughs in biology often arise from the development of new microscopy tools. Our understanding of biological systems has greatly benefited from the studies with electron microscopy, phase contrast microscopy, confocal fluorescence microscopy, scanning probe microscopy, and other imaging tools (Cheng, 2007). Confocal fluorescence microscopy has been widely used in material and life sciences for submicron level investigations through a fast beam scanning approach, allowing the specific visualization of microscopic structures of the stained molecular composition with chemical specificity (Rigaut & Vassy, 1991). Confocal fluorescence and multiphoton fluorescence microscopy permit 3D imaging of different cellular organelles or specific molecules. However, cells need to be labeled with fluorescent probes, which are prone to photobleaching and perturbations to cell functions (Cheng*, et al.*, 2002). For biomolecular species and cellular components that cannot tolerate fluorescence staining, other complementary contrast mechanisms for non-invasive characterization are used such as phase contrast and differential interference contrast (DIC) microscopy (Allen*, et al.*, 1981, Arnison*, et al.*, 2004).

These rely on the minor differences of the refractive indexes across the sample to highlight small particles and interfaces with index mismatch. However, these techniques are lacking in chemical sensitivity and usually have a low depth resolution (Cheng *et al*. 2002). Vibrational microscopy on the other hand provides a direct way of imaging unstained biological samples, such as cells and tissues with chemical selectivity.

Vibrational spectroscopy facilitates monitoring of bond vibrations as a consequence of interaction of light with the sample. Vibrational spectra are molecule-specific and unique to the nature of the specimen. Importantly, biological materials like proteins, carbohydrates, lipids, nucleic acids, etc. have unique structures and therefore unique spectral fingerprints, which can be obtained for these molecules (Singh*, et al.*, 2012). Vibrational spectroscopic techniques have been useful to understand a wide variety of interesting basic and applied scientific problems, ranging from applications in material characterization to biomedicine due to their fast and non-invasive nature. Vibrational microscopies, such as infrared and Raman microscopy (Kneipp*, et al.*, 1999, Long, 2002, Huang*, et al*., 2003, Ho*, et al*., 2008, Smith & Dent, 2013), have been used for chemically-selective imaging. Chemical imaging can be defined as the analytical capability to create a visual image of components distributed from simultaneous measurement of spectra and spatial information (Kozaris*, et al.*, 2012). Infrared spectroscopy works on the principle that the direct absorption of IR radiation can promote molecules from their vibrational ground state into the first vibrationally excited state. Vibrational transitions can also take place via an inelastic scattering process called the Raman effect which marks an indirect approach to excite molecular vibrations (Popp*, et al.*, 2011). The technical achievements on femtosecond or picosecond pulsed laser sources triggered the rapid development of nonlinear optical microscopy for life science applications (Masters & So, 2008). Recently, coherent anti-Stokes Raman scattering (CARS) imaging has been developed as a useful complementary technique for video-rate vibrational imaging based on the coherently enhanced Raman-active vibrations (Lawrence 2004, (Zumbusch*, et al.*, 1999, Zhu*, et al*., 2009).

1.5.1 Raman Spectroscopy

Sir Chandrashekara Venkata Raman first reported the light-scattering phenomenon in 1928. It has come to be known as the Raman effect for which he was honoured with the Nobel Prize for Physics in 1930. The potential of the Raman effect in chemistry and physics was realized very rapidly (Long, 1988). When light interacts with matter, photons may undergo various processes including absorption, dispersion, reflection, refraction, fluorescence and scattering. If the energy of an incident photon corresponds to the energy gap between the ground state of a molecule and an excited state, the photon may be absorbed and the molecule promoted to a higher state of energy. However, it is also possible for a photon to interact with a molecule in a way that results in scattering. In this case it is not necessary for the photon to have an energy which matches the difference between two energy levels of the molecule. The scattered photons can be observed by collecting light e.g. at an angle to the incident light beam, provided that there is no absorption from any electronic transitions, which have similar energies to that of the incident light. The scattering intensity increases as the fourth power of the frequency of the incident light. Classical Raman spectroscopy uses a single frequency of coherent light to irradiate the sample. The radiation scattered from the molecule, one vibrational unit of energy different from the incident beam, is then detected (Smith & Dent, 2013). Raman scattering does not require matching of the incident radiation to the energy difference between the ground and excited states.

The energy changes we detect in vibrational spectroscopy are those required to cause molecular vibrations. If a distortion of the electron cloud of a molecule is involved in the scattering process, the photons will be scattered with a frequency shift. This scattering process is regarded as elastic scattering and is the dominant process called Rayleigh scattering. However, if molecular vibration is induced during the scattering process, energy will be transferred either from the incident photon to the molecule or from the molecule to the scattered photon. In these cases the process is inelastic and the energy of the scattered photon is different from that of the incident photon by one vibrational unit. This inelastic scattering is usually referred to, as Raman scattering. It is inherently a weak process in that only one in every 10^6–10^8 photons which scatter is inelastically scattered. In itself this does not make the process insensitive since with modern lasers and microscopes, very high photon

densities can be delivered to very small samples, but as a consequence other processes such as sample degradation and fluorescence can readily occur.

1.5.2 Coherent anti-Stokes Raman Scattering (CARS) microscopy

Coherent anti-Stokes Raman scattering (CARS) microscopy provides a unique approach to imaging chemical and biological samples by using molecular vibrations as a contrast mechanism (Duncan*, et al.*, 1982, Zumbusch*, et al.*, 1999). In 1982, Duncan *et al*. reported the first CARS microscope using a non-collinear configuration of pump and Stokes beams to image onion cells with chemical specificity. In 1999, Zumbusch *et al*. demonstrated the first CARS microscope with collinear beam geometry for unstained live bacteria and cell imaging. Soon after, it was proved that in CARS microscopy the interaction length is only several micrometers or less under tightly focusing condition using large NA microscope objectives, thus the phase-mismatching condition can be relaxed within the large cone angle with collinear beam geometry (Cheng*, et al.*, 2001). Unlike spontaneous Raman scattering, CARS is highly sensitive and can be detected in the presence of background fluorescence induced by one-photon excitation (Cheng*, et al.*, 2001). Because of its nonlinear intensity dependence, the CARS signal is only generated at the focus, allowing three-dimensional sectioning of thick samples. This is similar and complementary to two photon fluorescence imaging (Denk*, et al.*, 1990) but requires no fluorophores (Cheng*, et al.*, 2001).

1.5.3 Applications of Vibrational Spectroscopy

Raman and IR techniques are particularly attractive as they provide biochemical information without the requirement of external contrast-inducing agents in comparison to popular instrumental techniques like MRI, PET, X-ray, etc. Compared with conventional methods of microorganism identification, Raman spectroscopy offers a significant time advantage because it can be used without amplification or enhancement steps. Excitation wavelengths in the ultraviolet and visible range were used to enhance signals from chromophores (carotenoids and chlorophyll) in bacteria utilizing the resonance Raman effect (Hering*, et al.*, 2008, Jarvis & Goodacre, 2008). Wide-field illumination and detection enabled imaging of single cells without scanning the laser or moving the sample (Tripathi, 2008). Ayca*, et al.* (2007) used FTIR to study the most common fungal (disseminated candidiasis) infection in hospitalized

patients using the mice model. The study revealed that the infection resulted in changes mainly in lipid profile (ratio of the saturated lipids to unsaturated lipids) and also caused lipid peroxidation. Edwards*, et al.* (1995) reported Fourier transform (FT) Raman spectra of the cell walls of three species of *Agaricus bisporus*, *Mortierella* genus and *Mucor* genus and proposed molecular assignments for the major vibrations attributed to chitin, *N*-acetyl glucosamine and (*R*)-glucan. Ghosal*, et al.* (2012) applied RMS for rapid characterization and identification of individual spores from several species of microfungi which has been used to compile a reference library of Raman spectra from several species of microfungi, typically associated with damp indoor environments. De Gussem*, et al.* (2005) reported for the first time the Raman spectra of spores of *Lactarius controversus* Pers. Fr., *Lactarius lacunarum* (Romagn.) ex *Hora*, *Lactarius quieticolor Romagn*. and *Lactarius quietus* Fr. These spectra were compared with the Raman spectra of substances known to occur in macrofungi, including saccharides, lipids and some minor compounds that may serve as specific biomarkers (adenine, ergosterol and glycine). In addition to different types of lipids and phospholipids, the polysaccharides chitin and amylopectin could be detected as well. The combination of Raman spectroscopy with chemometrical methods was capable of identifying spores of macrofungi/basidiomycetes (Gussem*, et al.*, 2007). Raman and surface enhanced Raman scattering (SERS) maps of *Aspergillus nidulans* hyphae grown on nanostructured gold-coated substrates have been recorded (Szeghalmi*, et al.*, 2007). Furthermore vibrational spectroscopy has been used to study the chemical compounds involved in cell differentiation of *S. commune* (Kawai*, et al.*, 1985, 1986) or which are produced by *S. commune* itself (Yamashita*, et al.*, 1985). In addition, vibrational spectroscopic characterization of fruiting bodies (Mohaček-Grošev*, et al.*, 2001) and Raman spectroscopical studies of fungi and spores (De Gussem*, et al.*, 2005, Stöckel*, et al.*, 2009) have been carried out. *S. commune* has been detected in wood and discriminated from another wood decaying fungal species by FTIR spectroscopy (Naumann*, et al.*, 2005) and a classification at strain level was achieved (Naumann, 2009). Raman and NIR Raman spectroscopy were used to characterize natural dyes produced by fungi (Li-Chan, 1996, Schrader*, et al.*, 1999). The cytochrome distribution in hyphal tip cells and branching regions of *S. commune* was visualized using resonance Raman mapping and CARS microscopy by Walter*, et al.* (2010). To date most biological applications of CARS have dealt with the investigation of lipids that play an important role in

biological membranes, as energy storage molecules, and as messengers in cellular communications. Lipids are comparatively easy to detect in cells by CARS microscopy due to their high local concentration and their high CH stretching vibration signal. The significance of CARS in single cell studies is expected to gain momentum in the near future due to the rapid acquisition, high spatial resolution and three-dimensional imaging capabilities (Krafft*, et al.*, 2009).

1.6 Mass spectrometry

John B. Fenn, the originator of electrospray ionization for biomolecules and the 2002 Nobel Laureate in Chemistry, probably gave the most fitting explanation for what mass spectrometry is: *"Mass spectrometry is the art of measuring atoms and molecules to determine their molecular weight. To practice this art one puts charge on the molecules of interest, i.e., the analyte, then measures how the trajectories of the resulting ions respond in vacuum to various combinations of electric and magnetic fields. Clearly, the sine qua non of such a method is the conversion of neutral analyte molecules into ions. For small and simple species the ionization is readily carried by gas-phase encounters between the neutral molecules and electrons, photons, or other ions."*

Genomics, proteomics, and metabolomics increasingly require the analysis of extremely complex mixtures, such as whole-cell lysates, and detection of analytes of a wide variety of types over a wide range of concentrations—from hormones and growth regulators present at pmole/L levels to ubiquitous as well as rare low copy number proteins. These challenges increasingly demand instruments with better performance characteristics including resolution, mass accuracy and dynamic range (Hu*, et al.*, 2005). In addition, tandem mass spectrometry (MS/MS) (Cooks*, et al.*, 1973, McLafferty, 1980, 1981, Holmes, 1984, Busch*, et al.*, 1988, de Hoffmann, 1996) serves as a requisite and invaluable tool for structure elucidation and peptide/protein sequencing (Hunt*, et al.*, 1986, Biemann & Scoble, 1987, Biemann, 1990). Mass spectrometric analysis of complex mixtures for particular analytes is often facilitated by tandem or multiple stage mass spectrometry (MSn) as well as by high resolution/ high-mass accuracy measurements. Mass spectrometry determines the mass-to-charge (*m/z*) ratio or a property related to *m/z*. A mass spectrum is a plot of ion intensity versus *m/z*. (Glish & Vachet, 2003)

1.3.1 Electrospray ionization (ESI)

Electrospray ionization - mass spectrometry (ESI-MS) provides a sensitive, robust, and reliable tool for studying, at femto-mole quantities in micro-litre sample volumes, non-volatile and thermally labile bio-molecules that are not amenable to analysis by other conventional techniques (Ho*, et al.*, 2003). Ions in ESI are generated at atmospheric pressure by passing a solution-based sample through a small capillary (internal diameter < 250 µm) that is at a potential difference relative to a counter electrode at voltages between +500 and +4,500 V. The actual voltage required depends on both the inner diameter of the needle and the solvents that make up the solution (Glish & Vachet, 2003)

1.3.2 Nanoelectrospray ionization using TriVersa NanoMate® technology

The TriVersa NanoMate is the latest in chip-based electrospray ionization technology. It combines the strengths of liquid chromatography, mass spectrometry, chip-based infusion, fraction collection, and direct surface analysis into one integrated system (www.advion.com). It allows analysts to obtain more information from complex samples than with LC/MS alone. It consists of the ESI chip which is a microfluidics chip containing an array of 400 nanoelectrospray emitters each one-fifth the diameter of a human hair, etched in a silicon wafer allowing for flow rates of 20 to 300 nL/min. The nozzles on the ESI Chip provide a long, efficient and stable spray with no sample-to-sample carryover. The TriVersa NanoMate can accomplish direct analysis of a sample using liquid extraction surface analysis (LESA). LESA can be used for discrete or consecutive spots as a profiling tool for a variety of samples like food for the detection of applied pesticides (Eikel & Henion, 2011), polymer coating additives and degradation products (Paine*, et al.*, 2012), and sensitive qualitative and quantitative (with internal standard) analysis of a variety of samples from solid phase extraction cards (Walworth*, et al.*, 2011). LESA in combination with high-resolution mass spectrometry can be used e.g., as a powerful tool to extract and detect bacterial antibiotics directly from spots of agar plates (Kai*, et al.*, 2012).

1.3.3 Mass spectrometric analysis using OrbitrapXL-MS

An orbitrap is a type of mass analyzer invented by Alexander Makarov. It consists of an outer barrel-like electrode and a coaxial inner spindle-like electrode that form an

electrostatic field with quadro-logarithmic potential distribution (Makarov, 2000, Hu*, et al.*, 2005). Image current from dynamically trapped ions is detected, digitized and converted using Fourier transform into frequency and then mass spectra. The orbitrap is the first new mass analyzer to be introduced as a commercial instrument (LTQ-Orbitrap hybrid mass spectrometers) in the last 20 years (Perry*, et al.*, 2008). It has become a powerful addition to the arsenal of mass spectrometric techniques for probing biological systems as well as increasing selectivity and confidence of routine analyses. The most prominent features of the Orbitrap include high mass resolution (up to 150 000), large space charge capacity, high mass accuracy (2–5 ppm), a mass/charge range of at least 6000, and dynamic range greater than 10 (Hu*, et al.*, 2005). Analytical performance of the trap can support a wide range of applications from routine compound identification to the analysis of trace-level components in complex mixtures, for example, in proteomics, drug metabolism, doping control, and detection of contaminants in food and feed (Zubarev & Makarov, 2013).

1.4 Research Objectives

A. Non invasive real-time imaging of nuclear migration in *S. commune*

The common techniques used to visualize the nuclei in fungi include fluorescence staining with DNA stains such as DAPI (4', 6-diamidino-2-phenylindole) and Hoechst 33258 (bis-benzimides). These stains are DNA-specific probes which interfere with replication gradually killing the cells, their cytotoxicity thus influencing the outcome of the experiments. In view of these caveats of DAPI/Hoechst DNA dyes, fluorescence microscopy is not favoured. As an alternative, chemical imaging is employed using vibrational spectroscopy to monitor the nuclear dynamics process *in vivo*. Thus, one focus of this study was to chemically image the process of nuclear migration and sorting in *S. commune* live *in vivo* with Raman spectroscopy and CARS microscopy. If successful, this will also set the experimental conditions for investigations of dikaryon formation in basidiomycete fungi showing no clamp formation, like *Tricholoma*.

B. Identification of secondary metabolites produced by *S. commune* upon interaction with wood rotting fungi

Previous studies by Hardiman (2012), have shown that *S. commune* secretes compounds in response to interactions with certain wood-rotting fungi and some antagonistic organisms in artificial media. The nature of these compounds and their biological activity was unknown, and thereby were of interest as they might have potentially anti-microbial properties. This study, therefore involves the identification of these compounds. On an ecological note, our study will give a greater insight into the working of the metabolite pathways involved in the various reactions that occur during fungal interactions. Of equal importance is the application of advanced analytical tools in the field of secondary fungal metabolites. To this end, we will use Raman micro-spectroscopy and mass spectrometry – based tool LESA, in order to quickly, efficiently and non-invasively identify, image and quantify the compounds present.

C. Identification of an auxin by wild type *S. commune* strains and monitoring its changes in fungal interactions in co-culture

It was reported that the mutant strains of *S. commune* producing indigo also synthesized IAA, and it was postulated that there may be a correlation between them in terms of synthesis. Thus, we conducted experiments with a pigmented mutant and quantified the amounts of indigo and IAA excreted into the media. It was also of interest to see if wild type *S. commune* synthesized auxins and if these auxins were influenced during interactions. We also seek to quantify the IAA and study aspects of its biosynthesis. We would like to monitor the changes in IAA concentration when *S. commune* is grown alongside antagonistic organisms. Because of the lack of basic knowledge, a study of the biosynthesis and the role of IAA in this organism is of interest.

2. Material and methods

2.1 Media and cultivation of *S. commune* for nuclear migration studies

S. commune 12-43 x 4-39, 12-43, 4-39 and F15 x F28 were cultured at 28 ^{o}C for 3–6 days on solid medium (CYM). For microscopic analysis, sterile objective slides, glass cover slips (for fluorescence microscopy), and calcium fluoride slides (for Raman microspectroscopy) were placed on an agar plate, such that the mycelium could attach and grow onto the slides. After 2–3 days at 28 ^{o}C, mycelium of *S. commune* grew over the slide with a monolayered growth front. For the Raman spectroscopy, the CaF_2 slide was removed directly before the measurements and kept under room conditions during the spectroscopic analysis.

2.2 Composition of media

Complex yeast medium (CYM) (Schwalb & Miles, 1967): 20 g/L glucose, 2 g/L trypticase peptone, 2 g/L yeast extract, 1 g/L K_2HPO_4, 0.5 g/L $MgSO_4$, 0.46 g/L KH_2PO_4, 18 g/L agar-agar (for solid medium).

CYM-T: CYM medium with 0.25 mM tryptophan

Potato dextrose agar (PDA): 0.4% potato extract, 2% glucose, and 1.5% agar (Merck, Germany)

Minimal Media (MM) (Raper & Hoffman, 1974): 20 g/L glucose, 2 g/L aspartic acid, 1 g/L K_2HPO_4,0.5 g/L $MgSO_4$, 0.46 g/L KH_2 PO_4, 120 µ g/L thiamin hydrochloride, pH 6.3, 18 g/L agar-agar (for solid medium).

MMNb (Modified Melin-Nokrans Medium) (Kottke*, et al.*, 1987): 0.05 g/L $CaCl_2$, 0.025 g/L NaCl, 0.5 g/L KH_2PO_4, 0.25 g/L $(NH_4)_2$ HPO_4, 1 µ g/L $FeCl_3.6H_2O$, 83 µl Thiamin hydrochloride (1.2 mg/ml), 0.15 g/L $MgSO_4$. 7 H_2O, 0.5 g/L Glucose, 1 g/L Peptone from Casein, 10 ml/L trace element solution (Fortin & Piche, 1979)

MMNb-T: MMNb medium with 0.25 mM tryptophan

2.3 Fungal cultures used in interaction studies

In order to analyse the metabolites produced during interactions S. commune strains were grown alongside other white and brown rot fungi on culture medium. The *Schizophyllum commune* strains used were12-43 x 4-39[2] (FSU2896 x FSU3214[3]), 12-43[2] (FSU3214[3]), 4-39[2] (FSU2896[3]) (Vermont, USA); *Schizophyllum commune* strains MG101028_06[1], F15[2], F15xF28[2] (Jena, Germany). The other fungal candidates included *Flammulina velutipes* MG091201_01[1] (Jena, Germany); *Ganoderma lucidum* MG100717_01[1] (Königsfeld, Germany); *Hypholoma fasciculare* MG100907_06[1] (Kauern, Germany); *Kuehneromyces mutabilis* MG091108_02[1] (FSU9992[3]) (Göttingen, Germany); *Pleurotus ostreatus* MG091105_01[1] (FSU9962[3]) (Jenaprießnitz, Germany) and *Serpula lacrymans* FSU2886[3] (Jena, Germany).

[1] Dr. Matthias Gube, Microbial Communication, University of Jena

[2] Strain collection of Microbial Communication, University of Jena

[3] Jena Microbial Resource Collection, University of Jena

2.3.1 Confrontation assays

One week-old cultures of wild-type *Schizophyllum commune* and each fungal candidate were cut into 0.5 cm agar cubes and placed 2 cm apart on the surface of CYM and PDA, and then incubated at 28 ^{o}C and 10 ^{o}C for 1 month. Plates inoculated with pure cultures of each fungus and incubated at the same conditions as the experimental cultures served as controls. Identical plates were made for IAA analysis. The plates were observed directly under a light microscope (Zeiss Axioplan 2, Jena, Germany). For sample preparation for Raman microspectroscopic measurements, 0.5 x 0.5 x 0.25 mm cubes of agar with hyphal mat were cut out from the interaction zones of the culture plates and placed on CaF_2 objective slides. The sample was trimmed in dimensions (if necessary) to accommodate it within the working distance of the microscope objective.

2.3.2 Metabolite extraction

From the co-culture plates, 4 x 1 x 0.3 cm mycelial strips were cut out from the interaction zone, and from the periphery of *S. commune* and *H. fasciculare* zones respectively. Each sample was added into a 1:1 (2 ml each) mixture of methanol:ethyl acetate and macerated. They were then ultra sonicated for 30 min and centrifuged at 10,000 rpm for 3 min. 500 µl of the clear supernatant was

retrieved and added to an equal amount of methanol along with 2 µl of 10 mM indole-3-propionic acid (internal standard). This mixture was vortexed for 30 s and allowed to stand for 30 min. It was then diluted 1:4 in methanol.

2.4 Fungal cultivation for auxin identification and quantification

In order to test the production of IAA in *S. commune* cultures, 2 x 2 cm agar cubes of the monokaryon 12-43 and dikaryon 12-43 x 4-39 were macerated and inoculated into 200 ml of liquid CYM with shaking (150 rpm) at 28 ^{o}C for 20 days. For quantification of IAA and comparison of its production with regard to different media, four liquid media were used: CYM, CYM-T, MMNb and MMNb-T. 2 x 2 cm agar cubes of 12-43 were macerated and inoculated into the 100 ml of media. These flasks were incubated for 28 ^{o}C with shaking (150 rpm) for 28 days. The tryptophan (0.25 mM) in CYM-T and MMNb-T was added after the seventh day. 2ml was retrieved from each culture filtrate every seven days for four weeks. These filtrates were immediately subjected to the extraction procedure. For sample preparation, 500 µl of methanol (hypergrade for LC MS, Merck KGaA, Darmstadt, Germany) was added to an equal amount of the filtered test culture broth and 2 µl of 10mM indole-3-propionic acid which was used an internal standard. This mixture was shortly agitated using a vortex, then incubated for 30 minutes at room temperature and further diluted 1:4 in methanol. 15 µl of the diluted extract was injected into the UHPLC binary solvent system of water (solvent A) and acetonitrile (solvent B, hypergrade for LC MS, Merck KGaA, Darmstadt, Germany), both containing 0.1% (v/v) formic acid (eluent additive for LC-MS, Sigma Aldrich Chemie GmbH, Steinheim, Germany).

2.5 Microscopy

In order to stain the nuclei of *S. commune*, fluorescent stains DAPI (4', 6-Diamidin-2'phenylindol-dihydrochloride) (0.1-1 µg/ml) and Hoescht 33258 (10 mg/ml stock solution) stains were used. DAPI preferentially binds to A-T rich regions (Loontiens, *et al*., 1990), and has the maxima of absorption and emission at ±350 and ±460 nm, respectively. Hoechst 33258 has the maxima of excitation and emission at ±352 and ±461 nm, respectively. The stain was added to the fungal sample under the cover slip and observed immediately.

Microscopy was carried out with an Axioplan 2 microscope (Carl Zeiss, Jena, Germany) using Filter set 02 for the nuclear staining. Differential interference contrast

(DIC) is another method of deriving contrast in an unstained specimen from differences in index of refraction of specimen components. As with phase contrast, DIC transforms the phase shift of light, induced by the specimen refractive index, into detectable amplitude differences. An advantage of interference-derived contrast is that an object will appear bright against a dark background but without the diffraction halo associated with phase contrast. However, because DIC utilizes optical path differences within the specimen (*i.e.*: product of refractive index and geometric path length) to generate contrast the three-dimensional appearance may not represent reality (Ruzin, 1999). Documentation was achieved with a digital camera (Insight Firewire 4 image sample, Diagnostic Instruments, Sterling Heights) and analyzed by the software Spot (version 4.6, Diagnostic Instruments, Sterling Heights).

2.6 Raman Microspectroscopy

Raman spectra were acquired using a WITec (Ulm, Germany) CRM Alpha-300Rplus confocal Raman microscope. Excitation (ca. 10 mW at the sample) was provided by 785 nm diode laser (TOPTICA Photonics AG). The exciting laser radiation is coupled into a Zeiss microscope through a wavelength-specific single mode optical fiber. The incident laser beam is collimated *via* an achromatic lens and passes a holographic band pass filter before it is focused onto the sample through the objective of the microscope. A Zeiss 50x/0.9 NA objective was used in the studies reported here. The sample is located on a piezo-electrically driven microscope scanning stage with an *x,y*-resolution of about 3 nm and a repeatability of ±5 nm, and *z*-resolution of about 0.3 nm and ±2 nm repeatability. The sample is scanned through the laser focus in a continuous line scan at a constant stage speed of fractions of a micrometer per second. Spectra are collected with a 0.33 µm step size and an illumination time of 3 s, using a 300/mm grating. The spectral resolution is about 6 cm^{-1} and the spectral window ranges from 300 to 3200 cm^{-1}. False color images were reconstructed using a spectral unmixing algorithm based on vertex component analysis (VCA), which decomposes a given dataset into fractions of most dissimilar spectral information (Miljkovic*, et al.*, 2010, Hedegaard*, et al.*, 2011).

The Raman spectrum of indigotin, isatin and indirubin (Sigma Aldrich, Taufkirchen, Germany) were obtained as references. Spectra were processed using the CytoSpec (Berlin, Germany) v. 1.4.00, Software for hyperspectral imaging as well as the MATLAB (Mathworks Inc.) software.

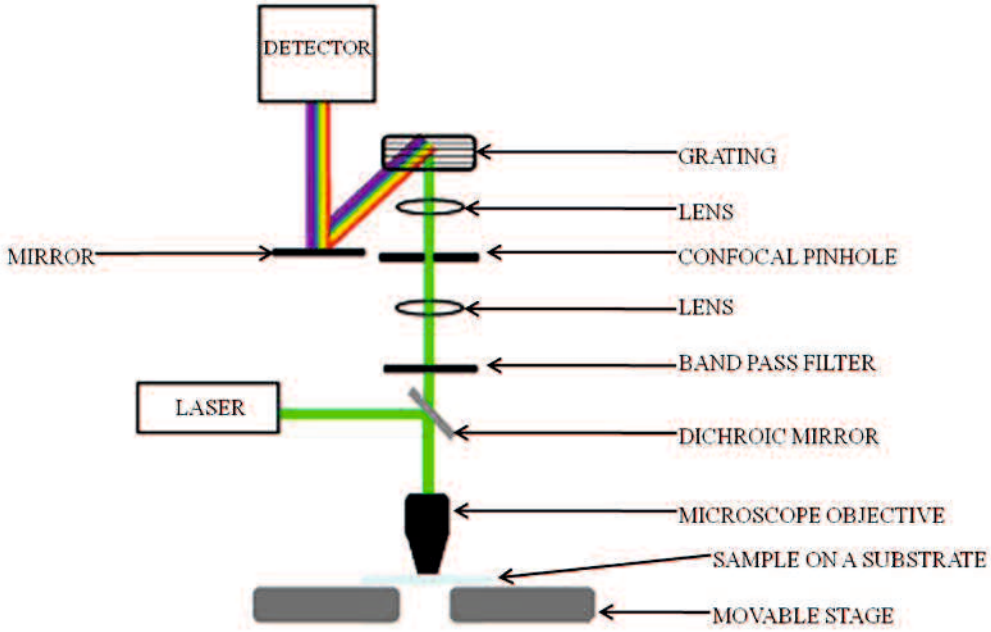

Figure 5: Instrumentation for a micro-Raman spectroscopy set-up to conduct sample imaging. The collimated laser light is directed through a dichroic mirror with appropriate wavelength selection and is focused through a microscope objective onto the sample. The backscattered light is collected through the objective and after filtering with either a notch or a bandpass filter to suppress the elastically scattered signal, the light is transmitted through the confocal pinhole into the spectrometer. The signal is then directed onto a grating which disperses the light and eventually guided onto the detector to collect the Raman spectrum.

For intensity plots of the Raman maps, the spectra were baseline corrected and approximated by linear segments with manually chosen points. For sample preparation, 0.5 x 0.5 x 0.3 cm^3 cubes of agar with hyphal mat were cut out from the interaction zones of the culture plates and placed on CaF_2 objective slides for Raman micro-spectroscopic measurements. The samples were trimmed in dimensions (if necessary) to accommodate it within the working distance of the microscope objective.

2.6.1. Image analysis and data processing

Various algorithms for image analysis of hyperspectral datasets have been developed. For extracting spectral information, several factor methods such as principle component analysis (PCA) or vector component analysis (VCA) have shown high potential for the evaluation of Raman datasets (Miljković*, et al.*, 2010, Hedegaard*, et al.*, 2011) In principle, these algorithms search for a basis that

describes the spectral variance optimally. Generally, the spectrum of a given image pixel is assumed to be a linear combination of the spectra of individual components:

$$p_{ij} = \sum_k e_{ik} c_{kj} ,$$

where p_{ij} is the i-th band of the j-th pixel, e_{ik} the i-th band of the k-th component spectrum and c_{kj} is the mixing proportion for the j-th pixel of the k-th component. The mixing proportions are assumed to be percentages and the proportions should add up to one:

$$\sum_k c_{kj} = 1 .$$

This new basis then consists of a few vectors, or in our case Raman spectra, which can be used to reconstruct the dataset or image by plotting their individual abundances. The different algorithms vary mainly in what constraints are set for this change of basis. In PCA, for instance, the vectors have to be orthogonal. In VCA the constraint is that the new vectors, usually referred to as endmembers, have to be all positive or real spectra. These endmembers normally represent the most dissimilar spectra within a dataset. For the evaluation of the endmembers the N-FINDR algorithm, described by Winter was employed (Winter, 1999, Du*, et al.*, 2008).

2.7 Coherent anti-Stokes Raman scattering (CARS) microscopy

The CARS microscopy setup used was described previously by Meyer*, et al.* (2008). The Ti:sapphire laser source was configured to generate pulses of 3 picoseconds in length. For these experiments, the Stokes beam was set to 831 nm and the pump beam at 669.5 nm for a Raman shift of 2900 cm^{-1}, and 671.35 nm for a Raman shift 2850 cm^{-1}. The laser radiation was focused into the object plane by a 63X NA 1.4 oil immersion objective (Zeiss Plan-Apochromat). The CARS signal was collected in the forward direction (F-CARS) by an NA 0.55 condenser, separated from the residual pump and Stokes light by filters (colored glass and Omega optics third millennium short pass filters), and detected by photomultipliers (Hamamatsu R6357). CARS is a coherent process; hence the signal is directional and laser-like. By tuning the difference frequency of the two lasers to Raman modes characteristic for different molecules present in the emulsion, the distribution of these molecular species can be imaged. The relevant Raman modes are chosen via nonresonant linear Raman spectroscopic measurements.

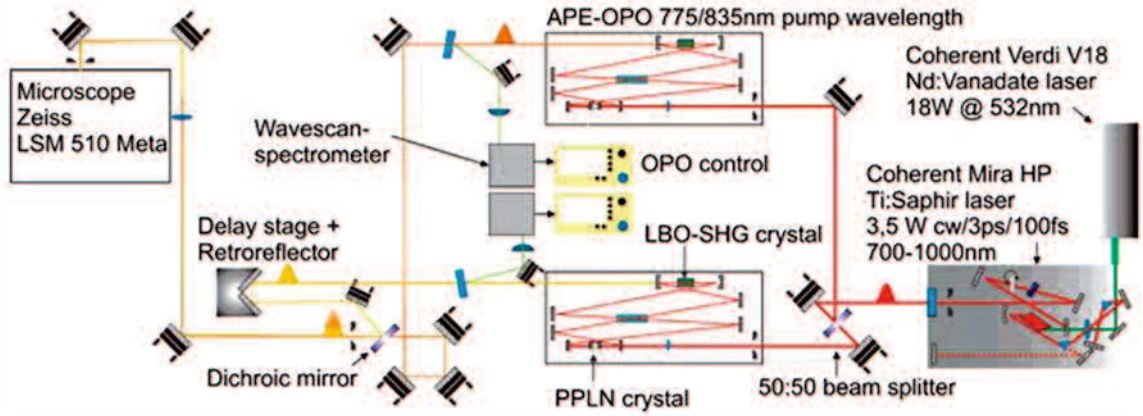

Figure 6: Scheme of the CARS microscopy setup. (Meyer *et al.* 2008)

The coverslips inoculated with the fungi were loaded onto a microscope slide, and measurements were carried out without further sample preparation. By tightly focused laser beams the CARS process generates a signal at the anti-Stokes frequency from a small volume and therefore providing high spatial resolution and three-dimensional sectioning capabilities. The electronic subsystem of the molecule is a source for the non resonant CARS signal, which has no chemical bond selectivity and limits the contrast.

2.8 Mass spectrometry with LESA-MS/MS and UHPLC-ESI-MS/MS

2.8.1 Liquid extraction surface analysis (LESA)

The liquid extraction surface analysis is an adaptation of the Nanomate robotic pipet chip-based infusion nanoESIsystem (Fig 7 A,B) (Kertesz & Van Berkel, 2010, Marshall*, et al*., 2010). It combines microliquid extraction from a solid surface with nanoelectrospray mass spectrometry. LESA is fully automated using disposable pipet tips creating liquid micro junctions (LMJs) with spatial resolutions of ±1 mm, and single-use nanoESI nozzles eliminating spot-to-spot sample carryover. Briefly, a robotic arm picks up a conductive pipet tip and moves the tip to a position above a specific well containing the extraction solvent, which is aspirated by lowering the pipet tip. Then the latter is positioned above the surface spot to be sampled and a liquid junction is created between the tip and the surface by dispensing a specific volume of the extraction solvent. Subsequently, the solution containing the dissolved sample is aspirated back into the tip, and is sprayed through a nanospray nozzle at flow rates of 20−500 nL min^{-1} for mass spectrometric analysis. The nanoelectrospray

is initiated by applying the appropriate high voltage to the pipet tip and gas pressure on the liquid.

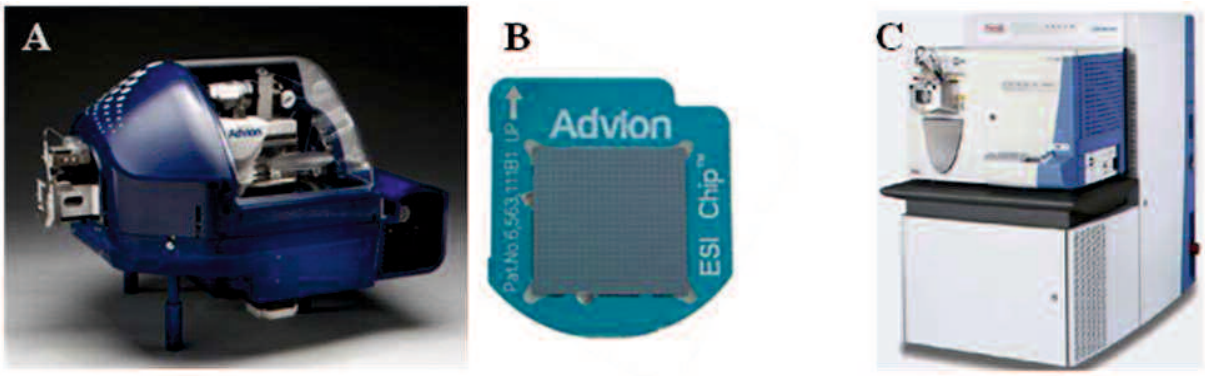

Figure 7: (A) LESA - Liquid Extraction Surface Analysis using Triversa NanoMate technology (B) TriVersa NanoMate® ESI Chip® (C) LTQ-OrbitrapXL

Liquid extraction surface analysis (LESA) was performed using Triversa Nanomate technology (Advion, Ithaca, NY, USA). For LESA, the confrontation zone on assay plates was directly extracted with 2 µl ethyl acetate in the Nanomate. After 8 s extraction time, 2.2 µl of solvent was aspirated and this extract was further ionized by nanoelectrospray using a voltage of 2 kV at a gas pressure of 0.5 psi.

2.8.2 Ultra-high performance liquid chromatography-electrospray ionization-tandem mass spectrometry (UHPLC-ESI-MS/MS) using the Orbitrap mass analyser

The Orbitrap mass analyzer (Fig 7C) consists essentially of three electrodes. Outer electrodes have the shape of cups facing each other and electrically isolated by a hair-thin gap secured by a central ring made of a dielectric. A spindle-like central electrode holds the trap together and aligns it via dielectric end-spacers. When voltage is applied between the outer and the central electrodes, the resulting electric field is strictly linear along the axis and thus oscillations along this direction will be purely harmonic. At the same time, the radial component of the field strongly attracts ions to the central electrode. Ions are injected into the volume between the central and outer electrodes essentially along a tangent through a specially machined slot with a compensation electrode (a “deflector”) in one of the outer electrodes. With voltage applied between the central and outer electrodes, a radial electric field bends the ion trajectory toward the central electrode while tangential velocity creates an opposing centrifugal force. With a correct choice of parameters, the ions remain on a

nearly circular spiral inside the trap, much like a planet in the solar system. At the same time, the axial electric field caused by the special conical shape of electrodes pushes ions toward the widest part of the trap initiating harmonic axial oscillations. Outer electrodes are then used as receiver plates for image current detection of these axial oscillations. The digitized image current in the time domain is Fourier-transformed into the frequency domain and then converted into a mass spectrum (Zubarev & Makarov, 2013).

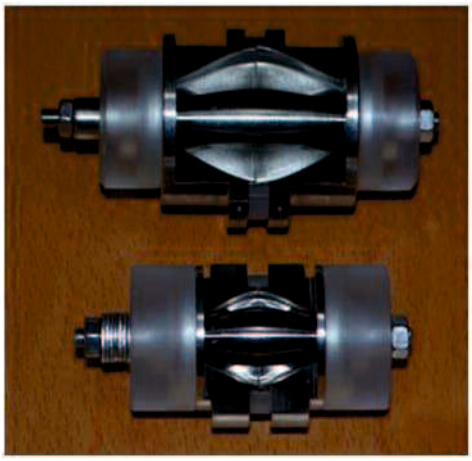

Figure 8: Cut-outs of a standard (top) and a high-field (bottom) Orbitrap analyzer. Copyright 2012 Thermo Fisher Scientific.

Methanol (gradient grade), and ethyl acetate (≥99%) were supplied by Sigma-Aldrich (St. Louis, USA). The water used in this work was UHPLC grade LC-MS Ultra CHROMASOLV® (Sigma-Aldrich Chemie GmbH, Taufkirchen, Germany). Standards of indole-3-acetic acid (>99%), indole-3-pyruvic acid (99%), L-tryptophan, indole-3-acetamide, tryptamine, indole-3-lactic acid and indole-3-propionic acid (99%) were purchased from Sigma-Aldrich Chemie GmbH (Taufkirchen, Germany). Indole-3-propionic acid was used as internal standard for the quantification of IAA. Stock solutions of the individual standards at a concentration of 10mM were prepared by dissolving the compounds in methanol and were stored at 4◦C. Working solutions of all the standards were prepared immediately before analyses by diluting the stock solution with mobile phase, to attain the required concentrations for calibration measurements.

Ultra-high-performance liquid chromatography–electrospray ionisation–tandem mass spectrometry (UHPLC-ESI-MS/MS) was performed with the diluted extract (see

metabolite extraction) using the Ultimate 3000 series RSLC (Dionex, Sunnyvale, CA, USA) system coupled to the Orbitrap XL mass spectrometer (Thermo Fisher Scientific, Bremen, Germany) equipped with an ESI source. 15 µl of the extract was injected into the UHPLC binary solvent system of water (solvent A) and acetonitrile (solvent B, hypergrade for LC MS, Merck, Darmstadt, Germany), both containing 0.1% (v/v) formic acid (eluent additive for LC-MS, Sigma Aldrich, Steinheim, Germany). Chromatographic separation was achieved using an Acclaim C18 Column (150×2.1 mm, 2.2 µm; Dionex, Sunnyvale, CA, USA) at a constant flow rate of 300 µl min^{-1} as follows: 0.5–10% (v/v) B (10 min), 10–80% B (4 min), 80% B (5 min), 80-0.5% (v/v) B (0.1 min), 0.5% B (6 min). ESI source parameters were set to 35 V for capillary voltage, 4 kV for spray voltage and 275°C for capillary temperature.

The samples were measured in positive ion mode in the range of *m/z* 50–1200 using the Orbitrap analyzer. Full scan mass spectra were generated using 30,000 m/Δm resolving power. Tandem mass spectra were acquired using collision induced dissociation in the LTQ trap with relative collision energies of 15, 25 and 35 % at 7500 m/Δm resolving power. Data interpretation was accomplished using XCALIBUR (Thermo Fisher Scientific, Waltham, MA, USA). In addition to mass of precursors, fragmentation patterns as well as retention time (UHPLC) were compared to those of reference compounds. Quantification was performed using calibration curves of reference compounds and the internal standard indole-3-propionic acid.

3. Results

3.1 Visualization of nuclei using fluorescence microscopy

Microscopic inspection of fungi revealed that central regions of tip hyphae showed more vacuoles and the nucleus is approximately located in the middle of the cell, while the length of the hyphal tip cell is bounded by the first septum. In branching regions, typical for subapical regions, vesicles and mitochondria are accumulated.

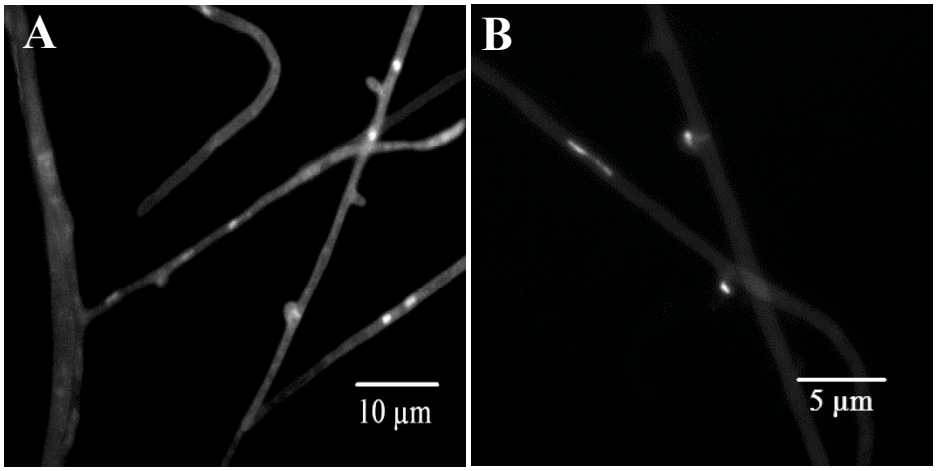

Figure 9: Nuclei seen in various stages of the cell cycle (A) 12-43x4-39 stained with DAPI (B) 12-43x4-39 stained with Hoechst 33258

Within the fungal cells an inhomogeneous distribution of cell components was observed. The chemical composition of filamentous cells varies due to the different functions of the hyphal section (Walter *et al.* 2010). In order to visualize the nuclei and distinguish them from other organelles, slides of young *S. commune* cultures were stained with nuclear stain DAPI and Hoechst 33258. Thus, nuclei could be observed in various stages of the cell cycle as seen in Fig. 9. Interphase nuclei were found to be elongated and thread-like. In some cases (Fig 9B), nuclei could be seen within unfused clamp cells, still in the process of formation. The nuclei were about 1 µm in diameter. Since staining with a nuclear stain halts any cell and nuclear division thus killing the cell, microscopy using differential interference contrast (DIC) and phase contrast was used to view them live and in motion. However, on merging the fluorescent stained cell and the DIC image of the same frame, it was observed that the location of the nuclei could not be observed or predicted (Fig 10). Vacuoles could be observed well with DIC, but they were not to be confused with nuclei. The

septum in filamentous fungi develops at the site that has previously been occupied by the dividing nuclei (Jersild, *et al.*, 1967, Trinci, 1978), particularly at the site occupied during the metaphase (Bourett & McLaughlin, 1986).

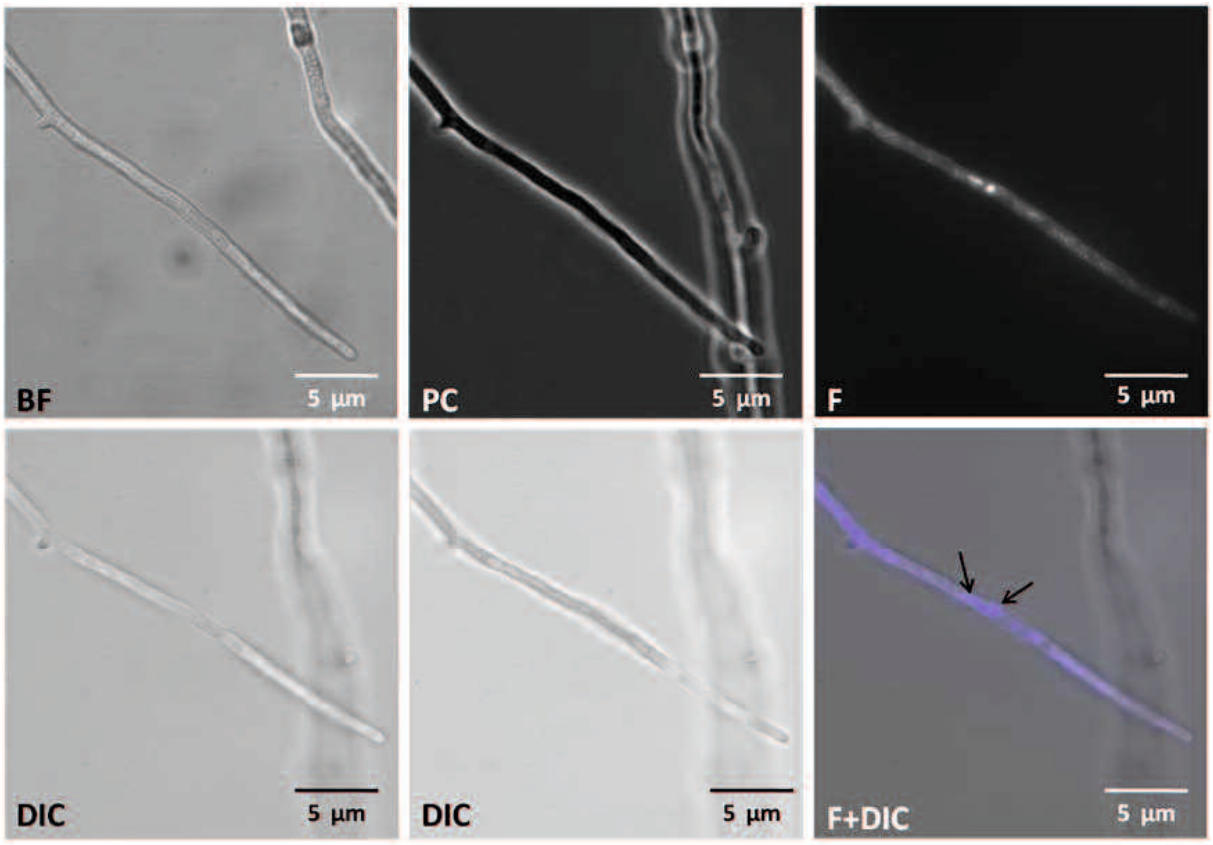

Figure 10: Images of *S. commune* 12-43x4-39 hypha. BF (bright field), PC (phase contrast), F (stained with DAPI), DIC (differential interference contrast), and F+DIC (merged DAPI and DIC image)

3.2 Raman and CARS microscopy of *S. commune* hyphae

Raman microscopic images were obtained from individual hyphae. Figure 11A shows a microscopic image of a typical *S. commune* hypha grown under normal, not competing, conditions. The resulting Raman image 11B was reconstructed by plotting the integrated scattering intensities of the CH stretching vibrations of the hypha components. The Raman image in 11C was generated by a spectral unmixing algorithm that decomposes the dataset into representative spectra and their individual abundance within the dataset. The associated spectral information is shown in 11D plots a and b. Both spectra show mainly Raman bands that are characteristic for glycogen or polysaccharides in general and proteins. Reference spectra for glycogen and a protein (albumin) are plotted in c and d.The cell wall of

S. commune is made up of N-acetyl-glucosamine and glucose residues, which occur in the in a polymerized form as chitin and glucans (Wang & Miles, 1966). In addition various structural proteins support the hyphae.

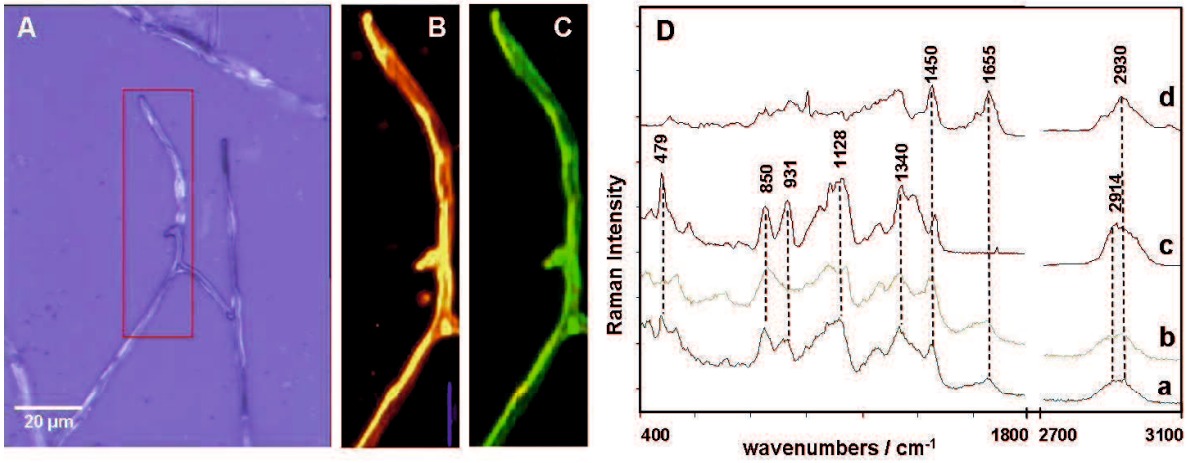

Figure 11: (A) Light microscopy image of *S. commune* 12-34 x 4-39 hypha in monoculture (B) Raman image of a hypha (C) Pseudo-coloured Raman image using a VCA algorithm (D) Raman spectra (a and b) of the fungal matrix plotted in C in corresponding colors, c and d show reference spectra of glycogen and proteins respectively.

All main Raman bands can be assigned to spectral features of either polysaccharides or proteins. However, the composition of polysaccharides and proteins varies along the hypha as indicated by the spectral differences associated with the green and yellow regions. The Raman bands of the polysaccharides can be assigned to different deformations of the glucose ring fractions. The main protein bands are for instance due to the carbonyl C=O stretching vibrations of the peptide backbone at 1665 cm^{-1}, often referred to as amide I band, or the CH_2 scissoring vibrations at 1450 cm^{-1}.

A comparison between the hyphal components of white-rot fungi *S. commune*, *F. velutipes* and *G. lucidum* (Fig 12) revealed some differences, thereby predicting that each genus has unique signatures and can be identified based on Raman spectra. The fungal wall is a heterogeneous structure consisting of lipids and carbohydrates such as chitin, 1,3-β-glucan and 1,6-β-glucan. As observed by spectroscopic analysis, the composition of the cell wall frequently varies in a noticeable way between species of fungi (Latgé, 2010). It was expected that strong peaks from either glucans or chitins would appear in the vibrational spectra of fungal cell walls. The

strong bands of chitin and β-glucans appeared in quite overlapping regions (Lee *et al.* 2013), but are however, absent in the spectra from these fungi in Fig 12.

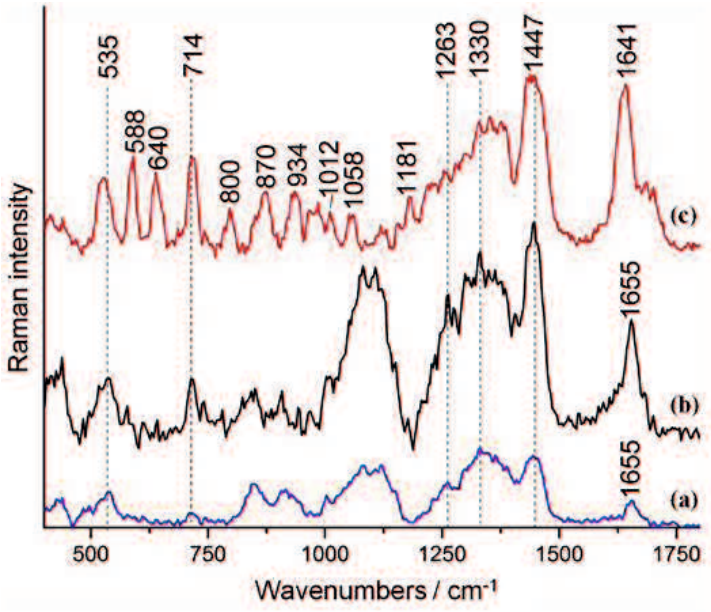

Figure 12: Raman spectra of the hyphae of (a) *S. commune,* (b) *F. velutipes* and (c) *G. lucidum.*

The bands which correspond to vibrations of protein components were found near 851 cm^{-1} (ring breathing in tyrosine, CCH deformation), 1003 cm^{-1} (symmetric ring breathing in phenylalanine), 1330 and 1656 cm^{-1}. In general, the presence of proteins can be noticed by the amide I and amide III bands at about 1655 and 1331 cm^{-1} (Tuma 2005). The strong peak at 1655 cm^{-1} is the so-called amide I band that corresponds to the sum of coupled modes of the polypeptide backbone. A major contribution to the amide I modes comes from the CO stretching of the peptide carbonyl groups. The amide III mode at 1331 cm^{-1} is another coupled vibration of the polypeptide backbone, mainly resulting from the coupled C–N stretching and N–H bending motions (Tuma 2005). In *S. commune*, the Raman band located at 1655 cm^{-1} results from a superposition of protein, lipid and polysaccharide vibrations and is therefore a marker of all relevant cell substances i.e. is typical for the fungal cell matrix (Walter *et al.* 2010). From the spectra, we can perceive that *Schizophyllum commune* and *Flammulina velutipes* have almost identical spectral features which are distinct from the *Ganoderma lucidum* spectra which exhibits the features attributed to proteins. However a large number from peaks in the *G. lucidum* spectrum lying between 500 – 1060 cm^{-1} remain unassigned.

Raman mapping was also performed on various clamp cell and hyphal tip regions in order to attempt to image the nuclei present within them (Fig 13). The nucleus consists of nucleic acids (DNA & RNA) and nuclear proteins. The excitation wavelength of 785 nm was used, because green laser excitation (such as 532 nm and 514.5 nm) generates significant native auto-fluorescence, which can obscure the Raman spectral features of biological specimens under investigation.

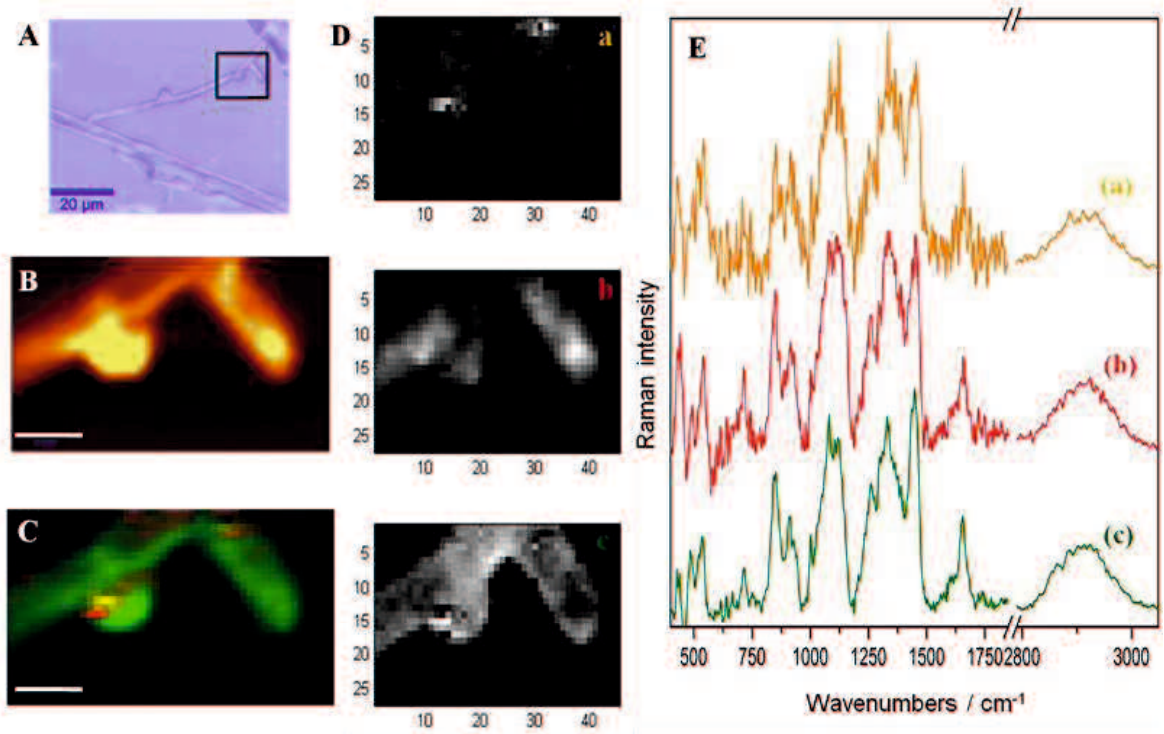

Figure 13: Raman mapping of a clamp cell and side branch of *S. commune* (A) Light microscopy image of *S. commune* 12-34 x 4-39 hypha. (B) Raman image at 2800-3020 cm^{-1}.(C) Pseudo-coloured Raman image using a VCA algorithm.(D) Abundance plot of representative end-member spectra corresponding to plot a,b and c in E.(E) Raman spectra (a, b and c) of the fungal matrix plotted in C in corresponding colors. Bar: 20 µm for A, 3 µm for B and C.

In general, cell specimens give rise to Raman spectra characterized by broad bands around 1650 cm^{-1}, the amide I protein C=O stretching vibration; 1575 cm^{-1} because of DNA and RNA components; 1440-1460 cm^{-1}, the methyl and methlyene deformation modes of lipids, polysaccharides, and proteins; around 1285-1350 cm^{-1}, the protein amide III deformation of N-H and C-H; and 1000-1200 cm^{-1} corresponding to C-C and C-O stretching modes of lipids and polysaccharides. Only a few vibrational modes of bio macromolecules give rise to sharp, signature peaks in their Raman spectra, such as the phenylalanine ring breathing mode around 1004 cm^{-1} (Szeghalmi, *et al*., 2007). Raman spectra characteristic of nucleic acids were not found in these maps.

While Raman mapping has numerous advantages, it cannot be performed at video rate, therefore dynamics of organelles cannot be observed. In contrast to linear Raman microspectroscopy, CARS microscopy allows for recording the distribution of a characteristic Raman mode within the sample with video rate. CARS images of a fungal hypha is shown in Fig. 14 recorded at 2900 cm^{-1}. The spectral region between 2800 and 3000 cm^{-1} represents the vibrations generated by C-H stretching vibrations that occur abundantly in lipids and proteins. This vibrational region was selected since the resonant CARS signal scales with the square of both the number of scatters and the large Raman scattering cross section of C-H vibrations. In biological samples $-CH_2-$ and $-CH_3$ containing compounds are highly abundant. Thus, a strong CARS signal results, exceeding the non-resonant background, which often hinders a convincing interpretation of CARS images in the finger print region. From previous findings (Lim*, et al.*, 2010, Medyukhina*, et al.*, 2012) it is known that nuclei show negative contrast in the C-H stretching region. Fig 14 B shows a CARS image of the hyphae recorded at 2850 cm^{-1}. As can be seen in Fig. 14 A, tuning the CARS signal to 2900 cm^{-1} (which is located between the $-CH_2-$ symmetrical stretching vibration and the $-CH_3$ Fermi resonance), yields a strong signal at the septal region. A hypha with clamp cells is shown. The signal is not entirely resonant and contains background noise.

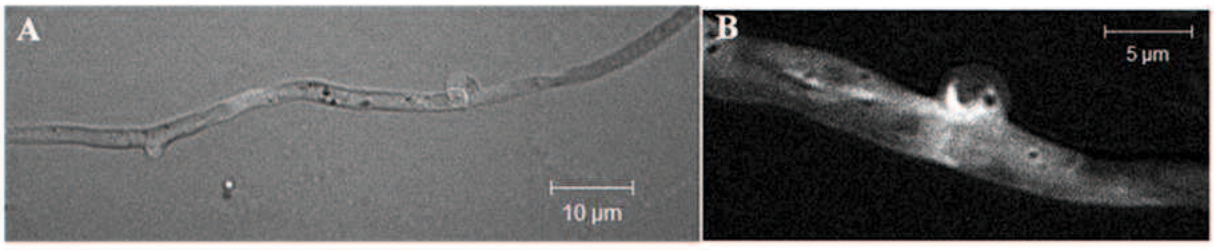

Figure 14: CARS images of hyphae recorded at (A) 2900 cm^{-1} (B) 2850 cm^{-1}

The region around the clamp cells was chosen because when dikaryons are formed, the clamp connection synthesis takes place and during this time there is nuclear migration via the clamp cells of the resultant fungi. Thus there was a higher probability of locating the nuclei in this region. In Fig 14 B the CARS signal from protein is obtained. Clamp cells contain dolipores which consist of proteins, which allows cytoplasmic continuity but prevents the movement of major organelles. Proteins, rich in aliphatic C-H bonds, are essential components of the entire cellular organization. In both images, some dark spots can be seen which might be

interpreted as vacuoles. In the scans, a chemical contrast for the nuclei could not be obtained. We also see what appears to be chitin dissolution due to clamp fusion.

3.3 Raman mapping of novel chromophores in *S. commune*

Raman mapping was performed on selected hyphae of *S. commune* dikaryon 12-43 x 4-39 pure culture. One such example is displayed in Fig. 15.

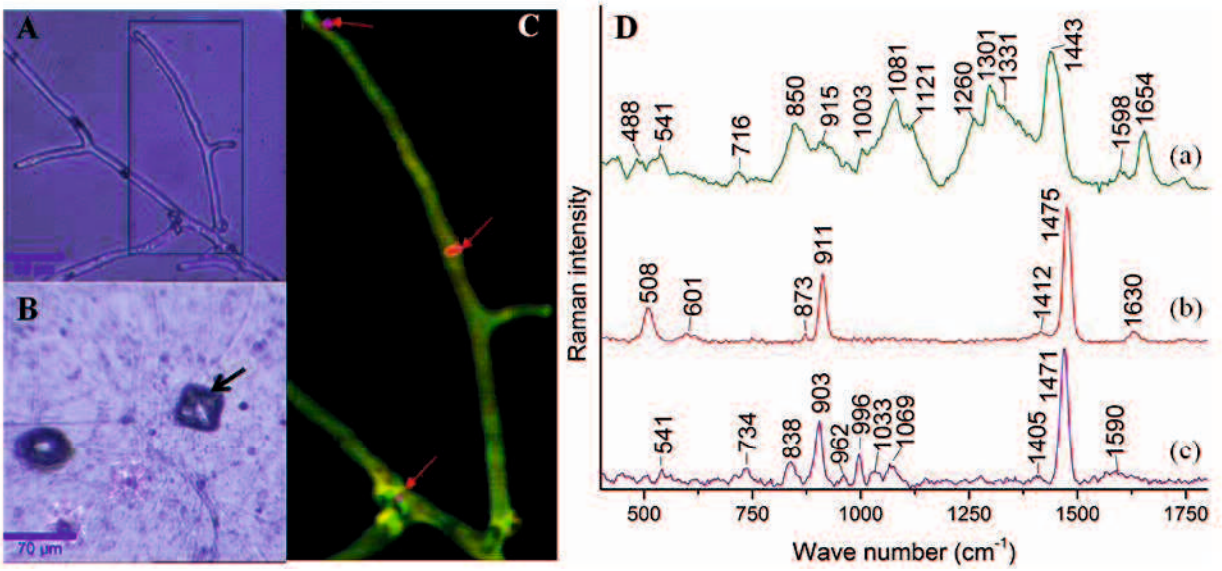

Figure 15: A) Bright field image of *S. commune* 12-43x4-39 hyphae (B) Bright field image of a crystal excreted by the F15 strain of *S. commune.* C) Intensity distribution of the most dissimilar spectra representative of the fungal matrix (green) and a chromophore (red). D) Representative Raman spectra of (a) hyphal cell of *S. commune* (b) the red regions in C and (c) spectra of the crystal seen in B. Bar: 20 µm for A and 70 µm for B

The Raman image in 15C was generated by a spectral unmixing algorithm that decomposes the dataset into representative spectra and their individual abundance within the dataset. The associated spectral information is shown in 15D plots a and b. End member spectra indicated the presence of very distinct spectra from the typical spectra of *S. commune* hypha. In the image in 15C, it was found that there was localization of a compound at the septal regions and near the formation of a branch (as indicated by arrows). The most intense peaks of the spectrum were located at 509, 912 and 1478 cm^{-1}, and some of lower intensities are observed at 601, 873, 1412 and 1630 cm^{-1}. Similarly, another distinct spectrum of an unidentified compound was measured from a crystal secreted by the *S. commune* F15 strain, with the most

intense bands occurring at 1471 and 903 cm^{-1} and the rest at 541, 734, 838, 962, 996, 1033, 1069, 1405, and 1590 cm^{-1}. These spectra did not correspond to that of any known compounds, thus, these two substances could not be identified.

3.4 Interaction of *S. commune* with wood-decay fungi

To investigate the interaction between *Schizophyllum commune* and *Ganoderma lucidum*, *Pleurotus ostreatus, Flammulina velutipes, Hypholoma fasciculare, Kuehneromyces mutabilis,* and *Serpula lacrymans,* agar plate based confrontation

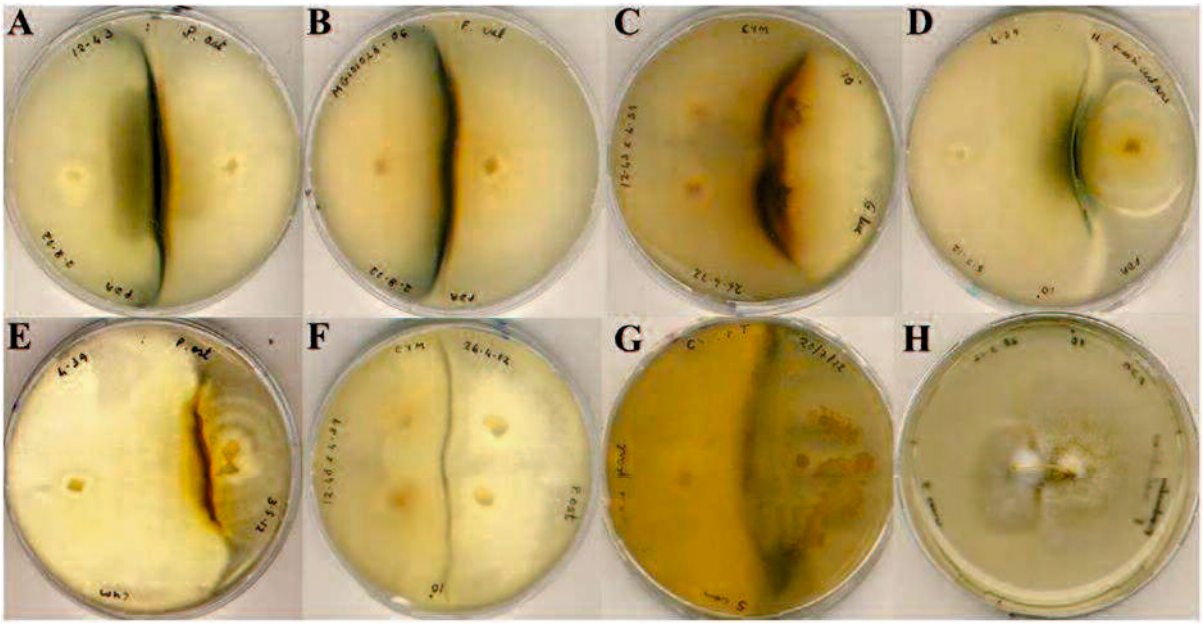

Figure 16: Interactions of (A) 12-43 with *P. ostreatus*, (B) MG101028-06 with *F. velutipes*, (C) 12-43x4-39 and *G. lucidum*, (D) 4-39 with *H. fasciculare*, (E) 4-39 and *P. ostreatus*, (F) 12-43x4-39 and *P. ostreatus*, (G) 12-43x4-39 and yeast and (H) 12-43x4-39 and *F. velutipes* with fruiting body.

assays were performed. Observation of the cultures revealed that coloured substances and discolouration of the media are produced by *S. commune* strains and some of the fungi with which they were grown alongside as seen in Figure 16. In the self-paired cultures of *S. commune* and other fungi, no induction of pigment production was observed (Fig 17 B). The response of *S. commune* to *G. lucidum*, *P. ostreatus*, *F. velutipes,* and *K. mutabilis* at 28 ^{o}C and *H. fasciculare* at 10 ^{o}C was initiated by the sealing off of the mycelial front and formation of mycelial barrage, at 24 and 48 h post-contact, respectively. In most cases, a blue/black/brownish, sometimes green pigment developed at the bottom of the plate within the interaction zone occupied by both fungi at 8h post contact.

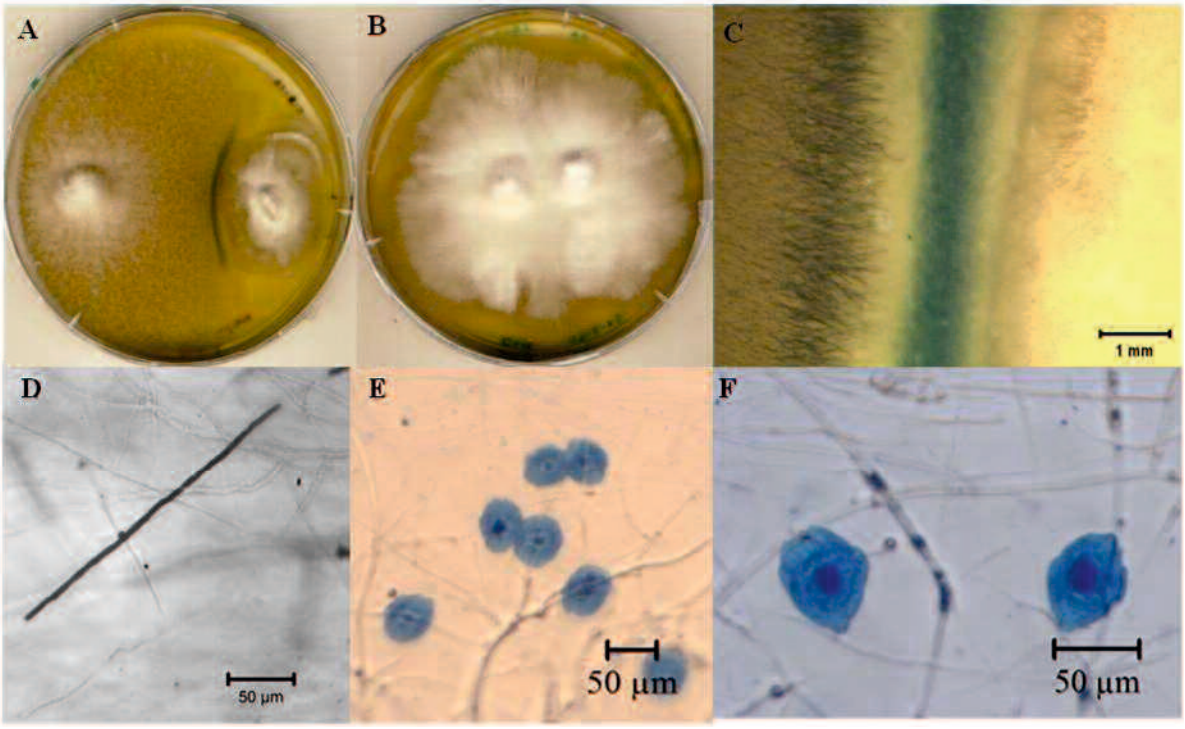

Figure 17: Pigments visible in and between hyphae in fungal interactions. (A) Culture of *S. commune* 12-43x4-39 (left) and *H. fasciculare* (right) showing pigmentation in zone of contact. B) Self-paired culture of *S. commune* after mycelial contact showing that no pigmentation is produced, (C) Blue coloration in the interaction zone of *S. commune* 4-39 (left) and *H. fasciculare* (right), (D) Pigment localized in *S. commune* hyphae in interaction with *F. velutipes*, (E) Pigment crystals excreted by the pigmented mutant strain of *S. commune* F15 into the media, and (F) F15 pigmented hyphae with pigment secretions in the media

The intensity of this pigmentation increased with the duration of contact. The substances were secreted into the agar. Microscopic observations of the solid media and the fungi showed the presence of blue crystals in the media (Fig 17 E) next to the hyphae and localization of the pigment within the hyphae of *S. commune* (Fig 17 D & F), while the fungi confronting *S. commune* did not show signs of any pigmentation. The pigment is excreted into the agar, where it crystallizes into various shapes and sizes. Time-lapse studies showed that growth of the pigment-filled *S. commune* hyphae came to a stop once the pigment was produced. New aerial hyphae then were formed, which grow over the region of the excreted pigment and continue to mature normally.

3.5 Identification of pigments produced by *S. commune* during interactions with fungi

Point Raman spectra were taken from *S. commune* hyphae, the fungal competitor hyphae and agar medium from the zone of interaction of *S. commune* and *H. fasciculare*. Raman mapping of *S. commune* hyphae (Fig 18) from these zones showed localization of the pigment.

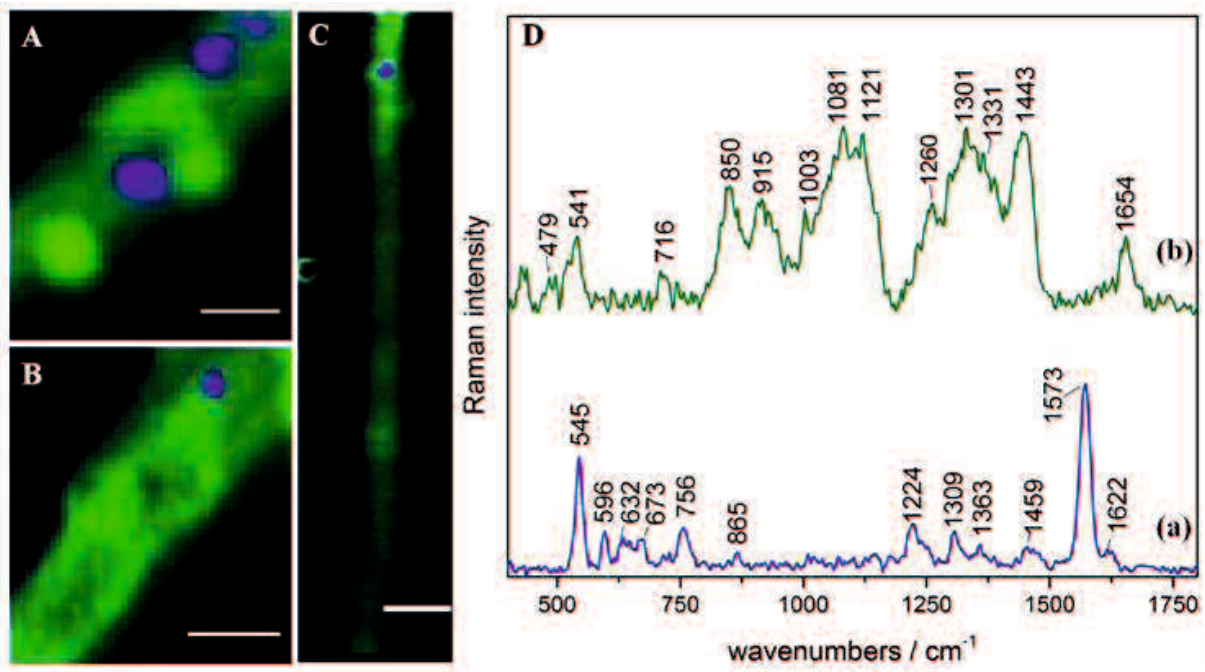

Figure 18: Pseudo-colour Raman maps based on Raman data recorded from three samples showing distribution of fungal matrix (green) and indigo pigment (blue). A) *S. commune* hypha from an interaction between *S. commune* 12-43x4-39 and *H. fasciculare,* (B) hypha of *S. commune* F15*,* and (C) hypha of F15xF28, a ΔGap1/ΔGap1 mutant dikaryon strain of *S. commune.* (D) End-member spectra of the three samples representing regions in blue (indigo) and green (fungal matrix) where (a) corresponds to the blue coloured areas, (b) corresponds the green regions. Bar: 1 µm for A and B, 2 µm for C

On analysis of the hyphae of the fungi with Raman microspectroscopy, the profile of indigo bands was recognized with reference to pure standard. The VCA algorithm was again used for spectral analysis of the Raman maps and image generation. Analysis of spectra of the samples taken from the interaction zone revealed that the most intense signal of the ring stretching mode is observed near 1573 cm^{-1} with a pronounced shoulder at 1581 cm^{-1} due to the stretching vibrations of the conjugated

system of C=C, C=O and N-H groups (Bauer, *et al.*, 1998). The vibration of this conjugated system gave rise also to bands near 1363, 1622 and 1700 cm^{-1}. The band attributed to N-H rocking vibration was observed at about 1224 cm^{-1}. Vibrations involving C–H rocking were recognized at 1247, 1459 and 1481 cm^{-1}, while the vibrations of five- and six- membered rings were observed at 756 & 1309 cm^{-1}. The band at 1573 cm^{-1} was used as a marker for identification of indigo (Baran *et al.* 2010). All Raman bands of indigo are resonance enhanced, because of a coupling of the vibrational modes with an electronic transition. As a consequence the band intensities of indigo are largely increased compared with the protein bands. Indigo was detected in the cultures of pigmented mutants 12-43 blue and F15, in dikaryon 12-43x4-39 co-cultured with *G. lucidum*, *P. ostreatus*, *H. fasciculare, K. mutabilis*, an ascomycete and a yeast, in wild type monokaryons 12-43 and 4-39 co-cultured with *P. ostreatus*, *G. lucidum*, *F. velutipes* and *H. fasciculare,* and in MG101028-06 with *F. velutipes, H. fasciculare* and *P. ostreatus*. Only *S. lacrymans* did not induce any pigment production in *S. commune*. Indigo localization could also be observed in ∆*gap1/*∆*gap1* dikaryon hyphae of *S. commune* (see Fig 18C). Isatin and indirubin could not be detected in these scans.

3.6 Analysis of co-cultivation of *S. commune* with *H. fasciculare* for release of indigo using LESA-MS and UHPLC-ESI-MS/MS

LESA-HRMS was performed on the confrontation assay plates directly from the surface of the agar (Fig 19A). Analyzing the blue boundary zone between *S. commune* and *H. fasciculare* a mass signal corresponding to indigo and indirubin was observed (Fig 19B). The accurate mass measurements of this ion revealed a *m/z* 263.0807 $[M+1]^+$ with a mass difference of 2.9 ppm to exact mass of protonated indigo and indirubin (calculated for $C_{16}H_{11}N_2O_2$, 263.0815). In order to confirm the presence of both molecules, the MS/MS spectrum of the parent ion signal was compared with the MS/MS spectrum of pure indigo and indirubin (Fig 19C-E). Thereby the MS/MS spectrum of the parent mass ion showed high similarity to the MS/MS spectra of pure indigo and indirubin. Fragment ion peaks were detected at *m/z* 219.09, 235.09 and 245.07. Same fragments were observed from both reference compounds. The indigo/indirubin mass signal was not visible when extracting and analyzing compounds from non-blue zones beneath the mycelium at the periphery of

S. commune and *H. fasciculare* cultures (Fig 19B) and neither from the surface of self-paired cultures.

To finally confirm the presence of indigo and to distinguish the signal from mass-identical indirubin, UHPLC-ESI-MS/MS measurements were conducted. Therefore we extracted the compounds present in the agar from different, defined zones of co- and mono-cultivated culture plates with methanol/ethyl acetate. In the extract obtained from the interaction zone we could determine two peaks with identical mass *m/z* 263.0813 $[M+1]^+$. By comparing the retention times and mass spectra, the more intensive peak has been assigned to protonated indigo while the less intensive peak has been assigned to protonated indirubin (Fig 19F). Quantification using calibration curves of reference compounds revealed 209.61 ± 67.3 pmol indigo and 0.87 ± 0.23 pmol indirubin per cm^3 agar to be present in the interaction zone. Analyzing at a detection limit of ca. 300 pmol of isatin, only single scans were detected at *m/z* 148.0391 $[M+H]^+$ with a mass difference of 1.1 ppm to exact mass of protonated isatin. The presence of isatin could not be confirmed by MS/MS data, because the amount of ions were insufficient to fragment the ion. Finally, neither the *S. commune* strain 12-43x4-39 nor *H. fasciculare* alone showed a signal for indigo, indirubin or isatin (Fig 19D). In 12-43 x 4-39 and 4-39 there was however the presence of a peak at RT 12.5 which corresponded to the mass of indigo. It was found that this was a contribution of the 4-39 partner as 12-43 did not produce such a peak. There is a possibility that this compound is another structural isomer of indigo.

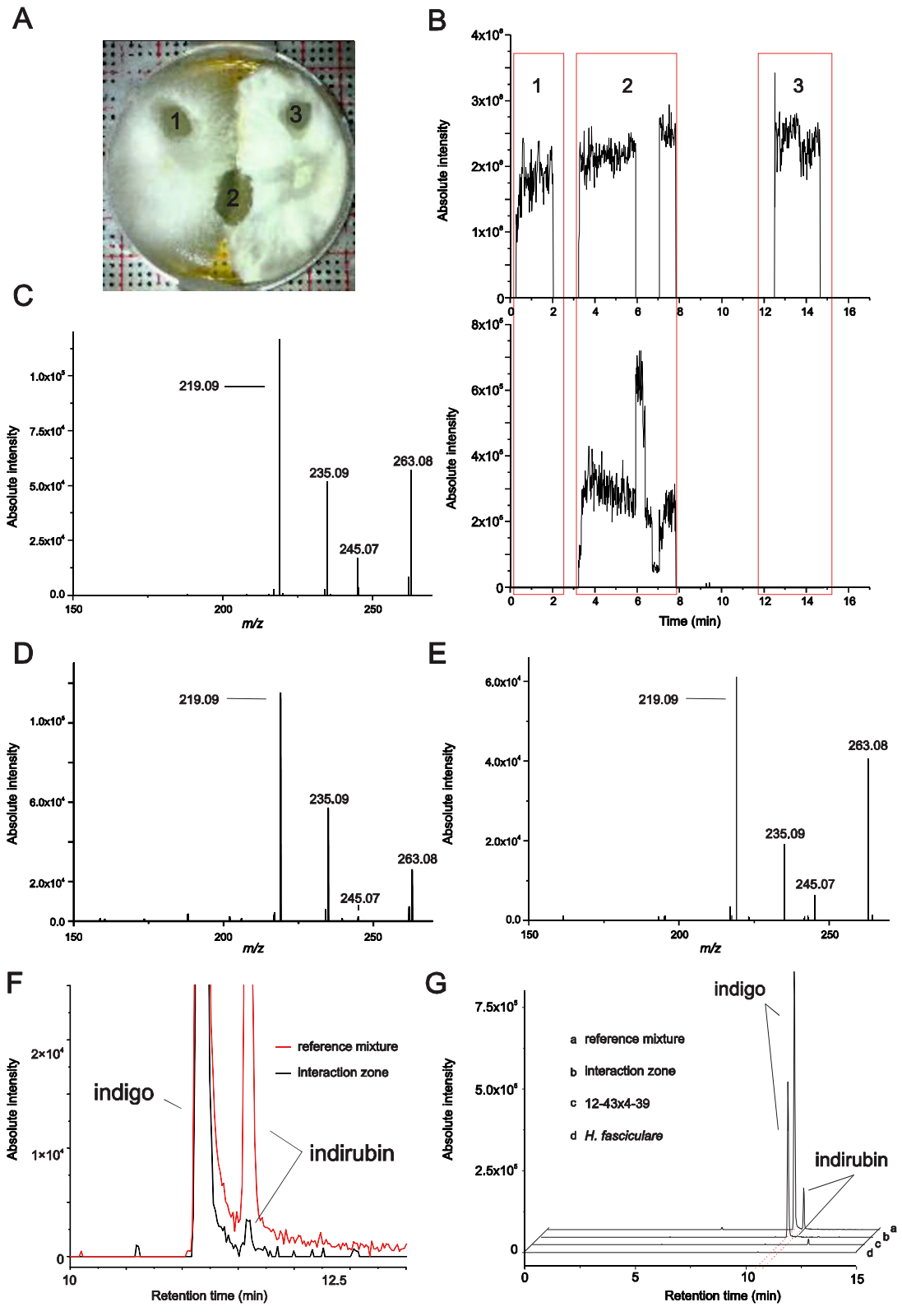

Figure 19: Co-cultivated strains of *S. commune* and *H. fasciculare* were analyzed for release of indigo using LESA-MS and UHPLC-ESI-MS/MS. (A) Confrontation assay of *S. commune* and *H. fasciculare* after LESA-MS analysis highlighting the investigation zones with numbers: (1) zone beneath *S. commune*, (2) interaction zone between the fungi and (3) zone beneath *H. fasciculare*. (B) LESA-MS ion intensity acquisition plots of the confrontation assay are depicted. The total ion acquisition (upper) and the ion trace of fungal indigo (*m/z* 263.078-263.084 in lower plot). The numbers of the boxes correspond to zones

in A. (C) The LESA-MS/MS spectrum of indigo is illustrated which is similar with the MS/MS spectrum of reference indigo (D) and the MS/MS spectrum of pure indirubin depicted in (E). For confirmation of indigo/indirubin production, UHPLC-ESI-MS/MS analysis was accomplished. (F) and (G) show the plots of extracted ion chromatograms (EIC) for mass trace of indigo and indirubin, respectively (*m/z* 263.078-263.084).

3.7 Determination of IAA in *S. commune*

As seen in table 1, the metabolites produced by *S. commune* as reported in this study and a list of those produced by mutant strains of *S. commune* as reported previously – indigo (Miles*, et al.*, 1956), indirubin, isatin (Epstein & Miles, 1966), IAA (Epstein & Miles, 1967) and anthranilic acid (Epstein, 1966) is summarized.

Table 1: Metabolites known to be produced by *S. commune*

S. commune secondary metabolites		Indigo	Indirubin	Isatin	IAA	Anthranilic acid
pigmented mutants	Epstein & Miles	+	+	+	+	+
non-pigmented strains	Epstein & Miles	-	-	-	-	-
WT 12-43 x 4-39	this study	-	-	-	+	+
WT 12-43	this study	-	-	-	+	+
WT *S. commune* interacting with fungi	this study	+	+	-	+	+
mutant12-43	this study	+	+	-	+	+
mutant F15	this study	+	+	-	+	+

3.7.1 Identification and quantification of indole-3-acetic acid in wild type *S. commune* cultures

Metabolites were extracted from agar pieces of plates cultured with WT strains *S. commune* dikaryon 12-43x4-39 and monokaryons 12-43 and 4-39 strains. Identification of indole-3-acetic acid (IAA) was performed using accurate mass measurements, and by comparison of fragmentation patterns and retention time with those of reference IAA. The LC/MS measurements revealed a chromatographic peak

from mass *m/z* 176.0706 which corresponds to protonated mass of IAA $[M+H]^+$ (calc. for $C_{10}H_{10}NO_2$ *m/z* 176.0706, 3.66 ppm). Verification by MS/MS fragmentation showed a fragment ion peak at *m/z* 130.06 which is most probably due to loss of COOH. Retention time and fragmentation patterns were similar for sample and reference IAA (Figure 20A, B).

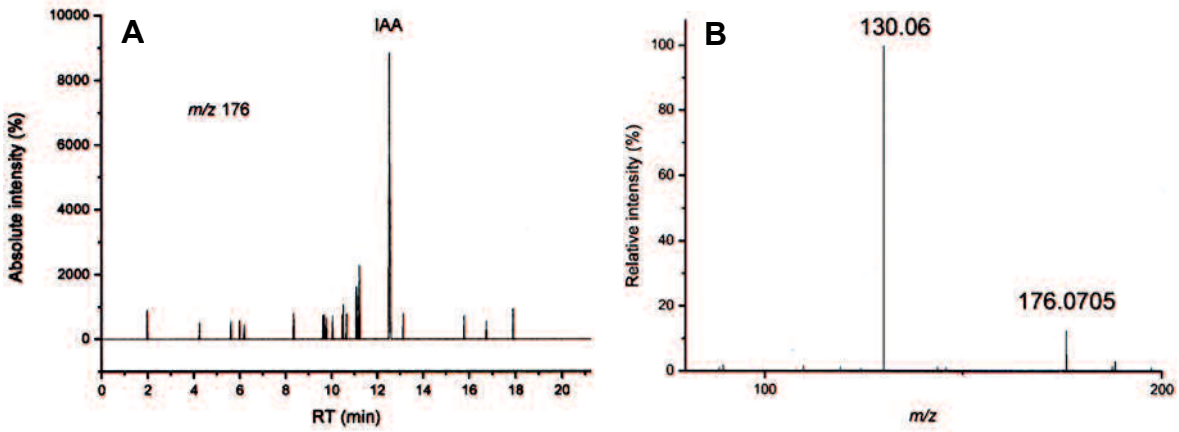

Figure 20: LC-MS analysis of *S. commune* 12-43 culture filtrate. (A) EIC chromatogram of *m/z* 176.07 (B) MS/MS of sample.

Quantification of IAA was accomplished from three replicates of liquid culture extracts of 12-43 using a calibration curve of reference IAA.

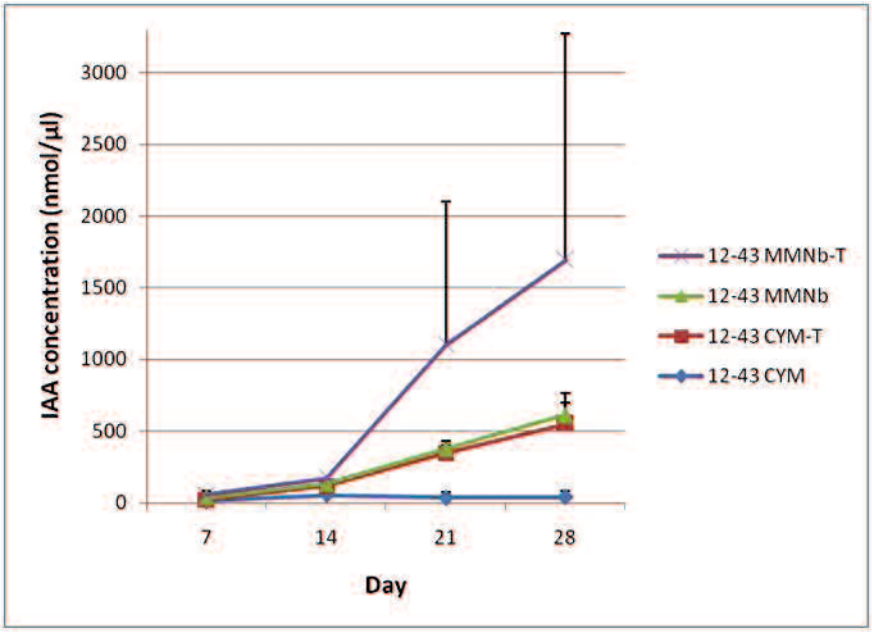

Figure 21: Graph showing the concentration of IAA produced by *S. commune* in four media CYM, CYM-T, MMNb and MMNb-T over a 28 day period.

Analysis revealed that 12-43 grew fairly well and produced IAA in the four different media (CYM; CYM-T, MMNb, MMNb-T) as seen in Fig 21. The amount of IAA produced was not necessarily proportional to the biomass of the fungal culture. Evidently, the addition of tryptophan greatly increases the amount of IAA synthesized. The production of IAA increased exponentially in MMNb-T after the addition of tryptophan. A gradual increase of IAA is seen in the CYM-T and MMNb cultures. In the case of CYM, data indicate that a plateau was reached in the production of IAA, after which the amount gradually decreases. The maximum IAA production (473.55 ± 3.32 $\mu g ml^{-1}$) was observed after 28 days of incubation using MMNb medium containing 0.25 mM tryptophan. However, its significance is debatable as the values deviate from the mean considerably.

3.7.2 Changes in IAA production in *S. commune* – *H. fasciculare* co-cultures

To determine whether the co-cultivation of *S. commune* with *H. fasciculare* influences the IAA production in *S. commune*, 4 x 1 x 0.3 cm mycelia strips with agar were cut out from a) the *S. commune* zone, b) the *H. fasciculare* zone and c) the interaction zone. Additionally, the self-paired cultures of the fungi were also sampled. *S. commune* monokaryon 4-39 and *S. commune* dikaryon 12-43x4-39 were used. The amount of IAA produced in pure cultures, co-cultures and in the interaction zones of the co-cultures were quantified (table 2 and figure 22).

Both the *S. commune* strains as well as *H. fasciculare* produce IAA on the CYM media. *S. commune* dikaryon produced 10 fold more IAA than the monokaryon. In co-culture with *H. fasciculare*, the IAA produced by 12-43 x 4-39 doubled, and that by 4-39 with *H. fasciculare* increased 7 times. The IAA produced in co-culture by *H. fasciculare* increased by 6 fold with 12-43x4-39 and by 14 fold with 4-39. Both interaction zones also showed an increase in IAA concentration as compared to the 4-39, 12-43x4-39 and *H. fasciculare* pure cultures, and the 4-39-*H. fasciculare* and the *H. fasciculare*-4-39 co-cultures. The concentration of anthranilate, a precursor of tryptophan, was also monitored, and it was found that it exhibited a similar trend as the changes in IAA concentration by the pure and co-cultures. In general, it was found that when the fungi were co-cultivated, their IAA production significantly increased.

Table 2: Concentration of IAA produced by pure and co-cultured fungi

Interactions	IAA concentration (nmol/cm^3 agar)
S. commune 12-43 x 4-39 pure culture	15.32
S. commune 4-39 pure culture	1.48
H. fasciculare pure culture	1.52
12-43 x 4-39 co-cultured with *H. fasciculare*	29.06
H. fasciculare co-cultured with 12-43 x 4-39	10.09
4-39 co-cultured with *H. fasciculare*	11.07
H. fasciculare co-cultured with 4-39	21.54
12-43 x 4-39 - *H. fasciculare* interaction zone	23.44
4-39 - *H. fasciculare* interaction zone	26.31

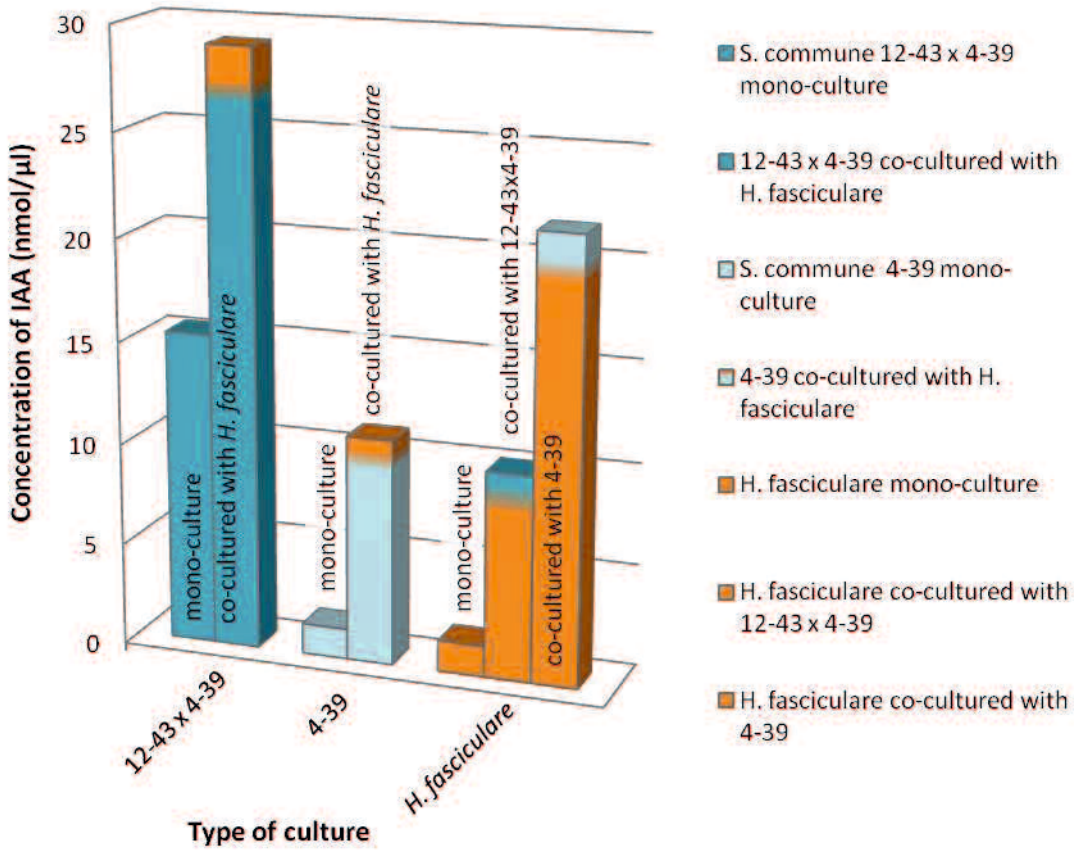

Figure 22: Concentration of IAA produced by *S. commune* 4-39 and 12-43x4-39 and, *H. fasciculare* in pure and co-cultures

3.7.3 Relationship between indigo and IAA synthesis in *S. commune*

In order to establish a correlation between indigo and IAA synthesis, the indigo-producing mutant strain of *S. commune* - F15 was cultivated in liquid CYM, since it was found that IAA, indigo and indirubin was produced by this mutant. 2ml samples were removed from the culture at regular intervals and analyzed to monitor the quantities of indigo, indirubin and IAA. The results can be seen in table 3.

Table 3: Concentrations of IAA, indigo and indirubin as produced by F15

Day	IAA (nmol/µl)	Indigo (nmol/µl)	Indirubin (nmol/µl)
7	21.48	16.00	0.72
9	17.57	13.60	0.52
16	25.73	5.97	0.16
23	243.43	11.78	0.24
30	498.39	20.06	0.57

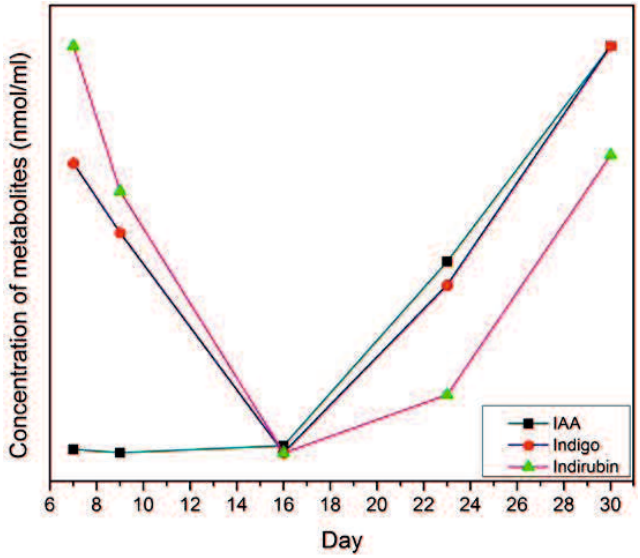

Figure 23: Plot showing concentration trend of IAA, indigo and indirubin. The values were normalized (0, 1).

The IAA concentration sharply increased by 8 fold from day 16 to day 23, after which it doubled on day 30. The concentration of indigo and indirubin exhibited similar trends in that it fell from day 7 to 16 and then started increasing again (Fig 23).

3.7.4 Degradation of indole

Since indole was thought to be an inhibitor of growth of the fungi during the interactions, minimal media containing 0.02% indole (MM-I) was inoculated with 12-43 x 4-39. The same setup without addition of indole was used as a control (MM).

Table 4: Concentrations of IAA, indirubin and indigo as produced by 12-43 x 4-39 in MM and MM-I

Day	IAA (pmol/ml)		Indirubin (pmol/ml)		Indigo (pmol/ml)	
	MM	MM-I	MM	MM-I	MM	MM-I
5	0	0	0	0	0	0
17	242.1793	4690.607	0	0	0	0
26	3.373801	63352.58	484.3586	9381.214	0	0
34	8.989141	1247.486	0	126705.2	0	0
42	4.876542	1359.171	0	2494.971	0	4989.9422

The effect of indole on the growth of *S. commune* and its degradation products, were determined. Addition of 0.02% indole (MM-I) to liquid culture of 12-43 x 4-39, showed an inhibition of growth of the fungi as compared to the control culture. The degradation products included greatly increased amounts of IAA as compared to the control, indirubin and, indigo. The addition of indole led to a 20 fold increase in the amount of IAA as compared to the control on day 17. It appears that IAA is broken down to indirubin in MM from day 17 to 26, and in MM-I from day 26 to 34, because as the amount of IAA exponentially falls, there is an exponential increase in the amount of indirubin. Indigo appears to be formed only on day 42 in MM-I, when the amount of IAA decreases.

.

4. Discussion

4.1 *In vivo* live imaging of nuclear migration in *S. commune*

In principle, Raman spectroscopy and its variants would be ideal methodologies to study nuclear migration given their non-invasive nature and high specificity. However, many practical obstacles were encountered, especially regarding the localization of the nuclei in the hyphae of *S. commune*. Raman microspectroscopy is usually hindered by the weakness of the Raman effect and as a consequence is a rather slow technique. Raman imaging is generally not fast enough to monitor nuclear migration (2–3 mm per hour in *S. commune*). In order to receive a reasonable Raman scattering signal, an integration time of 3 s per point had to be applied. Assuming a minimal image size of 50 × 50 pixels to follow the nuclei movement, this long pixel dwell time is orders of magnitude too slow to allow real-time measurements. Fluorescence is often generated under similar experimental conditions but generally generates much stronger signals. Raman spectra can be totally dominated by the broadband fluorescence. Moving to higher wavelengths for the excitation can significantly reduce fluorescence. Fluorescence can be, for instance, avoided by applying laser sources in the near-infrared. The sensitivity of the Raman spectrum is directly proportional to the exciting wavelength. Therefore, excitation in the near IR results intrinsically in a weaker signal. In resonance Raman spectroscopy, the incident wavelength is chosen to be close to the absorption maximum of a chromophore. The simultaneous transition of an electron into an excited state together with a vibrational excitation can give rise to very significant signal enhancement. However, this requires variable wavelengths, because all molecules do not exhibit the same absorbance spectrum. The Raman bands of the chromophore are generally much stronger than those of other groups (Spiro & Czernuszewicz, 1995).

In the CARS microscopy measurements, a significant amount of non-resonant background overlapped with the resonant CARS signal. A 63x oil immersion objective (NA 1.4) was used to obtain suitably magnified images of the fungal hyphae. A fair amount of resonant CARS signal was obtained for the 2850 cm^{-1} Raman shift in the clamp cell region. The signal can not only be attributed to the lipids, but also to the proteins present in this area (Krafft*, et al.*, 2012). It is known that the septal walls

within this clamp cell region contain two largely protein-containing pores (dolipores), which could result in a significant amount of scattering from the proteins. Most CARS studies are facilitated by the high density of CH_2 modes in lipids which produces a strong CARS signal at its symmetric stretch vibration at 2845 cm^{-1}. The lipid CARS response also benefits from having its major signatures in a relatively quiet region of the vibrational spectrum which prevents spectral interferences with neighbouring bands. Other dense CH_2- containing compounds and a concentrated substance like water can be relatively easily visualized in the high frequency range (2500 cm^{-1} – 3500 cm^{-1}). This is in contrast to the fingerprint region in which the vibrational modes for nucleic acids are situated. Because each vibrational band carries its own frequency dependent spectral phase, the coherent anti-Stokes Raman spectrum is affected by interferences among the different spectral signatures, in addition to interference with the non-resonant background. As a consequence, the spectral information in CARS spectra from the fingerprint region typically appears featureless and washed out (Potma, 2010).

As we know from *S. commune*, nuclear pairing initiates the formation of a clamp or crozier cell. However, clamp cell formation is not essential for stable and accurate dikaryon formation and is not seen in all species that can form dikaryons (Kues, 2000). In species that do not form clamp cells, different spindle lengths, different spindle elongation rates or simply a small enough starting distance between the two nuclei ensure that the spindles overlap in anaphase, enabling a ‘two-step’ swap of different sister nuclei. It has long been known that the nuclei in a dikaryon can communicate: exchange of genetic material and somatic recombination occurs between genotypes (Raper, 1966, Clark & Anderson, 2004). Interestingly, the exact position of the two nuclei in a dikaryon influences the specific genes that are expressed in these nuclei. For example, in *S. commune* dikaryons, when the nuclei are close together (<2 microns apart) a different set of hydrophobin-encoding genes is expressed than when the nuclei are further apart (Schuurs*, et al.*, 1998). Thus, the precise positions of the biparental nuclei in the dikaryon can specify the transcriptional programme of the cell. There are still many open questions to be answered, including how nuclei recognize one another as ‘different’ in a common cytoplasm, and how this information is converted to the signals that regulate the migration, positioning and sorting of the genotypes into dikaryons. Studying these

questions in model filamentous fungi will probably reveal new lines of communication between the genome and MT motor machinery (Gladfelter & Berman, 2009).
Various attempts to localize the nuclei were unsuccessful. RMS required high laser power and long integration times, limiting use for live imaging while with CARS microscopy, the applied experimental conditions did not provide sufficient contrast to image most molecules other than lipids.

Raman microspectroscopy was used in this study to also show that fungi can be distinguished or identified based on their Raman spectral features. Point spectra from *S. commune*, *F. velutipes* and *G. lucidum* showed enough differences to distinguish the fungi. From the spectra it could also be perceived that *S. commune* and *F. velutipes* are closely related to each other than to *G. lucidum,* which is in accordance with phylogentic classification, given that *S. commune* and *F. velutipes* belong to the Agaricales and *G. lucidum* belongs to the Polyporales (Hibbett, 2006).

4.2 Production of secondary metabolites by *S. commune* in pure culture

The white rot basidiomycetous fungi are the only organisms able to depolymerize and even completely oxidize (to CO_2 and H_2O) all the components of wood, which are primarily cellulose, hemicellulose and lignin (Kirk & Farrell, 1987, Eriksson*, et al.*, 1990, Hatakka, 2001, Kersten & Cullen, 2007) with also a remarkable ability to decompose the coloured, aromatic, heterogeneous and persistent lignin phenylpropanoid units, naturally synthesized by plants in their cell walls (Higuchi, 1997, 2006, Boerjan*, et al.*, 2003). Like most higher organisms, they possess a number of metalloproteins involved in various metabolic activities, including particular lignin-modifying enzymes (LMEs), which are extracellular and metal-containing oxidoreductases, mainly heme-containing peroxidases (Cullen, 1997, Gold, 2000, Martínez, 2002) and laccases (Thurston, 1994, Leonowicz*, et al.*, 2001, Mayer & Staples, 2002). We have shown the presence of two unique chromophores, one within the hyphae of *S. commune,* localized at the septal and branching regions and another secreted by it which crystallizes in the media. Although their identity or function could not be established due to lack of pertinent references, based on their Raman spectra, some conclusions can be drawn. The high signal intensity and limited number of peaks indicate that the compounds could be metal-containing

proteins consisting of chromophores in resonance with the 785 nm excitation wavelength. The limited number of spectral peaks also indicated that they may be crystalline in nature. Chromophores are often detected using resonance Raman microspectroscopy. Resonance Raman scattering occurs when a material is irradiated with monochromatic light corresponding to an allowed absorption band region (Spiro & Czernuszewicz, 1995). Thus, when the molecule is excited with a strong monochromatic light whose energy matches that of an electric-dipole allowed electronic transition, a vibronic coupling with the electronically excited state increases the probability of observing Raman scattering from vibrational transitions in the electronic ground state, and the modes that do show enhancement are localized on the chromophore (i.e., on the group of atoms that gives rise to the electronic transition) (Czernusxewicx, 1993). The origin of the observed resonance Raman signals from these substances synthesized by *S. commune* still need to be assigned.

4.3 Production of secondary metabolites by *S. commune* during interactions with fungi

In the fungal interaction study, we have shown that indigo is produced by *S. commune* as a general stress response towards antagonistic organisms whether they are basidiomycetes, ascomycetes, yeast or bacteria. Indigo appears to be produced by *S. commune* as an indication of a defense response against antagonistic microorganisms. It could also be a very specific reaction induced by communication molecules. The trypticase peptone present in the CYM media was probably used by *S. commune* as the nitrogen source to synthesize indigo. The pigments which seemed to be coloured black and green in the interactions zones also tested positive for indigo, meaning that the colours visualized were just a combination of concentration of indigo secreted and its appearance in the media. The pigments of mushrooms may protect the organisms from UV damage and bacterial attack or play a role as insect attractants (Velišek & Cejpek, 2011). Many of the pigments of higher fungi are quinones or similar conjugated structures that are mostly classified according to the perceived biosynthetic pathways, reflecting their structure, to pigments derived from the shikimate (chorismate) pathway, the acetate malonate (polyketide) pathway, the mevalonate (terpenoid) pathway, and pigments containing nitrogen. Various pigments and other fungal constituents show important biological activities (anti-oxidative, free radical scavenging, anti-carcinogenic, immune-

modulatory, antiviral, and antibacterial) that have generated intensive research interest (Steglich, 1981, Calìa*, et al.*, 2003, Liu, 2006, Schüffler & Anke, 2009). Indigo is an organic compound with a distinctive blue colour. The compound owes its deep color to the conjugation of the double bonds. In leuco-indigo (indigo white), the conjugation is interrupted because the molecule is nonplanar. Historically, indigo was a natural dye extracted from plants. It is one of the oldest dyes (Ensley*, et al.*, 1983) and is still used worldwide for textiles, with an annual production of $22x10^3$ tons, worth US $ $200x10^6$ (Wich, 1995). Indigo is an example of a class of textile dyes known as vat dyes. Vat dyes are typically insoluble in water and must undergo a chemical reaction to be converted to a water-soluble form (a leuco-base form) that effectively penetrates and interacts with the fibres (Mutnuri*, et al.*, 2009). Indigo was used in the textile industry by extracting the dye from plants. The *Indigofera tinctoria* variety for indigo production was domesticated in India. In 1897, 19,000 tons of indigo were produced from plant sources. Largely due to advances in organic chemistry, production by natural sources dropped to 1,000 tons by 1914 and continued to contract. The German chemist Adolf von Baeyer began working on the synthesis of indigo. He described his first synthesis of indigo in 1878 (from isatin) and a second synthesis in 1880 (from 2-nitrobenzaldehyde). The synthesis of indigo remained impractical, so the search for alternative starting materials continued. Indigo produced by pigmented *S. commune* mutants was first identified by Miles*, et al.* (1956) in artificial media and during interactions on wood by Peddireddi (2008). However, several conditions are required for indigo production, related to carbon sources, temperature, and pH. Only the medium containing the ammonium ion as the nitrogen source produced mycelium and pigment (Swack & Miles, 1960).The fact that indigo and indirubin was only produced by WT *S. commune* as a consequence of co-cultivation led us to assume that it is either a stress response towards antagonistic organisms or that they are produced as an indication of a defense response against antagonistic microorganisms. From the toxicity test, we see that indigo/indirubin did not inhibit growth of the fungi, which suggests that they may be by-products of a pathway induced by stress leading to a potent effector. They could also act as the detoxification products of some compounds, which might be toxic to *S. commune* itself. Accumulation to toxic levels could be prevented by the formation of an insoluble compound such as indigo. The possibility could also arise that *H. fasciculare* and the other fungi synthesize inhibitors towards *S. commune*, which

degrades them into indigo and indirubin. The presence of lignin-modifying enzymes like lignin peroxidases and/or manganese peroxidases and laccases in *S. commune* seemed to increase the degree of decolorization of individual commercial triarylmethane, anthraquinonic, and indigoid textile dyes by up to 25% using enzyme preparations (Abadulla *et al*. 2000). This indicated the ability of *S. commune* phenol oxidases to detoxify selected harmful substances. While indigo did not cause inhibition of growth, its presence did induce fruiting primodia formation in the other fungi, which is indicative of stress and unfavourable growth conditions. Indirubin on the other hand, is known as a potent anti-fungal and anti-cancer agent (Leclerc*, et al*., 2001). Indirubin extracted from *Wrightia tinctoria leaves* exhibit activity against dermatophytes such as *Epidermophyton floccosum* (MIC=6.25 µg/ml); *Trichophyton rubrum* and *T. tonsurans* (MIC=25 µg/ml); *T. mentagrophytes* and *T. simii* (MIC=50 µg/ml). It is also active against non-dermatophytes (*A. niger*, *C. albicans* and *Cryptococcus* sp.) within a MIC range of 0.75–25 µg/ml (Ponnusamy*, et al*., 2010). The indigo, produced in the cytoplasm of the hyphal cells is a by-product of tryptophan catabolism and was transported out of the hyphae. Tryptophan is transformed to hydroxyanthranilic acids that become the precursor of phenoxazines and other nitrogen-containing pigments (Velišek & Cejpek, 2011) such as the indigoids. Staining with membrane stain FM4-64 did not show localization of indigo within vacuoles present in the pigmented hyphae. Indigo localization could also be observed in Δ*gap1/*Δ*gap1* dikaryon hyphae of *S. commune,* wherein the production of indigo could not be visually observed either in the hyphae or in the media by light microscopy. Nevertheless, the presence of indigo could be displayed in some of the hyphae using Raman spectroscopy showing that this mutant strain of *S. commune* produces indigo. The gene gap1 encodes a GTPase-activating protein for Ras, a signaling molecule known to regulate various cellular processes in fungi. Δgap1 mutants are those in which the gene has been disrupted thus leading to production of phenotypes that are unable to maintain growth orientation and display altered clamp connections (Hatakka, 2001). Pigmented strains of *S. commune* have been shown to metabolize radioactive indole into radioactive isatin, indigo and indirubin (Epstein & Miles, 1966). It was postulated that a genetic block in the metabolism of tryptophan in the pigmented strains brings about the accumulation of indole which is oxidized to indoxyl by the fungus and further to isatin by air oxidation. Two molecules of indole

will form an indigotin molecule while a molecule of isatin and a molecule of indoxyl will produce indirubin (Epstein & Miles, 1966).

Various studies have reported the production of a variety of indole derivatives by *S. commune* as shown in Fig 24. Indigo, isatin and indirubin were found by Miles (1956) and Epstein (1966) respectively, in pigmented mutant strains of *S. commune*. Schizocommunin, was isolated along with indigo, indirubin, isatin, and tryptanthrin, from the liquid culture medium in which a culture of *S. commune*, isolated from the bronchus of a human patient with allergic bronchopulmonary mycosis, had been grown (Hosoe*, et al.*, 1999). However, in our studies we could confirm the production of only indigo and indirubin. The amount of indirubin found was very minute compared to indigo.

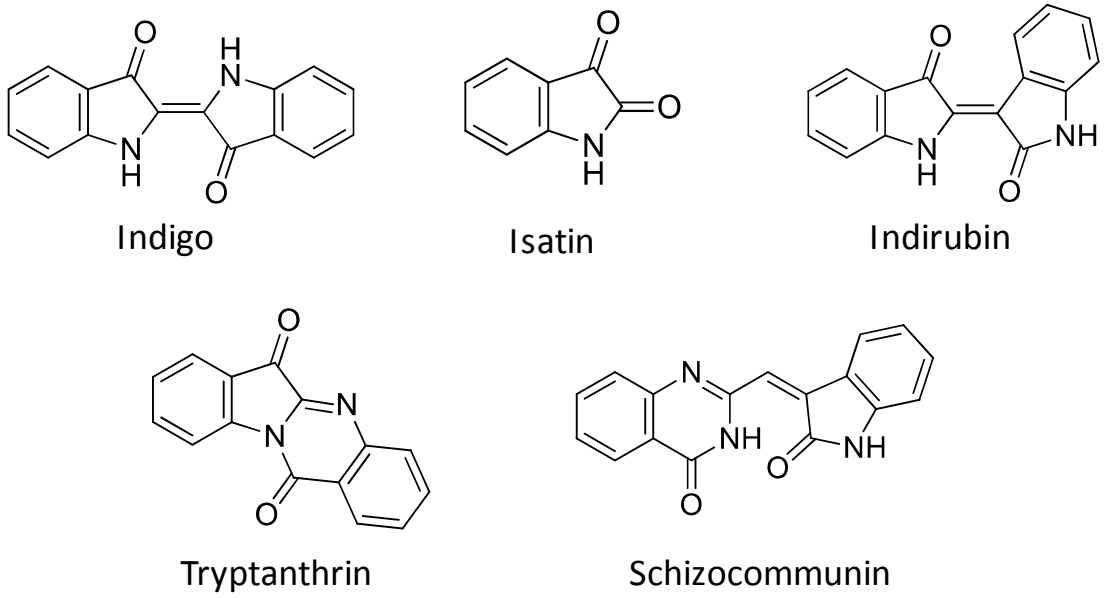

Figure 24: Structures of the indole derivatives produced by *S. commune* (Hosoe *et al.* 1999, Uehara, *et al.*2013)

In order to keenly observe the interactions and compounds produced, we focused our UHPLC-ESI-MS/MS study on the *S. commune* 12-43x4-39 – *H. fasciculare* pairing in liquid CYM media. The cell-free culture broths of *S. commune* and *H. fasciculare* had no effect on each other's growth and did not induce pigmentation. From this we deduce that in this case mycelial contact is necessary for pigmentation. The extraction was performed with methanol-water and the yield of the compounds obtained was low. Since the interactions could not be monitored well in the liquid cultures, we used instead, solid agar co-cultures of the pairing and modified the

extraction solvents to methanol-water-ethyl acetate. Thus, the interaction zone as well as the zones at the periphery of either fungus could be sampled easily and their metabolite profiles compared. The modified protocol resulted in higher yields of the compounds identified. In our studies we detected the production of indigo and indirubin which were present in the amounts of 207.92 ± 66.76 pmol and 0.87 ± 0.23 pmol per cm^3 agar respectively. Swack and Miles (1960) obtained average indigotin yields of 19.06 - 38.13 nmol/ml by pigmented mutants of *S. commune* in minimal media. Ujor, *et al.* (2012) conducted similar studies using gas chromatography-time of flight-mass spectrometry (GC-TOF-MS) for detection of the metabolites; however the presence of indigoids were not reported. GC/MS requires the analytes to be in an organic injection solvent and derivatization is often necessary to improve peak shape, ionization, and/or volatility, LC/MS however does not. As a result, the primary advantage HPLC/MS has over GC/MS is that it is capable of analyzing a much wider range of components including compounds that are thermally labile, exhibit high polarity or have a high molecular mass (www.agilent.com).

Although there was a hint of isatin, to date, its presence could not be confirmed by MS/MS fragmentation. Optimization of extraction is further needed to increase the amounts of metabolites and finally affirm the occurrence of isatin. Indirubin was also not detected by Raman spectroscopy due to its presence in a low concentration. The standard reference indirubin gave distinct spectra from that of indigo when tested with RMS (Fig 25). Indigo, due to its high molecular symmetry and conjugated bond system provides strong resonance enhanced Raman signals (Baran, *et al.*, 2010).

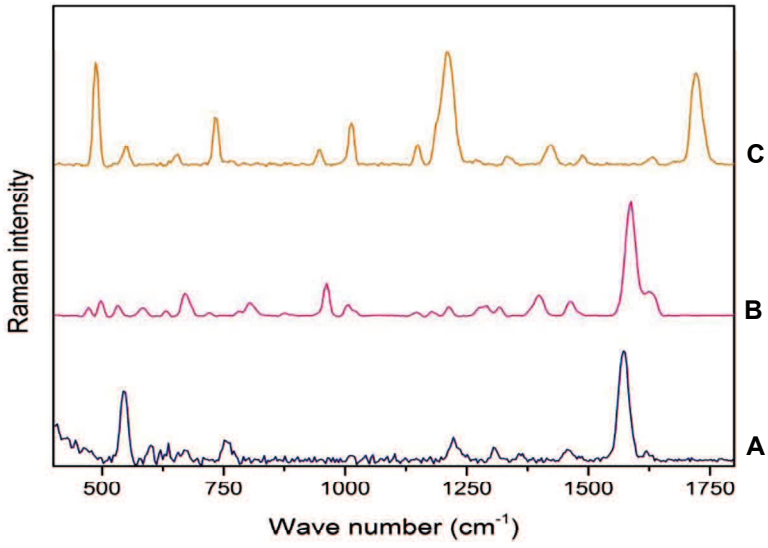

Figure 25: Raman spectra of (A) indigo (B) indirubin and (C) isatin

Raman microspectroscopy, exemplifies chemical imaging in the sense that it capable of non-invasive label-free imaging as presented in this study. Indigo localization could even be imaged in the pure culture of Δ*gap1*/Δ*gap1* mutant dikaryon hyphae of *S. commune* which microscopically did not show any sign of the production of the pigment in its hyphae. The study of these interactions (albeit on artificial media) is important because they give us a better insight into the working of the micro-organisms within an environment and their race for space and nutrient resources which have great implication in the forest eco system.

Today, most indigo dye is produced synthetically, and its production generates a significant amount of toxic waste. Therefore, biological fermentation by recombinant microorganisms may provide a cleaner alternative for large-scale indigo production (Murdock*, et al*., 1993). Indigoids also have the potential to be used for anticancer therapy, but also for Alzheimer's disease and diabetes (Kunikata*, et al*., 2000, Leclerc*, et al*., 2001, Eisenbrand*, et al*., 2004). Indigo, is uncharged and largely insoluble in most solvents. Raman spectroscopy has been shown to be a sensitive method to identify indigo even in the presence of pigment impurities (Baran*, et al*., 2010). Thus, we have shown that RMS is an efficient tool to identify the presence of compounds such as indigo, which have a relatively low solubility in water and organic solvents, without extensive sample preparation and measurement time. As second technique to analyze fungal interactions without sample preparation LESA-HRMS was performed. LESA was previously used to directly screen antibiotics from bacterial plates (Kai*, et al*., 2012). In our study, even though the mycelia covered the agar surface, the sample could be directly measured since the ethyl acetate solvent used dissolved the mycelium. Therefore, there was no need to scrape the mycelium from the agar before extraction and detection of indigo. The minor short-coming that isobaric compounds such as indigo and indirubin could not be differentiated by LESA-HRMS was overcome by implementing UHPLC-HRMS. Using this technique it has been demonstrated that there is about 2×10^5 fold more indigo present in the agar compared to indirubin. In combination, LESA-MS as a tool to rapidly extract, detect and analyze natural products like indigoids directly from the sample without any preparation protocols and UHPLC-HRMS for verification and quantification of those metabolites are powerful tools to study fungal interactions in situ.

Pigment formation in *S. commune*-fungal interactions might be a promising area in the commercialization of natural pigment and dye production for e.g. textile industry. Nevertheless, isolation and identification, as well as optimization of physical and chemical parameters of pigment production are still required before up-scaling to larger scope of production.

4.4 IAA metabolism in *S. commune*

Indole-3-acetic acid has been identified for the first time as a metabolic product of wildtype *S. commune*. The identification of this compound is based upon UHPLC-ESI-MS/MS with the sensitive LTQ-OrbitrapXL mass spectrometer. We have shown that wild type *S. commune* strains we used 12-43, 4-39 and 12-43 x 4-39 produce IAA constitutively, without the addition of tryptophan to the CYM media, and that its synthesis increased with the addition of tryptophan. Brian (1957) mentioned that none of the 25 fungal species he studied produced more than a trace of auxin without added tryptophan, but that auxin was produced by all 25 species with tryptophan. In our quantification study, out of the four media that *S. commune* 12-43 was inoculated into, it produced the highest amount of IAA (473.55 ± 3.32 $\mu g ml^{-1}$) in MMNb containing 0.25 mM tryptophan after 28 days. Although a large quantity was IAA was produced in MMNb, the data showed a large deviation from the mean. This was because the IAA values between the replicates varied vastly, which could be due to heterogenous growth of the fungi in each of the 3 replicates. Early studies used activity assays or qualitative colorimetric techniques to indicate the presence of IAA. Lately HPLC, GC and SPE (Solid-phase extraction) procedures have been described for separation and detection of IAA (Kim*, et al.*, 2006, Barkawi*, et al.*, 2008). However, we have shown that UHPLC-OrbitrapMS is also a sensitive and fast method to detect, analyze and quantify IAA. It is not known why a saprophytic wood-rotting fungus like *S. commune* would need to produce IAA. In general, pathogenic bacteria and fungi are known to produce IAA, but a direct link to pathogenicity has not been demonstrated in these pathogens (Rao*, et al.*, 2010). *S. cerevisiae* synthesizes and secretes IAA into the culture environment where it is available to function as a signal that regulates filamentation. Filamentation is a pathogenic trait because it contributes directly to virulence of pathogenic fungi like *C. albicans*. The study suggested that the secondary metabolite IAA is a chemical signal that regulates fungal pathogenesis (Rao*, et al.*, 2010). Epstein and Miles (1967) assumed

that since IAA was produced in excess in *S. commune* it did not have a growth regulating role. It was postulated that the indigo-producing mutant strains which incidently also synthesized IAA, contained a partial genetic block accumulating indole. This indole could be converted to IAA or broken down to anthranilic acid. Non-pigmented strains do not accumulate indole but possess the enzyme which converts indole to indole-3-acetic acid (Epstein & Miles, 1966). Experiments with labeled indole and IAA showed that when supplied in a small concentration the fungus was able to metabolize indole to IAA and indigo, and IAA to indole and indigo (Epstein, 1966). Richards (1949) reported that IAA caused abnormalities and changes in colony morphology usually at high concentrations. *S. commune* was strongly inhibited by a wide range of concentrations of IAA (10^{-2} to 10^{-3} M), naphthalene acetic acid, 2, 4-D, and 2,4,5-T (Richards, 1949). The inhibition of growth of *Aspergillus candidus*, *S. commune* and *Neurospora tetrasserma* by IAA in concentrations of 10^{-2} to 10^{-3} M was also reported. Indole, indole-3-acetic acid and indole-3-butyric acid were said to be among the most active of the substances inducing laccase formation in cultures of *Polyporus versicolor* (Féhraeus & Tullander, 1956). Laccases in turn are known to catalyse reactions involving actively secreted fungal metabolites like phenolic and other aromatic compounds (pigments), smaller peptides and organic acids, and lignocellulose-derived compounds and metal ions (Guillen*, et al.*, 2000, Hammel & Cullen, 2008, Ruiz-Dueñas & Martínez, 2009). A number of studies have clearly shown that IAA can be a signaling molecule in microorganisms, in both IAA-producing and IAA-nonproducing species (Spaepen*, et al.*, 2007). No similarity between the well-known effects of IAA on higher plants and the growth response of fungi can be said to exist. *S. commune* produced roughly twice the amount of IAA when co-cultured with *H. fasciculare* than its mono-culture, as did *H. fasciculare* implying that increased IAA production in the fungus is an indication of stress.

Roberts and Roberts (1939) tested several unidentified soil fungi with the *Avena* curvature test and found that only 46 per cent of 39 synthesized auxin on beef extract-peptone; none of 15 synthesized auxin on a medium without tryptophan. The mechanism of conversion of tryptophan to IAA is not known with certainty in *S. commune.* A summary of intermediates and pathways proposed by the synthesis of IAA in plants and microbes is shown in Fig. 26. Although a growth-promoting hormone, IAA is toxic at high levels, and is also an unstable compound, which makes it plausible to suggest that IAA metabolism may be tightly controlled. Indeed, this

seems to be the case as only small amounts of free IAA in plants, bacteria or fungi are present, most of it existing in the form of conjugates (Spaepen*, et al.*, 2007). Yet, we have found free IAA in amounts of 1.08 µmol/µl after 28 days of cultivation of *S. commune* in liquid culture suggesting that it has no regulatory role. Why it is produced then can only be speculated upon. Interestingly the amount of IAA and anthranilate doubled in *S. commune* present in a co-culture with another fungus than its axenic culture. This shows that the tryptophan metabolism and in turn IAA production is up-regulated during an interaction with non-self mycelia.

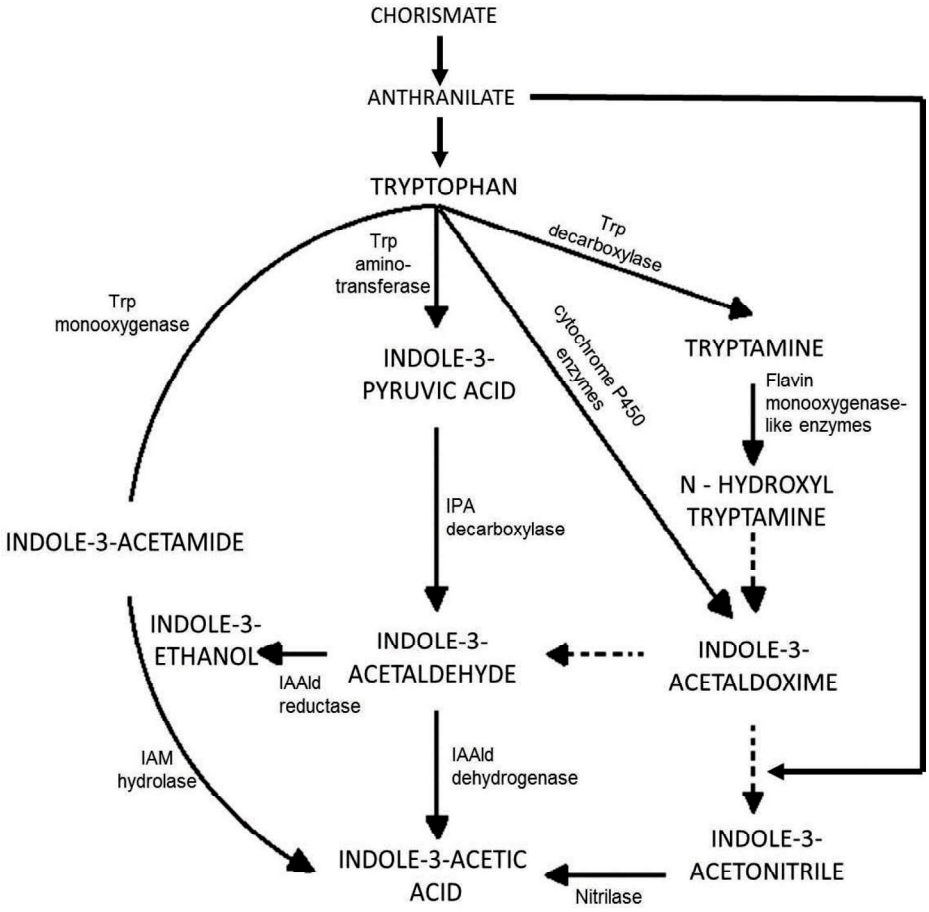

Figure 26: Scheme of IAA pathways and key intermediates proposed for plants and microorganisms. Trp, tryptophan; IPA, indole-3-pyruvic acid; IAAld, indole-3-acetaldehyde; IAA, indole-3-acetic acid; Tol, indole-3-ethanol; TAM, tryptamine; N-TAM, N-hydroxyl tryptamine; IAOx, indole-3-acetaldoxime; IAN, indole-3-acetonitrile; IAM, indole-3-acetamide. Enzymes involved in these pathways are: Trp aminotransferase (1), IPA decarboxylase (2), IAAld dehydrogenase (3), IAAld reductase (4), Trp decarboxylase (5), flavin monooxygenase-like enzymes (6), cytochrome P450 enzymes (7); nitrilase (8); Trp monooxygenase (9); IAM hydrolase (10). Possible intermediates or by-products of IAA formation thus far reported for fungi are typtamine, indole-3-pyruvic acid, indole-3-acetaldehyde and indole-3-ethanol. Enzymes for the conversion of intermediates connected by dashed arrows are elusive. Tol emerges as a by-product from IAAld in the absence of IAAld dehydrogenase activity (Reineke *et al*. 2008; Spaepen *et al.* 2007).

Plants have multiple pathways to synthesize, inactivate, and catabolize IAA (Delker, *et al.*, 2008, Lau, *et al.*, 2008, Normanly, 2010). In fungi, IAA biosynthesis was always tryptophan-dependent and the amounts of IAA produced increased with increasing tryptophan concentrations (Furukawa, *et al.*, 1996, Furukawa & Syono, 1998, Robinson, *et al.*, 1998). Time course experiments showed that the amount of IAA in media usually reached a peak after several days of growth and then either remained constant or declined. (Furukawa & Syono, 1998, Robinson, *et al.*, 1998). Most plant pathogenic bacteria produce IAA through indole-3-acetamide (IAM). In this pathway, tryptophan is converted to IAM by tryptophan-2-monooxigenase (*iaaM*), and IAM is metabolized to IAA by IAM-hydrolase (*iaaH*). The capacity to produce IAA through the IAM pathway is associated with bacterial virulence and with gall formation (Sciaky & Thomashow, 1984, Manulis, *et al.*, 1991, Yamada, 1993, Manulis, *et al.*, 1998). The tryptamine (TAM) pathway is prevalent in plants (Bartel, *et al.*, 2001). Many fungi can produce auxins in axenic cultures (Gruen, 1959, Buckley & Pugh, 1971). Most species use tryptophan to produce IAA, mainly through the indole-3-pyruvic acid and tryptamine pathways (Frankenberger & Arshad, 1995, Tudzynski & Sharon, 2002).

We could show hints of the presence of tryptamine and indole-3-pyruvic acid in the culture. But this can be confirmed only after further experimentation in this direction. We also showed for the first time that *H. fasciculare* is capable of synthesizing IAA. Epstein and Miles (1967) showed that *S. commune* mutants that produce the pigment indigo also produced IAA which indicated a possible relationship between the formation of IAA and indigo. Their study did not detect IAA production by wild type strains. Our LC-MS measurement of the culture filtrate of wildtype strains *S. commune* dikaryon 12-43 x 4-39 and monokaryon 12-43 showed a number of indolic compounds one of them being IAA, thus showing that wildtype *S. commune* strains constitutively produce IAA in detectable quantities, but not indigoid pigments. On comparing of the concentrations of indigo, IAA and indirubin in the liquid culture of pigmented mutant F15, no correlation between the formation and breakdown of the compounds was evidenced. Indole was found to be to be toxic to *S. commune* in a very small concentration (Miles, unpublished observations). Experiments with labeled indole and IAA (Epstein, 1966) showed that when supplied in a small concentration the fungus was able to metabolize indole to IAA and indigo. This raised the possibility that IAA, as well as indigo, were produced by the fungus as a means of detoxification of indole. Fungi are known to degrade various xenobionts e.g. indole,

but the degradation mechanism and products in *S. commune* have not been completely studied. Addition of 0.02% indole to liquid cultures of 12-43 x 4-39, showed an inhibition of growth of the fungi as compared to control cultures. The degradation products of indole included IAA, indirubin, indigo and anthranilate. Although the indole inhibited the growth of the fungus, nevertheless increased concentrations of IAA, indirubin and anthranilate were observed.

4.5 Outlook

This research work involved the application of advanced techniques such as confocal Raman imaging, CARS microscopy and mass spectrometry to investigate the basic metabolic processes in the white-rot fungus *Schizophyllum commune*.

Firstly, aspects of nuclear migration and sorting, and chromophores present in *S. commune* were investigated using a range of tools including live-cell imaging with Raman microspectroscopy and coherent anti-Stokes Raman scattering (CARS) microscopy, and fluorescent microscopy. The presence of previously unknown chromophores was revealed. The nuclei could not be located in this study using vibrational spectroscopy, as spontaneous Raman microscopy requires high laser power and long integration times, limiting use in live specimens and CARS microscopy lacks the contrast to image most molecules beyond lipids. The tagging of a protein localized in the nucleus with GFP could be the subject of future studies in order to monitor nuclear migration in real-time. Since microtubules play a role in this process, studies should be conducted on how dynamics of microtubules are coupled to nuclear movement.

The second study comprised of the identification of secondary metabolites produced by *S. commune* during interactions with wood-decay fungi and investigation of their role. *S. commune* being a wood-rotting fungus encounters other competitor microorganisms competing for space and the same nutrient sources in the forest ecosystem. We developed a fast and less-invasive way to identify, quantify and image metabolites of *S. commune* interacting with competitor species, using the pigment indigo as an example. This combination of Raman micro spectroscopy and LESA-HRMS (Liquid Extraction Surface Analysis coupled with high-resolution mass spectrometry) opens new avenues to investigate the fungal and bacterial metabolites directly from the sample plates without extensive preparation. It would be interesting to compare the metabolites produced by *S. commune* during various mycelial interactions with wood-decay fungi in for example, deadlock and replacement. The metabolomic data combined with transcriptome data from such interactions will enable one to paint a larger picture of the genes and metabolic pathways involved in such interactions. In addition to diffusible metabolites, the profiling of volatile fungal metabolites produced during interactions would make for a definitive study. Proton Transfer Reaction- MS (PTR-MS) allows the simultaneous

real-time monitoring of volatile (organic) compounds (VOCs). It must be noted that the metabolites identified in *in vitro* studies need not necessarily be present in nature; therefore studies involving the fungi in their natural environment must be conducted to correctly assess the occurrence of these metabolites.

Finally, the role of an auxin in wood-degrading fungi, its biosynthesis and significance using UHPLC-ESI-MS/MS was investigated. It was shown that wild type *S. commune* strains constitutively produced indole-3-acetic acid. Most fungal species use tryptophan to produce IAA, mainly through the indole-3-pyruvic acid and tryptamine pathways. We could show hints of the presence of tryptamine and indole-3-pyruvic acid in the medium, but to be certain, feeding experiments using labeled intermediates of the tryptophan dependent pathway need to be conducted in order to confirm their presence, and thus, enabling the elucidation of the biosynthetic pathway of IAA in *S. commune*. These intermediates include indole-3-acetamide, indole-3-pyruvic acid, tryptamine and indole-3-acetamide. Gene expression studies combined with metabolite profiling only can truly determine the genetics behind this mechanism.

5. Summary

Schizophyllum commune is a wood-rotting fungus that causes white-rot. It belongs to the family Schizophyllaceae of Basiodiomycetes and is ubiquitously found world-over. The abundance of *S. commune* can be attributed not only to its prolific outbreeding (>23,000 mating types), but also to its superior competition ability. This thesis, therefore, focuses mainly on studying (1) secondary metabolites produced by *S. commune* upon interaction with various white-rot fungi, (2) identification of auxins synthesized by *S. commune* and (3) nuclear migration, a step in the life cycle of *S. commune.* It also showcases the various ways in which already well established techniques like micro-Raman spectroscopy and mass spectrometry can be effectively employed in microbiology.

(1) From previous studies it was reported that *S. commune* secreted compounds in response to interactions with certain wood-rotting fungi and some antagonistic organisms on artificial media. The nature of these compounds and their biological activity was unknown, thereby were of interest as they might have potentially anti-microbial properties. To this end, Raman micro-spectroscopy and mass spectrometry – based tool LESA were employed to image, identify, and quantify these secondary metabolites. Thus, it was revealed that the pigments, indigo and indirubin are produced by *S. commune* in the zone of contact with basidiomycetes, ascomycetes, yeast or bacteria. The fact that the indigo and indirubin were only detected in wildtype *S. commune* due to co-cultivation led to the assumption that it is either a stress response or that *S. commune* detoxifies inhibitors produced by antagonistic microorganisms into indigo. They could also be detoxification products of substances such as indole which in high concentrations might be toxic to *S. commune* itself. Accumulation to toxic levels could be prevented by the formation of an insoluble compound such as indigo. On an ecological note, this work provided a greater insight into the metabolite pathways involved in the various reactions that occur during fungal interactions.

(2) The auxin indole-3-acetic acid (IAA) is a phytohormone and is best known for its role in plant cell elongation, division, and differentiation. It was reported that indigo-producing mutant strains of *S. commune* also synthesized IAA, and postulated that there may be a correlation between them in terms of synthesis. Thus, in this study

the amounts of indigo and IAA excreted into the media by a pigmented mutant were quantified and analyzed showing that there is no evidence to suggest that IAA is broken down into indigo and vice versa. On the other hand, it was shown that wild type *S. commune* strains 12-43, 4-39 and 12-43 x 4-39 produce IAA constitutively and that its synthesis was augmented by the addition of tryptophan. To test the effect of tryptophan (T) and other components on the production of IAA, *S. commune* 12-43 was inoculated into the media CYM, CYM-T, MMNb and MMNb-T. After quantification, it was found that *S. commune* produced the highest amount of IAA (473.55 ± 3.32 $\mu g ml^{-1}$) in MMNb containing 0.25 mM tryptophan after 28 days. It is not known why a saprophytic wood-rotting fungus like *S. commune* would need to produce IAA. There have been indications that IAA can be a signaling molecule in both IAA-producing and non-producing species of microorganisms (Spaepen and Remans 2007). *S. commune* produced nearly twice the amount of IAA when co-cultured with *H. fasciculare* than its monoculture, as did *H. fasciculare,* which implied that increased IAA production is an indication of stress. The functions of IAA differ with changing concentrations and therefore might also act as communication molecules. Interestingly the amount of IAA and anthranilate (precursor of tryptophan) doubled in the fungi present in a co-culture. This shows that the tryptophan metabolism and in turn IAA synthesis is up-regulated during an interaction with non-self mycelia.

(3) Nuclear migration is necessary for the dikaryotization process in *S. commune*, which consequently is necessary for mushroom formation. The common techniques used to visualize the nuclei in fungi include fluorescence staining. These stains are DNA-specific probes which interfere with replication, gradually killing the cells. Therefore, chemical imaging was employed using Raman and coherent anti-Stokes Raman scattering (CARS) microscopy to monitor nuclear dynamics *in vivo*. While in principle, Raman spectroscopy and its variants would have been ideal tools to study nuclear migration; in reality many hurdles were encountered. In order to receive a reasonable Raman scattering signal to noise ratio, an integration time of 3 s per point had to be applied. However, given that nuclear migration in *S. commune* occured at a rate of 2-3 mm per hour such a long pixel dwell time was orders of magnitude too slow to allow real-time measurements. With CARS microscopy, a good enough spectral contrast could not be obtained. During the course of this study however, two unique chromophores were discovered, one within the hyphae of *S. commune* and

another secreted by it. Although their identity or function could not be established due to lack of pertinent references, based on their Raman spectra, some conclusions could be drawn. The high signal intensity and limited number of peaks indicated that the compounds could be metallo-proteins consisting of chromophores in resonance with the 785 nm excitation wavelength. The limited number of spectral peaks also suggests that they may be crystalline in nature.

6. Zusammenfassung

Schizophyllum commune ist ein holzabbauender Pilz, welcher eine Weißfäule verursacht. Er gehört zur Familie der Schizophyllaceae der Basidiomyceten und kann weltweit gefunden werden. Die Vielfalt von *S. commune* beruht nicht nur auf der produktiven Auskreuzung (>23,000 Kreuzungstypen) sondern auch auf seiner guten Konkurrenzfähigkeit. Diese Arbeit untersucht (1) die Bildung von Sekundärmetaboliten durch *S. commune* während der Interaktion mit verschiedenen Weißfäulepilzen, (2) die Identifizierung von Auxinen in *S. commune* und (3) die Kernwanderung, einem Abschnitt im Lebenszyklus dieses Pilzes. Es wird gezeigt, wie die gut etablierten Methoden wie Mikro-Raman-Spektoskopie und Massenspektrometrie effektiv in der Mikrobiologie angewandt werden können.

(1) Es ist bekannt, dass *S. commune* auf künstlichen Medien als Antwort auf Interaktionen mit bestimmten holzabbauenden Pilzen und einigen antagonistischen Organismen verschiedene Stoffe abgibt. Deren Natur und biologische Aktivität ist unbekannt, aber wegen potentieller antimikrobieller Eigenschaften von Interesse. Daher wurden Mikro-Raman-Spektroskopie und das auf Massenspektrometrie basierende LESA zur Abbildung, Identifikation und Quantifizierung dieser Sekundärmetabolite genutzt. Es wurde gezeigt, dass die Pigmente Indigo und Indirubin in der Kontaktzone von *S. commune* mit Basidiomyceten, Ascomyceten oder Bakterien gebildet werden. Indigo und Indirubin wurden nur im *S. commune* Wildtyp während der Ko-Kultivierungen gefunden. Dies lässt vermuten, dass es sich dabei entweder um eine Stressantwort handelt, oder dass der Pilz Inhibitoren anderer antagonistischer Mikroorganismen zur Entgiftung in Indigo umwandelt. Diese könnten ebenfalls Entgiftungsprodukte von Substanzen wie Indol sein, welches für *S. commune* in hohen Konzentrationen vielleicht selbst giftig ist. Der Akkumulation toxischer Mengen könnte durch die Bildung unlöslicher Verbindungen wie Indigo vorgebeugt werden. Aus ökologischer Sicht liefert diese Arbeit einen Einblick in den Metabolitweg, der in verschiedene Reaktionen bei pilzlichen Interaktionen involviert ist.

(2) Das Auxin Indol-3-essigsäure (IAA) ist ein Phytohormon und für seine Rolle in Zell-Verlängerung, Teilung und Differenzierung bekannt. Es wurde gezeigt, dass Stämme von *S. commune,* die Indigo produzieren auch IAA synthetisieren und ein

ähnlicher Syntheseweg postuliert. In dieser Arbeit wurde das durch einen pigmentierten Mutantenstamm ins Medium abgegebene Indigo und IAA quantifiziert und analysiert. Es gibt aber keinen Beweis, dass IAA zu Indigo abgebaut wird oder umgekehrt. Andererseits konnten die Wildtypstämme 12-43, 4-39 und 12-43 x 4-39 viel IAA produzieren und dessen Synthese durch Tryptophan gesteigert werden. Um den Effekt von Tryptophan und anderen Komponenten auf die Produktion von IAA nachzuweisen wurden verschiedene Medien mit *S. commune* 12-43 inokuliert. Mit der Quantifizierung wurde gezeigt, dass *S. commune* nach 28 Tagen in MMNb mit Tryptophan die höchste Menge IAA produziert. Noch ist unbekannt, wozu ein holzabbauender Pilz wie *S. commune* IAA produziert. Es gibt Anhaltspunkte, dass IAA als Signalmolekül sowohl in IAA-produzierenden als auch nicht-IAA-produzierenden Spezies von Mikroorganismen vorkommt. In einer Ko-Kultur mit *H. fasciculare* produziert *S. commune* nahezu die doppelte Menge von IAA als beide Monokulturen, was zeigt, dass die erhöhte IAA-Produktion ein Anzeichen für Stress ist. Die Funktion von IAA unterscheidet sich mit wechselnden Konzentrationen, weshalb es ebenfalls als Molekül zur Kommunikation dienen könnte. Interessanterweise ist die Menge von IAA und Anthranilat, einer Tryptophanvorstufe, in den Pilzen einer Kokultur verdoppelt. Dies zeigt, dass der Tryptophan-Metabolismus und die IAA-Synthese während einer Interaktion mit fremdem Myzel hochreguliert sind.

(3) Die Kernwanderung ist in *S. commune* für die Bildung eines Dikaryons und somit für die Fruchtkörperbildung notwendig. Zu den Standardmethoden, welche zur Visualisierung der Zellkerne in Pilzen eingesetzt werden, gehören Fluoreszenzfärbungen. Diese färben DNA-spezifisch, inhibieren aber die Replikation und führen schließlich zum Zelltod. Daher wurden neue chemische Darstellungsverfahren mit Raman- und CARS-Mikroskopie eingesetzt um Zellkerndynamiken in vivo darzustellen. Obwohl die Raman-Spektroskopie und deren verschiedene Varianten für diese Untersuchungen prinzipiell ein geeignetes Instrument darstellen, gibt es in der Realität viele Hürden. Um eine auswertbare Raman-Streuung mit gutem Signal/Rausch-Verhältnis zu erhalten muss eine Integrationszeit von 3 s/Punkt eingesetzt werden. Die Kernwanderung in *S. commune* erfolgt mit einer Geschwindigkeit von 2-3 mm/Stunde, sodass eine lange Pixel-Halbwertszeit/Verweildauer um mehrere Größenordnungen zu langsam ist um Echtzeit-Messungen durchzuführen. Mit CARS-Mikroskopie kann kein

ausreichend guter spektraler Kontrast erreicht werden. Während dieser Arbeit konnten zwei einzelne Chromophore detektiert werden, eines innerhalb der Pilzhyphe das andere wurde ausgeschieden. Obwohl ihre Identität oder Funktion wegen fehlender geeigneter Referenzen nicht geklärt werden konnte waren einige Schlußfolgerungen möglich. Die hohe Signalintensität und geringe Anzahl von Peaks zeigt, dass es sich bei diesen Verbindungen um Metalloproteine mit Chromophoren handeln könnte, in Resonanz mit 785 nm Anregungswellenlänge. Die geringe Menge der spektralen Peaks spricht für eine natürliche kristalline Struktur.

7. References

Abel S & Athanosios T (2010) Odyssey of auxin. *Cold Spring Harb Perspect Biol* **2**.

Allen RD, Allen NS & Travis JL (1981) Video-enhanced contrast, differential interference contrast (AVEC-DIC) microscopy: a new method capable of analyzing microtubule-related motility in the reticulopodial network of Allogromia laticollaris. *Cell Motil* **1**: 291-302.

Anker L (1949) *Koninkl. Ned. Akad. Wetenschap. Proc.* **52**: 875-881

Arnison MR, Larkin KG, Sheppard CJR, Smith NI & Cogswell CJ (2004) Linear phase imaging using differential interference contrast microscopy. *J Microsc* **214**: 7-12.

Ásgeirsdóttir SA, Schuren FHJ & Wessels JGH (1994) Assignment of genes to pulse-field separated chromosomes of *Schizophyllum commune*. *Mycol Res* **98**: 689-693.

Asiimwe T (2010) Molecular characterization of a fungal aldehyde dehydrogenase in the *Tricholoma vaccinum* - spruce ectomycorrhiza. Thesis, Friedrich-Schiller-Universität, Jena, Germany.

Ayca D, Kivanc E, Fatma B & Feride S (2007) Evaluation of disseminated candidiasis on an experimental animal model: a Fourier transform infrared study. *Appl. Spectrosc.***61**: 199-203.

Badalyan SM, Polak E, Hermann R, Aebi M & Kues U (2004) Role of peg formation in clamp cell fusion of homobasidiomycete fungi. *J Basic Microbiol* **44**: 167-177.

Baran A, Fiedler A, Schulz H & Baranska M (2010) In situ Raman and IR spectroscopic analysis of indigo dye. *Anal. Methods* **2**: 1372.

Barkawi LS, Tam Y-Y, Tillman JA, *et al.* (2008) A high-throughput method for the quantitative analysis of indole-3-acetic acid and other auxins from plant tissue. *Anal. Biochem.***372**: 177-188.

Bartel B, LeClere S, Magidin M & Zolman BK (2001) Inputs to the active indole-3-acetic acid pool: de novo synthesis, conjugate hydrolysis, and indole-3-butyric acid beta-oxidation. *J Plant Growth Regul.***20**: 198-216.

Bauer H, Kowski K, Kuhn H, Lüttke W & Rademacher P (1998) Photoelectron spectra and electronic structures of some indigo dyes. *J Mol Struct.***445**: 277-286.

Berends E, Lehle L, Henquet M, Hesselink T, Wosten HA, Lugones LG & Bosch D (2013) Identification of alg3 in the mushroom-forming fungus *Schizophyllum commune* and analysis of the Delta alg3 knockout mutant. *Glycobiology* **23**: 147-154.

Biemann K (1990) Sequencing of peptides by tandem mass spectrometry and high-energy collision-induced dissociation. *Methods Enzymo l***193**: 455-479.

Biemann K & Scoble H (1987) Characterization by tandem mass spectrometry of structural modifications in proteins. *Science* **237**: 992-998.

Boddy L (2000) Interspecific combative interactions between wood-decaying basidiomycetes. *FEMS Microbiol. Ecol.***31**: 185-194.

Boddy L, Owens EM & Chapela IH (1989) Small scale variation in decay rate within logs one year after felling: Effect of fungal community structure and moisture content. *FEMS Microbiol. Ecol.* **62**: 173-184.

Boerjan W, Ralph J & Baucher M (2003) Lignin biosynthesis. *Annu. Rev. Plant Biol.***54**: 519-546.

Bourett TM & McLaughlin DJ (1986) Mitosis and septum formation in the basidiomycete *Helicobasidium mompa*. *Can. J. Bot.***64**: 130-145.

Brian PW (1957) The effects of some microbial metabolic products on plant growth. *Symposia Soc. Exptl. Biol.***11**: 166-182.

Brown AJ & Casselton LA (2001) Mating in mushrooms: increasing the chances but prolonging the affair. *Trends in genetics : TIG* **17**: 393-400.

Buckley NG & Pugh GJF (1971) Auxin production by phylloplane fungi. *Nature***231**: 332-332.

Busch KL, Glish GL & McLuckey SA (1988) *Mass spectrometry/mass spectrometry: techniques and applications of Tandem mass spectrometry*. VCH, New York.

Butin H & Lonsdale D (1995) *Tree diseases and disorders: Causes, biology, and control in forest and amenity trees*. Oxford University Press, Oxford.

Calìa V, Spatafora C & Tringali C (2003) Polyhydroxypterphenyls and related p-terphenylquinones from fungi: Overview and biological properties. *Stud. Nat. Prod. Chem.***29**.

Cartwright KSG & Findlay WPK (1946) *Decay of timber and its prevention*. Her Majesty's Stationary Office, London.

Chapela I & Boddy L (1988) The fate of early fungal colonizers in beech branches decomposing on the forest floor. *FEMS Microbiol. Ecol.***53**: 273-284.

Chapela I, Boddy L & Rayner ADM (1988) Structure and development of fungal communities in beech logs four and a half years after felling. *FEMS Microbiol.Ecol.***53**: 59-70.

Cheng J-X, Volkmer A, Book LD & Xie XS (2001) An epi-detected coherent anti-Stokes Raman scattering (E-CARS) microscope with high spectral resolution and high sensitivity. *J. Phys. Chem. B* **105**: 1277-1280.

Cheng J-X, Jia YK, Zheng G & Xie XS (2002) Laser-scanning coherent anti-Stokes Raman scattering microscopy and applications to cell biology. *Biophys J* **83**: 502-509.

Cheng J (2007) Coherent anti-Stokes Raman scattering microscopy. *Appl Spectrosc* **61**: 197-208.

Clark TA & Anderson JB (2004) Dikaryons of the basidiomycete fungus *Schizophyllum commune*: evolution in long-term culture. *Genetics* **167**: 1663-1675.

Clémençon H (2004) Anatomie der Hymenomyceten: eine Einführung in die Cytologie und Plectologie der Krustenpilze. Porlinge, Keulenpilze, Leistlinge, Blätterpilze und Röhrlinge.

Coates D & Rayner ADM (1985) Fungal population and community development in cut beech logs. *New Phytol.***101**: 153-171.

Cooke RC & Rayner ADM (1984) *Ecology of saprotrophic fungi*. Longman, London ; New York.

Cooks RG, Beynon JH, Caprioli RM & Lester GR (1973) *Metastable ions*. Elsevier, Amsterdam.

Cullen D (1997) Recent advances on the molecular genetics of ligninolytic fungi. *J Biotechnol* **53**: 273-289.

Czernusxewicx RS (1993) *Resonance Raman spectroscopy of metalloproteins using CW laser excitation*. Humana Press.

De Gussem K, Vandenabeele P, Verbeken A & Moens L (2005) Raman spectroscopic study of *Lactarius spores* (Russulales, Fungi). *Spectrochim. Acta A* **61**: 2896-2908.

de Hoffmann E (1996) Tandem mass spectrometry: A primer. *J. Mass Spectrom.***31**: 129-137.

Delker C, Raschke A & Quint M (2008) Auxin dynamics: the dazzling complexity of a small molecule's message. *Planta* **227**: 929–941.

Denk W, Strickler JH & Webb WW (1990) Two-photon laser scanning fluorescence microscopy. *Science* **248**: 73-76.

Dolk HE & Thimann KV (1932) Studies on the growth hormone of plants: I. *Proc Natl Acad Sci U S A* **18**: 30-46.

Du Q, Raksuntorn N, Younan NH & King RL (2008) End-member extraction for hyperspectral image analysis. *Appl Opt* **47**: F77-F84.

Duncan MD, Reintjes J & Manuccia TJ (1982) Scanning coherent anti-Stokes Raman microscope. *Opt Lett* **7**: 350-352.

Edwards HGM, Russell NC, Weinstein R & Wynn-Williams DD (1995) Fourier transform Raman spectroscopic study of fungi. *J. Raman Spectrosc.***26**: 911-916.

Eikel D & Henion J (2011) Liquid extraction surface analysis (LESA) of food surfaces employing chip-based nano-electrospray mass spectrometry. *Rapid Commun. Mass Sp.***25**: 2345-2354.

Eisenbrand G, Hippe F, Jakobs S & Muehlbeyer S (2004) Molecular mechanisms of indirubin and its derivatives: novel anticancer molecules with their origin in traditional Chinese phytomedicine. *J. Cancer Res. Clin.***130**: 627-635.

Ensley B, Ratzkin B, Osslund T, Simon M, Wackett L & Gibson D (1983) Expression of naphthalene oxidation genes in *Escherichia coli* results in the biosynthesis of indigo. *Science* **222**: 167-169.

Epstein E (1966) Studies of the biosynthesis of indigotin by the basidomycete *Schizophyllum commune Fr.* Ph.D Thesis, State University of New York, Buffalo, New York, U.S.A.

Epstein E (1966) Identification of 1-(o-Carboxyphenylamino)-1-deoxyribulose and anthranilic acid in cultures of the basidiomycete *Schizophyllum commune*. *Nature* **211**: 855-856.

Epstein E & Miles P (1966) Indole metabolism in *Schizophyllum commune*. *Am. J. Bot.***53**: 626.

Epstein E & Miles P (1966) Identification of indirubin as a pigment produced by mutant cultures of the fungus *Schizophyllum commune*. *Shokubutsugaku Zasshi***79**: 566-571.

Epstein E & Miles PG (1967) Identification of indole-3-acetic acid in the basidiomycete *Schizophyllum commune*. *Plant Physiol.***42**: 911-914.

Eriksson KEL, Blanchette RA & Ander P (1990) *Microbial and enzymatic degradation of wood and wood components*. Springer-Verlag.

Falconer RE, Bown JL, White NA & Crawford JW (2008) Modelling interactions in fungi. *J R Soc Interface***5**: 603-615.

Féhraeus G & Tullander V (1956) Effect of indole-3-acetic acid on the formation of oxidases in fungi. *Physiol. Plantarum***9**: 494-501.

Fortin AJ & Piche Y (1979) Cultivation of *Pinus strobus* root-hypocotyl explants for synthesis of ectomycorrhizae. *New Phytol.***83**: 109-119.

Frankenberger WT & Arshad M (1995) *Phytohormones in soils*. Marcel Dekker, New York, NY.

Furukawa T & Syono K (1998) Increased production of IAA by *Rhizoctonia solani* is induced by culture filtrate from rice suspension cultures. *Plant Cell Physiol.***39**: 43-48.

Furukawa T, Koga J, Adachi T, Kishi K & Syono K (1996) Efficient conversion of L-tryptophan to indole-3-acetic acid and/or tryptophol by some species of *Rhizoctonia*. *Plant Cell Physiol.***37**: 899-905.

Ghosal S, Macher JM & Ahmed K (2012) Raman microspectroscopy-based identification of individual fungal spores as potential indicators of indoor contamination and moisture-related building damage. *Environ. Sci. Technol.***46**: 6088-6095.

Giasson L, Specht CA, Milgrim C, Novotny CP & Ullrich RC (1989) Cloning and comparison of A alpha mating-type alleles of the basidiomycete *Schizophyllum commune*. *Mol. Gen. Genet.***218**: 72-77.

Gladfelter A & Berman J (2009) Dancing genomes: fungal nuclear positioning. *Nat. Rev. Microbiol.***7**: 875-886.

Glick BR, Patten CL, Holguin G & Penrose DM (1999) Auxin production. Imperial College Press, London.

Glish GL & Vachet RW (2003) The basics of mass spectrometry in the twenty-first century. *Nat Rev Drug Discov* **2**: 140-150.

Gold MH, Youngs, H.L., Sollewijin Gelpke, M.D. (2000) Manganese peroxidase. Marcel Dekker, NewYork-Basel.

Griffith GS, Rayner ADM & Wildman HG (1994) Interspecific interactions, mycelial morphogenesis and extracellular metabolite production in Phlebia radiata (Aphyllophorales). *Nova Hedwigia* **59**: 331-344.

Gruen HE (1959) Auxins and fungi. *Ann. Rev. Plant Physiol.***10**: 405-440.

Guillen F, Gomez-Toribio V, Martinez MJ & Martinez AT (2000) Production of hydroxyl radical by the synergistic action of fungal laccase and aryl alcohol oxidase. *Arch. Biochem. Biophys.***383**: 142-147.

Gussem K, Vandenabeele P, Verbeken A & Moens L (2007) Chemotaxonomical identification of spores of macrofungi: possibilities of Raman spectroscopy. *Anal. Bioanal. Chem.***387**: 2823-2832.

Halliday KJ, Martinez-Garcia JF & Josse EM (2009) Integration of light and auxin signaling. *Cold Spring Harb Perspect Biol.***1**: a001586.

Hammel KE & Cullen D (2008) Role of fungal peroxidases in biological ligninolysis. *Curr. Opin. Plant. Biol.***11**: 349-355.

Hancock R (2004) A role for macromolecular crowding effects in the assembly and function of compartments in the nucleus. *J. Struct. Biol.***146**: 281-290.

Hardiman I (2012) Microbial interactions of *Schizophyllum commune*. Master's Thesis, Friedrich-Schiller-Universität, Jena, Germany.

Hatakka A (1994) Lignin-modifying enzymes from selected white-rot fungi: production and role from in lignin degradation. *FEMS Microbiol Rev* **13**: 125-135.

Hatakka A (2001) *Biodegradation of lignin*. Wiley-VCH, Weinheim.

Hazelwood LA, Daran JM, van Maris AJ, Pronk JT & Dickinson JR (2008) The Ehrlich pathway for fusel alcohol production: a century of research on *Saccharomyces cerevisiae* metabolism. *Appl. Environ. Microbiol.***74**: 2259-2266.

Hedegaard M, Matthäus C, Hassing S, Krafft C, Diem M & Popp J (2011) Spectral unmixing and clustering algorithms for assessment of single cells by Raman microscopic imaging. *Theor. Chem. Acc.***130**: 1249–1260.

Hedegaard M, Matthäus C, Hassing S, Krafft C, Diem M & Popp J (2011) Spectral unmixing and clustering algorithms for assessment of single cells by Raman microscopic imaging. *Theor Chem Acc* **130**: 1249-1260.

Hering K, Cialla D, Ackermann K*, et al.* (2008) SERS: a versatile tool in chemical and biochemical diagnostics. *Anal. Bioanal. Chem.***390**: 113-124.

Hibbett, DS (2006) A phylogenetic overview of the Agaricomycotina. Mycologia **98**:6. 917-925

Higuchi T (1997) Biochemistry and molecular biology of wood. Springer-Verlag GmbH.

Higuchi T (2006) Look back over the studies of lignin biochemistry. *J. Wood Sci.***52**: 2-8.

Hintz W, Anderson JB & Horgen PA (1988) Nuclear migration and mitochondrial inheritance in the mushroom *Agaricus bitorquis*. *Genetics* **119**: 35-41.

Hirsch AM, Bhuvaneswari TV, Torrey JG & Bisseling T (1989) Early nodulin genes are induced in alfalfa root outgrowths elicited by auxin transport inhibitors *Proc. Natl. Acad. Sci. USA***86**: 1244-1248.

Ho CS, Lam CW, Chan MH*, et al.* (2003) Electrospray ionisation mass spectrometry: principles and clinical applications. *Clin. Biochem. Rev.***24**: 3-12.

Ho KY, Teh M, Yeoh KG, Huang Z, Teh SK & Zheng W (2008) Diagnosis of gastric cancer using near-infrared Raman spectroscopy and classification and regression tree techniques. *J Biomed Opt***13**: 034013-034013-034018.

Holmes JL (1984) Tandem mass spectrometry. Wiley–Interscience, New York, 1983. *Org. Mass Spectrom.***19**: 530-530.

Horton JS, Palmer GE & Smith WJ (1999) Regulation of dikaryon-expressed genes by FRT1 in the basidiomycete *Schizophyllum commune*. *Fungal. Genet. Biol.***26**: 33-47.

Hosoe T, Nozawa K, Kawahara N, Fukushima K, Nishimura K, Miyaji M & Kawai K (1999) Isolation of a new potent cytotoxic pigment along with indigotin from the pathogenic basidiomycetous fungus *Schizophyllum commune*. *Mycopathologia* **146**: 9-12.

http://www.advion.com/products/triversa-nanomate/mode-3-liquid-extraction-surface-analysis-lesa/ ed.^eds.), p.^pp.

http://www.chem.agilent.com/Library/selectionguide/Public/5989-6328EN.pdf ed.^eds.), p.^pp.

Hu Q, Noll RJ, Li H, Makarov A, Hardman M & Graham Cooks R (2005) The Orbitrap: a new mass spectrometer. *J. Mass. Spectrom.***40**: 430-443.

Huang Z, McWilliams A, Lui H, McLean DI, Lam S & Zeng H (2003) Near-infrared Raman spectroscopy for optical diagnosis of lung cancer. *Int. J. Cancer* **107**: 1047-1052.

Hunt DF, Yates JR, Shabanowitz J, Winston S & Hauer CR (1986) Protein sequencing by tandem mass spectrometry. *P. Natl. Acad. Sci. USA* **83**: 6233-6237.

Iwasa M, Tanabe S & Kamada T (1998) The two nuclei in the dikaryon of the homobasidiomycete *Coprinus cinereus* change position after each conjugate division. *Fungal Genet. Biol.***23**: 110-116.

Jarvis RM & Goodacre R (2008) Characterisation and identification of bacteria using SERS. *Chem. Soc. Rev.***37**: 931–936.

Jersild RA, Mishkin S & Niederpruem DJ (1967) Origin and ultrastructure of complex septa in *Schizophyllum commune* development. *Arch. Microbiol.* **57**: 20-32.

Johnson D, Krsek M, Wellington EMH*, et al.* (2005) Soil invertebrates disrupt carbon flow through fungal networks. *Science* **309**: 1047.

Kai M, Gonzalez I, Genilloud O, Singh SB & Svatos A (2012) Direct mass spectrometric screening of antibiotics from bacterial surfaces using liquid extraction surface analysis. *Rapid Commun. Mass Spectrom.***26**: 2477-2482.

Kai M, González I, Genilloud O, Singh SB & Svatoš A (2012) Direct mass spectrometric screening of antibiotics from bacterial surfaces using liquid extraction surface analysis. *Rapid Communications in Mass Spectrometry* **26**: 2477-2482.

Kawai G, Ikeda Y & Tubaki K (1985) Fruiting of *Schizophyllum commune* induced by certain ceramides and cerebrosides from *Penicillium funiculosum*. *Agr. Biol. Chem. Tokyo* **49**: 2137-2146.

Kawai G, Ohnishi M, Fujino Y & Ikeda Y (1986) Stimulatory effect of certain plant sphingolipids on fruiting of *Schizophyllum commune*. *J.Biol. Chem.***261**: 779-784.

Kersten P & Cullen D (2007) Extracellular oxidative systems of the lignin-degrading basidiomycete *Phanerochaete chrysosporium*. *Fungal Genet. Biol.***44**: 77-87.

Kertesz V & Van Berkel GJ (2010) Fully automated liquid extraction-based surface sampling and ionization using a chip-based robotic nanoelectrospray platform. *J Mass Spectrom* **45**: 252-260.

Kim Y-J, Oh YJ & Park WJ (2006) HPLC-based quantification of indole-3-acetic acid in the primary root tip of maize. *J. Nano & Bio Tech.***3**: 40–45.

Kirk TK & Farrell RL (1987) Enzymatic "combustion": the microbial degradation of lignin. *Annu. Rev. Microbiol.***41**: 465-505.

Kneipp K, Kneipp H, Itzkan I, Dasari RR & Feld MS (1999) Ultrasensitive chemical analysis by Raman spectroscopy. *Chem. Rev.***99**: 2957-2976.

Kniep H (1915) Beitrage zur Kenntnis der Hymenomyceten. III. Uber die konjugierten Teilungen und die phylogenetische Bedeutung der Schnallenbildungen. *Zeitschr. Botanik.* **7**: 369–398.

Kniep H (1920) Uber morphologische und physiologische Geschlechtsdifferenzierung (Untersuchungen an Basidiomyzeten). *Verhandlungen der Physikalisch-Medizinischen Gesellschaft in Wuerzburg* **46**: 1-18.

Kniep H (1928) *Die Sexualitaet der niederen Pflanzen*. Gustav Fischer Verlag, Jena.

Kögl F & Deijs WB (1935) Untersuchungen über Pilzfarbstoffe. XI. Über Boletol, den Farbstoff der blau anlaufenden Boleten. *Justus Liebigs Annalen der Chemie* **515**: 10-23.

Kögl F, Erxleben H & Jänecke L (1930) Untersuchungen über Pilzfarbstoffe. IX. Die Konstitution der Thelephorsäure. *Justus Liebigs Annalen der Chemie* **482**: 105-119.

Kothe E (1996) Tetrapolar fungal mating types: Sexes by the thousands. *FEMS Microbiol Rev***18**: 65-87.

Kottke I, Guttenberger M, Hampp R & Oberwinkler F (1987) An *in vitro* method for establishing mycorrhizae on coniferous tree seedlings. *Trees* **1**: 191-194.

Kozaris IA, Pavidou E, Salzer R, Capitani D, Spinella A & Caponetti E (2012) *Identification techniques I*. Springer, Heidelberg.

Krafft C, Dietzek B & Popp J (2009) Raman and CARS microspectroscopy of cells and tissues. *Analyst* **134**: 1046-1057.

Krafft C, Dietzek B, Schmitt M & Popp J (2012) Raman and coherent anti-Stokes Raman scattering microspectroscopy for biomedical applications. *J. Biomed. Opt.***17**: 0408011-04080115.

Kues U (2000) Life history and developmental processes in the basidiomycete Coprinus cinereus. *Microbiol Mol Biol Rev* **64**: 316-353.

Kunikata T, Tatefuji T, Aga H, Iwaki K, Ikeda M & Kurimoto M (2000) Indirubin inhibits inflammatory reactions in delayed-type hypersensitivity. *Eur J Pharmacol.* **410**: 93-100.

Kwon NR, Chae JC, Choi KY*, et al.* (2008) Identification of functionally important amino acids in a novel indigo-producing oxygenase from *Rhodococcus* sp. strain T104. *Appl. Microbiol. Biotechnol.***79**: 417-422.

Latgé J-P (2010) Tasting the fungal cell wall. *Cell. Microbiol.***12**: 863-872.

Lau S, Jurgens G & De Smet I (2008) The evolving complexity of the auxin pathway. *Plant Cell* **20**: 1738–1746.

Leclerc S, Garnier M, Hoessel R*, et al.* (2001) Indirubins inhibit glycogen synthase kinase-3β and CDK5/P25, two protein kinases involved in abnormal Tau phosphorylation in Alzheimer's Disease: A property common to most cyclin-dependent kinase inhibitors? *J. Biol. Chem.***276**: 251-260.

Leonowicz A, Cho N, Luterek J*, et al.* (2001) Fungal laccase: properties and activity on lignin. *J. Basic Microbiol.***41**: 185-227.

Li-Chan ECY (1996) The applications of Raman spectroscopy in food science. *Trends Food Sci. Tech.***7**: 361-370.

Li CY (1981) Phenoloxidase and peroxidase activities in zone lines of *Phellinus weirii*. *Mycologia* **73**: 811-821.

Lim RS, Kratzer A, Barry NP*, et al.* (2010) Multimodal CARS microscopy determination of the impact of diet on macrophage infiltration and lipid accumulation on plaque formation in ApoE-deficient mice. *J. Lipid Res.***51**: 1729-1737.

Liu J-K (2006) Natural terphenyls: Developments since 1877. *Chem. Rev.***106**: 2209–2223.

Long DA (1988) Early history of the Raman effect. *Int. Rev. Phys. Chem.***7**: 317-349.

Long DA (2002) The Raman Effect: A unified treatment of the theory of Raman scattering by molecules. Wiley.

Loontiens FG, Regenfuss P, Zechel A, Dumortier L & Clegg RM (1990) Binding characteristics of Hoechst 33258 with calf thymus DNA, poly[d(A-T)] and d(CCGGAATTCCGG): multiple stoichiometries and determination of tight binding with a wide spectrum of site affinities. *Biochemistry* **29**: 9029-9039.

Lundell TK, Mäkelä MR & Hildén K (2010) Lignin-modifying enzymes in filamentous basidiomycetes – ecological, functional and phylogenetic review. *J. Basic. Microbiol.***50**: 5-20.

Makarov A (2000) Electrostatic axially harmonic orbital trapping: a high-performance technique of mass analysis. *Anal. Chem.***72**: 1156-1162.

Manulis S, Valinski L, Gafni Y & Hershenhorn J (1991) Indole-3-acetic acid biosynthetic pathways in *Erwinia herbicola* in relation to pathogenicity on *Gypsophila paniculata*. *Physiol. Mol. Plant Path.***39**: 161-171.

Manulis S, Haviv-Chesner A, Brandl MT, Lindow SE & Barash I (1998) Differential involvement of indole-3-acetic acid biosynthetic pathways in pathogenicity and epiphytic fitness of *Erwinia herbicola* pv. *gypsophilae*. *Mol. Plant-Microbe Int.***11**: 634-642.

Marshall P, Toteu-Djomte V, Bareille P, Perry H, Brown G, Baumert M & Biggadike K (2010) Correlation of skin blanching and percutaneous absorption for glucocorticoid receptor agonists by matrix-assisted laser desorption ionization mass spectrometry imaging and liquid extraction surface analysis with nanoelectrospray ionization mass spectrometry. *Anal Chem* **82**: 7787-7794.

Martínez AT (2002) Molecular biology and structure-function of lignin-degrading heme peroxidases. *Enzyme Microb.Tech.***30**: 425-444.

Masters BR & So P (2008) Handbook of biomedical nonlinear optical microscopy. Oxford University Press, USA.

May G & Taylor JW (1988) Patterns of mating and mitochondrial DNA inheritance in the agaric basidiomycete *Coprinus cinereus*. *Genetics* **118**: 213-220.

Mayer AM & Staples RC (2002) Laccase: new functions for an old enzyme. *Phytochemistry* **60**: 551-565.

McClay K, Boss C, Keresztes I & Steffan RJ (2005) Mutations of toluene-4-monooxygenase that alter regiospecificity of indole oxidation and lead to production of novel indigoid pigments. *Appl Environ Microbiol.* **71**: 5476-5483.

McLafferty F (1981) Tandem mass spectrometry. *Science* **214**: 280-287.

McLafferty FW (1980) Interpretation of Mass Spectra. University Science Books.

McSteen P (2010) Auxin and monocot development. *Cold Spring Harb Perspect Biol* **2**: a001479.

Medyukhina A, Meyer T, Schmitt M, Romeike BFM, Dietzek B & Popp J (2012) Towards automated segmentation of cells and cell nuclei in nonlinear optical microscopy. *J Biophotonics* **5**: 878-888.

Meyer T, Akimov D, Tarcea N*, et al.* (2008) Three-dimensional molecular mapping of a multiple emulsion by means of CARS microscopy. *J Phys Chem B* **112**: 1420-1426.

Miles PG, Lund H & Raper JR (1956) The identification of indigo as a pigment produced by a mutant culture of *Schizophyllum commune*. *Arch. Biochem. Biophys.***62**: 1-5.

Miljkovic M, Chernenko T, Romeo MJ, Bird B, Matthaus C & Diem M (2010) Label-free imaging of human cells: algorithms for image reconstruction of Raman hyperspectral datasets. *Analyst* **135**: 2002-2013.

Misteli T (2007) Beyond the sequence: Cellular organization of genome function. *Cell* **128**: 787-800.

Mohaček-Grošev V, Božac R & Puppels GJ (2001) Vibrational spectroscopic characterization of wild growing mushrooms and toadstools. *Spectrochim. Acta A* **57**: 2815-2829.

Moller B & Weijers D (2009) Auxin control of embryo patterning. *Cold Spring Harb Perspect Biol* **1**: a001545.

Munoz-Rivas A, Specht CA, Drummond BJ, Froeliger E, Novotny CP & Ullrich RC (1986) Transformation of the basidiomycete, *Schizophyllum commune*. *Mol. Gen. Genet.***205**: 103-106.

Murdock D, Ensley BD, Serdar C & Thalen M (1993) Construction of metabolic operons catalyzing the de novo biosynthesis of Indigo in *Escherichia coli*. *Nat. Biotech.***11**: 381-386.

Mutnuri S, Bandi C & Ganguly A (2009) Biocatalytic production of a commercial textile dye (Indigo) from a xenobiont. *Res. J. Microbiol* **4**: 82-88.

Naumann A (2009) A novel procedure for strain classification of fungal mycelium by cluster and artificial neural network analysis of Fourier transform infrared (FTIR) spectra. *Analyst* **134**: 1215-1223.

Naumann A, Navarro-González M, Peddireddi S, Kües U & Polle A (2005) Fourier transform infrared microscopy and imaging: Detection of fungi in wood. *Fungal Genet. Biol.***42**: 829-835.

Niederpruem DJ (1980) Direct studies of dikaryotization in *Schizophyllum commune*. II. Behavior and fate of multikaryotic hyphae. *Arch. Microbiol.***128**: 172-178.

Nielsen N (1931) Uber Wuchsstoffe der Hefe. *Biochem. Z.* **237**: 244–246.

Normanly J (2010) Approaching cellular and molecular resolution of auxin biosynthesis and metabolism. *Cold Spring Harb Perspect Biol* **2**: a001594.

Ohm RA, de Jong JF, Lugones LG*, et al.* (2010) Genome sequence of the model mushroom Schizophyllum commune. *Nat Biotechnol* **28**: 957-963.

Paine MRL, Barker PJ, Maclauglin SA, Mitchell TW & Blanksby SJ (2012) Direct detection of additives and degradation products from polymers by liquid extraction surface analysis employing chip-based nanospray mass spectrometry. *Rapid Commun. Mass Sp.***26**: 412-418.

Papazian HP (1950) The physiology of the incompatibility factors in *Schizophyllum commune*. *Bot. Gaz. 112:143-163*.

Peddireddi S (2008) Hydrophobins in wood biology and biotechnology. Thesis, Georg-August-University, Göttingen, Germany.

Perry RH, Cooks RG & Noll RJ (2008) Orbitrap mass spectrometry: instrumentation, ion motion and applications. *Mass Spectrom Rev* **27**: 661-699.

Pinan-Lucarre B, Balguerie A & Clave C (2005) Accelerated cell death in *Podospora* autophagy mutants. *Eukaryot. Cell* **4**: 1765-1774.

Pliss A, Kuzmin AN, Kachynski AV & Prasad PN (2010) Biophotonic probing of macromolecular transformations during apoptosis. *PNAS* **107**: 12771-12776.

Ponnusamy K, Petchiammal C, Mohankumar R & Hopper W (2010) In vitro antifungal activity of indirubin isolated from a South Indian ethnomedicinal plant *Wrightia tinctoria* R. Br. *J. Ethnopharmacol.***132**: 349-354.

Popp J, Tuchin VV, Chiou A & Heinemann SH (2011) Handbook of Biophotonics. Wiley.

Potma EO (2010) Tissue imaging with coherent anti-Stokes Raman scattering microscopy. McGraw Hill.

Rao RP, Hunter A, Kashpur O & Normanly J (2010) Aberrant synthesis of indole-3-acetic acid in *Saccharomyces cerevisiae* triggers morphogenic transition, a virulence trait of pathogenic fungi. *Genetics* **185**: 211-220.

Raper CA (1983) Controls for development and differentiation of the dikaryon in basidiomycetes. *Secondary metabolism and differentiation in fungi,*(Ciegler JWBA, ed.^eds.), p.^pp. 195-238. Taylor & Francis, New York.

Raper JR (1966) Genetics of sexuality in higher fungi Ronald Press, New York.

Raper JR & Miles PG (1958) The genetics of *Schizophyllum commune*. *Genetics* **43**: 530-546.

Raper JR & Hoffman RM (1974) *Schizophyllum commune*. Plenum Press, New York.

Raudaskoski M (1998) The relationship between B-mating-type genes and nuclear migration in *Schizophyllum commune*. *Fungal Genet. Biol.***24**: 207-227.

Rayner ADM (1991) The challenge of the individualistic mycelium. *Mycologia* **83**: 48-71.

Rayner ADM & Todd NK (1980) Population and community structure and dynamics of fungi in decaying wood. Academic Press.

Rayner ADM & Todd NK (1982) Population structure in wood-decomposing basidiomycetes. Cambridge University Press, Cambridge.

Rayner ADM & Webber JF (1984) Interspecific mycelial interactions - an overview. Cambridge University Press, Cambridge.

Rayner ADM & Boddy L (1988) Fungal decomposition of wood : its biology and ecology. Wiley, Chichester ; New York.

Rayner ADM, Griffith GS & Howard GW (1994) Induction of metabolic and morphogenetic changed during mycelial interactions among species of higher fungi. *Biochem. Soc. Trans.* **22**: 389–394.

Reineke G, Heinze B, Schirawski J, Buettner H, Kahmann R & Basse CW (2008) Indole-3-acetic acid (IAA) biosynthesis in the smut fungus *Ustilago maydis* and its relevance for increased IAA levels in infected tissue and host tumour formation. *Mol. Plant Pathol.***9**: 339-355.

Richards RR (1949) Effects of auxins. *Botan Gaz.***110**: 523-550.

Rigaut JP & Vassy J (1991) High-resolution three-dimensional images from confocal scanning laser microscopy. Quantitative study and mathematical correction of the effects from bleaching and fluorescence attenuation in depth. *Anal. Quant. Cytol. Histol.***13**: 223-232.

Roberts JL & Roberts E (1939) Auxin production by soil microorganisms. *Soil Science***48**: 135-140.

Robinson M, Riov J & Sharon A (1998) Indole-3-acetic acid biosynthesis in *Colletotrichum gloeosporioides f. sp. Aeschynomene*. *Appl. Environ. Microbiol.***64**: 5030-5032.

Ross IK (1976) Nuclear migration rates in *Coprinus congregatus*: a new record? . *Mycologia* **68**: 418–422.

Royo JL, Moreno-Ruiz E, Cebolla A & Santero E (2005) Stable long-term indigo production by overexpression of dioxygenase genes using a chromosomal integrated cascade expression circuit. *J Biotechnol.***116**: 113-124.

Ruiz-Dueñas FJ & Martínez AT (2009) Microbial degradation of lignin: How a bulky recalcitrant polymer is efficiently recycled in nature and how we can take advantage of this. *Microb.Biotechnol.***2**: 164–177.

Ruzin SE (1999) Plant microtechnique and microscopy. Oxford University Press.

Scarpella E, Barkoulas M & Tsiantis M (2010) Control of leaf and vein development by auxin. *Cold Spring Harb Perspect Biol* **2**: a001511.

Schmidt O (2006) Wood and tree fungi biology, damage, protection, and use *; with 49 tables*. Springer, Berlin [u.a.].

Schmidt O & Liese W (1980) Variability of wood degrading enzymes of *Schizophyllum commune*. *Holzforsch* **34**: 67-72.

Schrader B, Dippel B, Erb I*, et al.* (1999) NIR Raman spectroscopy in medicine and biology: results and aspects. *J. Mol. Struct.***480–481**: 21-32.

Schubert D, Raudaskoski M, Knabe N & Kothe E (2006) Ras GTPase-activating protein gap1 of the homobasidiomycete *Schizophyllum commune* regulates hyphal growth orientation and sexual development. *Eukaryot. Cell* **5**: 683-695.

Schüffler A & Anke T (2009) *Secondary metabolites of basidiomycetes*. Springer, New York.

Schuurs TA, Dalstra HJ, Scheer JM & Wessels JG (1998) Positioning of nuclei in the secondary mycelium of *Schizophyllum commune* in relation to differential gene expression. *Fungal Genet. Biol.***23**: 150-161.

Schwalb MN & Miles PG (1967) Morphogenesis of *Schizophyllum commune*. II. Effect of microaerobic growth. *Mycologia* **59**: 610-622.

Sciaky D & Thomashow MF (1984) The sequence of the tms transcript 2 locus of the *A. tumefaciens* plasmid pTiA6 and characterization of the mutation in pTiA66 that is responsible for auxin attenuation. *Nucleic Acids Res.***12**: 1447-1461.

Shin M, Shinguu T, Sano K & Umezawa C (1991) Metabolic fates of L-tryptophan in *Saccharomyces uvarum* (*Saccharomyces carlsbergensis*). *Chem Pharm Bull (Tokyo).***39**: 1792-1795.

Singh B, Gautam R, Kumar S*, et al.* (2012) Application of vibrational microspectroscopy to biology and medicine. *Cur. Sci. India* **102**: 232-244.

Smith E & Dent G (2013) Modern Raman Spectroscopy: A Practical Approach. Wiley.

Spaepen S, Vanderleyden J & Remans R (2007) Indole-3-acetic acid in microbial and microorganism-plant signaling. *FEMS Microbiol. Rev.***31**: 425-448.

Spiro TG & Czernuszewicz RS (1995) Resonance Raman spectroscopy of metalloproteins. *Methods Enzymol.***246**: 416-460.

Stankis MM, Specht CA, Yang H, Giasson L, Ullrich RC & Novotny CP (1992) The A alpha mating locus of *Schizophyllum commune* encodes two dissimilar multiallelic homeodomain proteins. *Proc Natl Acad Sci USA* **89**: 7169-7173.

Steglich W (1981) Biologically active compounds from higher fungi. *Pure Appl. Chem* **53**: 1233-1240.

Stöckel S, Meisel S, Böhme R, Elschner M, Rösch P & Popp J (2009) Effect of supplementary manganese on the sporulation of *Bacillus* endospores analysed by Raman spectroscopy. *J. Raman Spectrosc.***40**: 1469-1477.

Sundberg E & Ostergaard L (2009) Distinct and dynamic auxin activities during reproductive development. *Cold Spring Harb Perspect Biol* **1**: a001628.

Swack NS & Miles PG (1960) Conditions affecting growth and indigotin production by strain 130 of *Schizophyllum commune*. *Mycologia* **52**: 574-583.

Szeghalmi A, Kaminskyj S, Rösch P, Popp J & Gough KM (2007) Time fluctuations and imaging in the SERS spectra of fungal hypha grown on nanostructured substrates. *J. Phys. Chem. B* **111**: 12916-12924.

Thurston CF (1994) The structure and function of fungal laccases. *Microbiology* **140**: 19-26.

Trinci APJ (1978) Wall and hyphal growth. *Science Progress, Oxford* **65**: 75-99.

Tripathi A, Jabbour, R.E., Treado, P.J., Neiss, J.H., Nelson, M.P., Jensen, J.L., Snyder, A.P. (2008) Waterborne pathogen detection using Raman spectroscopy. *Appl. Spectrosc.* **62**: 1-9.

Tudzynski B & Sharon A (2001) *Biosynthesis, biological role and application of fungal phytohormones*. Springer-Verlag, Berlin.

Tudzynski B & Sharon A (2002) *Biosynthesis, biological role and application of fungal phytohormones*. Springer-Verlag, Berlin, Germany.

Uehata K, Kimura N, Hasegawa K*, et al.*(2013) Total synthesis of schizocommunin and revision of its structure. *J. Nat. Prod.***76**: 2034-2039.

Ueyama A (1966) Studies on the succession of higher fungi on felled beech logs (Faguscrenata) in Japan. *Mat.Org.* **1**: 325-332.

Ujor VC, Monti M, Peiris DG, Clements MO & Hedger JN (2012) The mycelial response of the white-rot fungus, *Schizophyllum commune* to the biocontrol agent, *Trichoderma viride*. *Fungal Biol.***116**: 332-341.

Velišek J & Cejpek K (2011) Pigments of higher fungi– a review. *Czech J. Food Sci.***29**: 87–102.

Walter A, Erdmann S, Bocklitz T*, et al.* (2010) Analysis of the cytochrome distribution via linear and nonlinear Raman spectroscopy. *Analyst* **135**: 908-917.

Walworth MJ, ElNaggar MS, Stankovich JJ, Witkowski C, Norris JL & Van Berkel GJ (2011) Direct sampling and analysis from solid-phase extraction cards using an automated liquid extraction surface analysis nanoelectrospray mass spectrometry system. *Rapid Commun. Mass Sp.***25**: 2389-2396.

Wang CS & Miles PG (1966) Studies of the cell walls of *Schizophyllum commune*. *Am J Bot* **53**: 792-800.

White NA & Boddy L (1992) Extracellular enzyme localization during interspecific fungal interactions. *FEMS Microbiol Lett* **98**: 75-79.

Wich CB (1995) Genencor international takes a green route to blue dye. *Genet. Eng. News* **15**: 22-25.

Willstaedt H (1935) Über die Farbstoffe des echten Reizkers (*Lactarius deliciosus* L.) (I. Mitteil.). *Berichte der deutschen chemischen Gesellschaft (A and B Series)* **68**: 333-340.

Willstaedt H (1936) Über die Farbstoffe des echten Reizkers (*Lactarius deliciosus* L.) (II. Mitteil.). *Berichte der deutschen chemischen Gesellschaft (A and B Series)* **69**: 997-1001.

Winter ME (1999) N-FINDR: an algorithm for fast autonomous spectral end-member determination in hyperspectral data. *Proc. SPIE. Imaging Spectrometry V* **3753**: 266-275.

Yamada T (1993) The role of auxin in plant-disease development. *Annu Rev Phytopathol.***31**: 253-273.

Yamashita H, Tsubokawa S & Endo A (1985) Microbial hydroxylation of Compactin (ML-236B) and Monacolin K. *J. Antibiot.***38**: 605-609.

Yorimitsu T & Klionsky DJ (2005) Autophagy: molecular machinery for self-eating. *Cell Death Differ* **12 Suppl 2**: 1542-1552.

Zazímalová E, Murphy AS, Yang H, Hoyerová K & Hosek P (2010) Auxin transporters - why so many? *Cold Spring Harb. Perspect. Biol.* **March 2010; 2 : a001552**.

Zhu J, Lee B, Buhman KK & Cheng J-X (2009) A dynamic, cytoplasmic triacylglycerol pool in enterocytes revealed by ex vivo and in vivo coherent anti-Stokes Raman scattering imaging. *J Lipid Res* **50**: 1080-1089.

Zubarev RA & Makarov A (2013) Orbitrap mass spectrometry. *Anal Chem* **85**: 5288-5296.

Zumbusch A, Holtom GR & Xie XS (1999) Three-dimensional vibrational imaging by coherent anti-Stokes Raman scattering. *Phys Rev Lett* **82**: 4142-4145.

8. Selbständigkeitserklärung

Ich erkläre, dass ich die Dissertation “Application of Raman spectroscopy and mass spectrometry to study growth and interaction processes of the white-rot fungus *Schizophyllum commune*” selbständig und nur mit der darin angegebenen Hilfe verfasst habe. Die Dissertation wurde in keiner anderen Fakultät oder Universität eingereicht.

I hereby declare that this dissertation “Application of Raman spectroscopy and mass spectrometry to study growth and interaction processes of the white-rot fungus *Schizophyllum commune*” is an original work. I guarantee that the content of this dissertation has not, in part or whole, been accepted for the award of any degree in any university or institution.

Jena, 14.03.2014 Riya Christina Menezes

9. Acknowledgement

First and foremost, I would like to express my sincere gratitude to my advisors Prof. Dr. Erika Kothe and Prof. Dr. Jürgen Popp, who offered me the opportunity to pursue the PhD degree with delightfully interdisciplinary projects in their groups. I am indebted to the both of them for their professional advice, guidance, and patience throughout my studies. I also thank Dr. Katrin Krause and Prof. Dr. Benjamin Dietzek for advice on projects and for reviewing my articles.

Many thanks to Dr. Christian Matthäus for being a mentor and a friend. Apart from teaching me the nitty-gritties of Raman spectroscopy, he has been a source of support through these years with his kind and encouraging words. Our discussions over Black Bean coffee were truly enlightening and fun.

I want to thank my “de facto” advisor Dr. Marco Kai for introducing me to mass spectrometry and for his extensive advice during my research. He is truly a researcher with both, creativity and diligence. He has been incredibly patient and attentive while dealing with my daily onslaught of questions. Every discussion with him resulted in fresh ideas or suggestions on how to improve the current ones. His profound knowledge of MS, his zeal for research and his kind encouragement inspired me to be a better researcher.

I’m thankful to Elke-Martina Jung for introducing me to *Schizophyllum* and for reintroducing me to microscopy. She’s always been kind and helpful in various ways and I appreciate that. Her endless knowledge on all things Thüringian, from bees to bratwurst, has led to very entertaining conversations over lunch and otherwise. I also thank Dr. Gero Bergner and Sandro Heuke for assistance with µCARS measurements and, Dr. Aleš Svatoš for allowing me to use his research lab at the MPI-Chemical Ecology. My sincere gratitude to all my co-workers at the Institute of Microbial Communication, the Leibniz Institute of Photonic Technology and the Mass spectrometry research group at the MPI-Chemical Ecology for a cheerful and enriching research ambiance. Many thanks to Mrs. Ulrike Schleier and Dr. Carsten Thoms of the JSMC for welcoming me warmly to Jena in the very cold winter of Jan 2011 and for their dedicated service to the graduate school.

Last but not least, I thank warmly, my parents Victor and Lucy and my siblings Reema, Roopa and Rohan for their constant love and support, for tolerating my eccentricities and always having faith in me. Thanks to Aunty Ceci and Nana for keeping me in their prayers. I thank my dear friends Preetha, Bhavya, Harish, Elizabeth, Terenia and the Thikkal Club back in India for always having my back.

The financial support of the Jena School for Microbial Communication is gratefully acknowledged.

10. Curriculum vitae

Riya Christina Menezes

Work Address Institute of Microbiology, Neugasse 25, 07743 Jena, Germany

Phone +49 151 66803753

E-mail riya.menezes@jsmc.info

Nationality Indian

Date of Birth August 16, 1986

EDUCATION

2011 - present: Ph.D. student at the Institute of Microbiology and the Institute of Photonic Technology, Friedrich Schiller University, Jena, Germany, supervised by Professors Erika Kothe and Jürgen Popp
Fellow of the Jena School for Microbial Communication (JSMC)

2009 - 2010: Junior research fellow at the Centre for Ecological Sciences, Indian Institute of Science, Bangalore, India. Member of the Kartik Shanker Lab

2007 - 2009: MSc. Biotechnology at St. Aloysius College (affiliated to Mangalore University), Mangalore, India. Thesis "Development of technology for the bio-control of *Salmonella* in poultry"

2004 - 2007: BSc. Biotechnology at Mount Carmel College (affiliated to Bangalore University), Bangalore, India

SCHOLARSHIPS

- JSMC MikroInter PhD fellowship from the Graduate School *Jena School for Microbial Communication* (JSMC) funded by the German Excellence Initiative – *Deutsche Forschungsgemeinschaft* (DFG)
- Received a Junior Research Fellowship with a 3 year grant (2009-2012) from the Council for Industrial and Scientific Research (CSIR), Govt. of India to carry out research on the scheme "Models of diversification in the Western Ghats frogs"

EMPLOYMENT HISTORY

01/2011- present: PhD candidate, Institute of Microbiology and Leibniz Institute of Photonic Technology. Friedrich-Schiller-Universität, Jena, Germany

07/2009- 12/2010: Research fellow, Center for Ecological Sciences, Indian Institute of Science, Bangalore, India

PUBLICATIONS

- Menezes, RC., Kai, M., Matthäus, C., Krause, K., Svatoš, A., Popp, J., Kothe, E. (2014) Monitoring metabolites produced in interactions of *S. commune* with wood-degrading fungi - new analytical potential combining Raman microscopy and LESA-HR mass spectrometry (submitted)
- Menezes, RC., Kai, M., Svatoš, A., Kothe, E. (2014) Metabolomic profiling of fungal co-cultures from different zones of the petri dish (in preparation)
- Vijaykumar, SP., Menezes, RC., Jayarajan, A., Shanker, K. (2013) Radiation in a refugium: contrasting patterns of in situ diversification in the Western Ghats bush frogs (submitted)
- Menezes, RC. (2009) Development of technology for the bio-control of *Salmonella* in poultry. Master's thesis. St. Aloysius College, Mangalore University.

CONFERENCES

- Kai, M.,Menezes, RC., Krause, K., Kothe, E., Svatoš, A. (Mar '14) "Investigation of fungal metabolites using LESA, DESI and UHPLC OrbitrapXL mass spectrometry". 47. Jahrestagung der Deutschen Gesellschaft für Massenspektrometrie, Goethe Universität, Frankfurt, Germany (Poster).
- Menezes, RC. (Oct '13). "Direct detection of secondary fungal metabolites using Raman spectroscopy and liquid extraction surface analysis''. JSMC Symposium, Jena, Germany (Oral presentation).
- Menezes, RC., Kai, M., Matthäus, C., Jung, E-M, Krause, K, Dietzek, B, Kothe, E and Popp, J. (Sep '13)."Raman spectroscopy to detect secondary fungal metabolites". 10th Confocal Raman Imaging Symposium, Ulm, Germany. (Poster).

- Krause, K., Menezes, RC., Hardiman, I., Jung, E-M., Formann, S., Matthäus, C., Kai, M., Popp, J.. Kothe, E. (Sep '13) "Biotic and abiotic interactions of *Schizophyllum commune* and identification of produced compounds". 12th Symposium on remediation in Jena (Poster).
- Menezes, RC., Matthäus, C., Jung, E-M, Krause, K, Dietzek, B, Kothe, E and Popp, J. (Jun '13). "Raman Spectroscopy- A simple and reliable tool for the detection of secondary fungal metabolites". 6th International Biophotonics Graduate Summer school, Ven, Sweden (Poster).
- Menezes, RC. IPHT Retreat, Dornburg, Germany (Nov '12). "Raman investigation of compounds produced in fungal interactions" (Oral presentation).
- Menezes, RC., Matthäus, C., Jung, E-M, Krause, K, Dietzek, B, Kothe, E and Popp, J. (Aug '12) "Spectral analysis of secondary metabolites produced during fungal interactions". 4th Congress of the European Association for Chemical and Molecular Sciences (EuCheMS2012), Prague, Czech Republic (Poster).
- Menezes, RC. JSMC Retreat, Bad Sulza, Germany (Jul '12). "Spectral analysis of secondary metabolites produced in fungal interactions" (Oral presentation).
- Menezes, RC., Bergner, G.,Dietzek, B., Kothe, E. and Popp, J (Sep '11). "Characterization of the cellular components of *S. commune* by chemical imaging 11th European conference on Fungal Genetics. Philipps-Universität Marburg (Poster).
- Menezes, RC., Bergner, G., Dietzek, B., Kothe, E. and Popp, J. (Sep '11)."Characterization of the cellular components of *S. commune* by chemical imaging". MiCom 2nd international student conference on microbial communication, Jena, Germany (Poster).